University of South-Eastern Norway

www.usn.no

FMH606 Master's Thesis 2022

Masters in Energy and Environment Technology

Modeling and analysis of secondary oil recovery through advanced wells

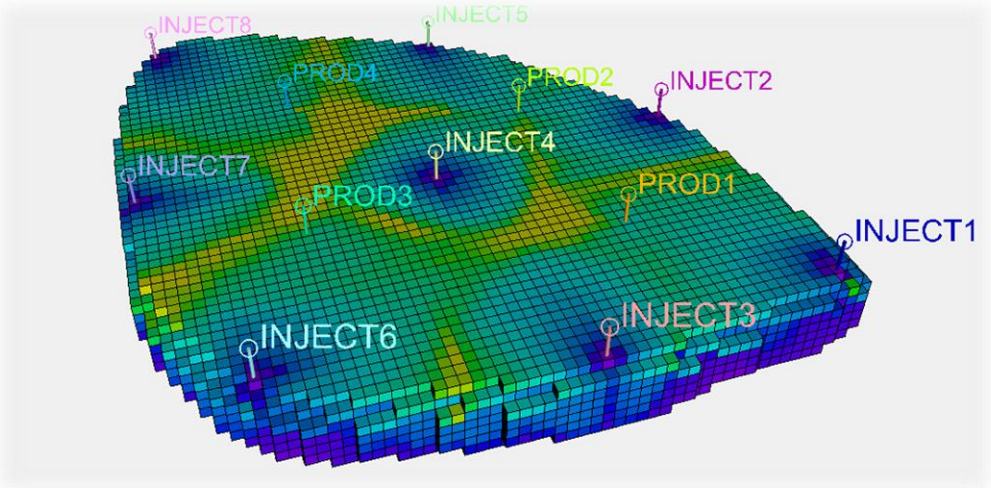

Onkar Prakash Bhujange

Faculty of Technology, Natural sciences and Maritime Sciences

Campus Porsgrunn

University of South-Eastern Norway

www.usn.no

Course: FMH606 Master's Thesis, 2022

Title: Modeling and analysis of secondary oil recovery through advanced wells

Number of pages: 86

Keywords: Egg Model, secondary oil recovery, horizontal well, ICD, AICD, AICV, Advance well.

Student:	Onkar Prakash Bhujange
Supervisor:	Prof. Britt M. E. Moldestad, Associate Prof. Amaranath S. Kumara, and Ali Moradi
External partner:	Equinor and SINTEF

The University of South-Eastern Norway takes no responsibility for the results and conclusions in this student report.

University of South-Eastern Norway

www.usn.no

Summary: Oil and gas will remain the most important source of energy for the foreseeable future and there is an urgent need to improve oil and gas recovery with less carbon footprint to meet the future energy demands. The extraction of oil from a reservoir starts by drilling a well into the oil zone. Initially, due to the high pressure, the oil is pushed towards the surface. But as the pressure inside the reservoir drops a mechanism such as water injection is required to maintain the pressure high inside the reservoir. Th process is called secondary oil production. One of the main principles to achieve cost-effective and efficient oil recovery is maximizing the well-reservoir contact by using long horizontal wells. One of the main challenges of using such wells is early gas and/or water breakthrough due to the heel-toe effect and heterogeneity along with the horizontal wells. To tackle this problem, advanced wells are used. Advanced wells are horizontal wells equipped with downhole Flow Control Devices (FCDs), which are passive Inflow Control Devices (ICDs), Autonomous Inflow Control Devices (AICDs), Autonomous Inflow Control Valves (AICVs), and Interval Control Valves (ICVs). To achieve a successful design of horizontal wells, a suitable dynamic model of oil field and advanced wells must be developed.

With and objective of comparing the vertical well production with horizontal good production and analyzing the effect of horizontal good length on the productivity of the well different reservoir model has been developed using Petrel 2021 software. Also, the flow control devices such as ICD, AICD, and AICV have been mathematically modeled.

The result of the study shows that the production rate of the reservoir with a horizontal well is higher than the reservoir with a vertical well. Different phenomenon such as early water breakthrough in horizontal wells is also presented. Also, the effect of high permeability zones on well production and injection is presented. Moreover, it is observed that doubling the length of horizontal well have increased the oil production by 70%. Hence it can be concluded that Petrel is a very good platform to create the dynamic reservoir model and the simulation results show that the field with horizontal wells is more effective than the field with vertical wells.

The University of South-Eastern Norway takes no responsibility for the results and conclusions in this student report.

Preface

This master's thesis presents the outcome of the research work carried out in spring 2021 at the University of South-Eastern Norway (USN), Porsgrunn. It has been written to fulfill the graduation requirements of the Master of Science degree at USN.

The main objective of the thesis is to study and develop a simulation model for secondary oil recovery through advanced wells. The thesis description has been presented in Appendix A.

This thesis was a great learning opportunity for me to indulge in a research project under the supervision of Prof. Britt Margrethe Emilie Moldestad, Associate Prof. Amaranath S. Kumara, and Ali Moradi.

I would like to especially thank Ali Moradi for his immense support from day one. The guidance and knowledge I got from his profound and I couldn't have completed my study without it.

A very special thanks to Mr. Aleksander Svanberg and the IT team for their never-ending support regarding Petrel.

Also, a very special thanks to my Mom, Dad, Sister, Suraj, Suzan, and other friends who believed in me and supported me during every step of my life.

At last I gratefully acknowledge the economic support from The Research Council of Norway and Equinor ASA through Research Council project "308817 - Digital wells for optimal production and drainage" (DigiWell).

Porsgrunn, 1st June 2022

Onkar Prakash Bhujange

Contents

1 Introduction 10

1.1 Background 10
1.2 Problem Description 11
1.3 Objective 13
1.4 Thesis Outline 13

2 Literature Review 14

2.1 Water flooding 14
2.1.1 Water flooding pattern 14
2.2 Horizontal wells 16
2.2.1 Heterogeneity in Horizontal well 17
2.2.2 Hill-toe effect 18
2.3 Inflow Control Devices 19
2.3.1 Channel-type (Helical channel) ICD 20
2.3.2 Orifice/Nozzle type ICD 21
2.4 Autonomous Inflow Control Device (AICD) 21
2.5 Autonomous Inflow Control Valve (AICV) 23
2.6 Multi-segmenting 24

3 Theoretical background 27

3.1 Reservoir Properties 27
3.1.1 Porosity 27
3.1.2 Absolute Permeability 29
3.1.3 Effective Permeability 31
3.1.4 Relative Permeability 32
3.1.5 Wettability 33
3.1.6 Capillary Pressure 34
3.2 Models and Calculation 35
3.2.1 The horizontal well production mechanism 35
3.2.2 Modeling of Nozzle ICDs 36
3.2.3 Modeling of AICDs 37
3.2.4 Modeling of AICVs 42

4 Reservoir Model 46

4.1 Geological Model 46
4.1.1 Egg Model 46
4.1.2 Simple model with one producer and one injector. 47
4.1.3 Enlarged Egg Model 48
4.1.4 Fluid Contacts 49
4.2 Fluid Model 50
4.2.1 Reservoir conditions 50
4.2.2 Oil 51
4.2.3 Water 52
4.2.4 Rock Physics 52
4.3 Well Model 54
4.3.1 Well, Design. 54
4.3.2 Well Completion 57
4.3.3 Development Strategy 59

5 Simulation Result 62

5.1 Analyzing Egg model in Petrel. 62
5.2 Vertical open hole production vs Horizontal open hole production of reservoir. 64
5.2.1 Producer 1 65
5.2.2 Producer 2 65
5.2.3 Producer 3 66
5.2.4 Producer 4 67
5.2.5 Cumulative field production rate. 67
5.3 Impact of horizontal well length on production. 68
5.3.1 Production rate. 69
5.3.2 Water-oil ratio. 69
5.4 3D simulation results of Oil Saturation. 70

6 Discussion 71

6.1 Egg Model 71
6.2 Oil production in vertical vs horizontal wells. 71
6.3 Effect of horizontal well length on reservoir production. 72
6.4 Observation from the 3D plots with respect to time. 72

7 Conclusion 73

8 References 74

Table of Figures.

Figure 1.1: Global fossil fuel consumption [1] 10
Figure 1.2: Change in oil demand by a scenario from 2020 to 2030. [3] 11
Figure 1.3: Waterflooding technique for oil production. [5] 12
Figure 2.1: Direct inline drive pattern [6] 15
Figure 2.2: Staggered line drive [6] 15
Figure 2.3: Flooding efficiency of direct line (1) and staggered line drive (2 and 3) well networks as a function of d/a. At a mobility ratio of 1. [6] 16
Figure 2.4: Representation of horizontal well. [7] 16
Figure 2.5: Breakthrough of oil and gas in the heterogeneous reservoir. [8] 17
Figure 2.6: Uniform inflow profile after installation of ICD in heterogeneous reservoir [8] 17
Figure 2.7: Hill toe effect in a horizontal well. [9] 18
Figure 2.8: The variation of cumulative oil production with the Well length [7] 19
Figure 2.9: Schematic diagram of orifice ICD. [7] 20
Figure 2.10: Helical channel type ICD. [7] 20
Figure 2.11: Nozzle type ICD. [7] 21
Figure 2.12: AICD design [11] 22
Figure 2.13: AICD flow path and operation. [11] 22
Figure 2.14: AICV pressures. [12] 23
Figure 2.15: AICV components. [12] 24
Figure 2.16: ICDs implemented in multisegmented model as individual segments. [16] 25
Figure 2.17: Well related equations. [13] 25
Figure 2.18: Inflow in the segment [13] 26
Figure 2.19: Pressure equation for each segment. [13] 26
Figure 3.1: Sandstone sample. [18] 27
Figure 3.2: Conceptual representation of pore space. [17] 28
Figure 3.3: Different types of pores. [17] 28
Figure 3.4: Effect of wettability on relative permeability data. [6] 33
Figure 3.5: Flow-through nozzle ICD in well. [23] 36
Figure 3.6: Performance curves for nozzle ICD for oil, water, and gas. [23] 37
Figure 3.7: AICD flow path. [23] 38
Figure 3.8: Performance curve of ICD and RCP for oil, water, and gas. [23] 38

Figure 3.9: AICD performance modeling versus testing. [11] 39
Figure 3.10: Multi variable non-linear regression for AICD curve. 41
Figure 3.11: Open AICV (left) and Closed AICV (right) [23] 42
Figure 3.12: Performance curve of AICV and ICD for oil, water, and gas. [23] 43
Figure 3.13: Multi variable non-linear regression for AICD curve. 45
Figure 4.1: Egg model of the reservoir showing 8 injectors and 4 producers. [24] 46
Figure 4.2: Input properties of the simulation case. 47
Figure 4.3: Staggered line drive pattern of egg model. 48
Figure 4.4: Simple reservoir model. 48
Figure 4.5: Model description and the model. 49
Figure 4.6: Relationship of contacts in a pool (right) to reservoir capillary pressure and fluid production curves (left). [25] 49
Figure 4.7: Gas-oil contact(Green) & water-oil contact(Blue). 50
Figure 4.8: Make a fluid model tab in the Petrel. 51
Figure 4.9: Dead oil [26] 51
Figure 4.10: Make a fluid model tab for water in the Petrel. 52
Figure 4.11: Relative permeability values. 53
Figure 4.12: Relative permeability curve obtained from data in Figure 4.11. 53
Figure 4.13: Pattern of injectors and producers in egg model. 54
Figure 4.14: Top view of the enlarged egg model showing the wells 55
Figure 4.15: Top view of the reservoir showing horizontal good directions (left) and high permeability zones(Right). 56
Figure 4.16: Horizontal producer and vertical injector in a simple model. 56
Figure 4.17: ICD attributes. 58
Figure 4.18: AICD attributes (Left) and AICV attributes (Right) 59
Figure 4.19: Development strategy for waterflooding in the Petrel software. 60
Figure 5.1: Oil and water production of producer 1. 62
Figure 5.2: Oil and water production of producer 2. 63
Figure 5.3: Oil and water production of producer 3 63
Figure 5.4: Oil and water production of producer 4. 64
Figure 5.5: Horizontal vs Vertical well production of Producer 1. 65
Figure 5.6: Horizontal vs Vertical well production of Producer 2. 65
Figure 5.7: Oil saturation w.r.t time of Enlarged Egg Model with vertical well 66
Figure 5.8: Horizontal vs Vertical well production of Producer 3. 66

Figure 5.9: Oil saturation results of horizontal well case after 365 days. 67
Figure 5.10: Horizontal vs Vertical well production of Producer 4. 67
Figure 5.12: Cumulative production rate of horizontal vs vertical wells. 68
Figure 5.13: Oil and water production for PROD1. 69
Figure 5.15: Water-oil ration of PROD1 at varying length. 69
Figure 5.16: 3D simulation results at the interval of 4 years. 70

1 Introduction

1.1 Background

Ever since the industrial revolution, we have been burning fossil fuels. Although, over the past few centuries the consumption of fossil fuels has changed significantly in terms of what we burn and how we burn. From 1950 to 2020 the consumption of fossil fuel has increased eight-fold, and it is doubled since 1980. But the type of fossil fuel has changed from coal to oil and gas. Coal consumption is falling in many parts of the world while oil and gas are still increasing. Below Figure 1.1 shows the consumption of oil, gas, and coal since 1800. [1]

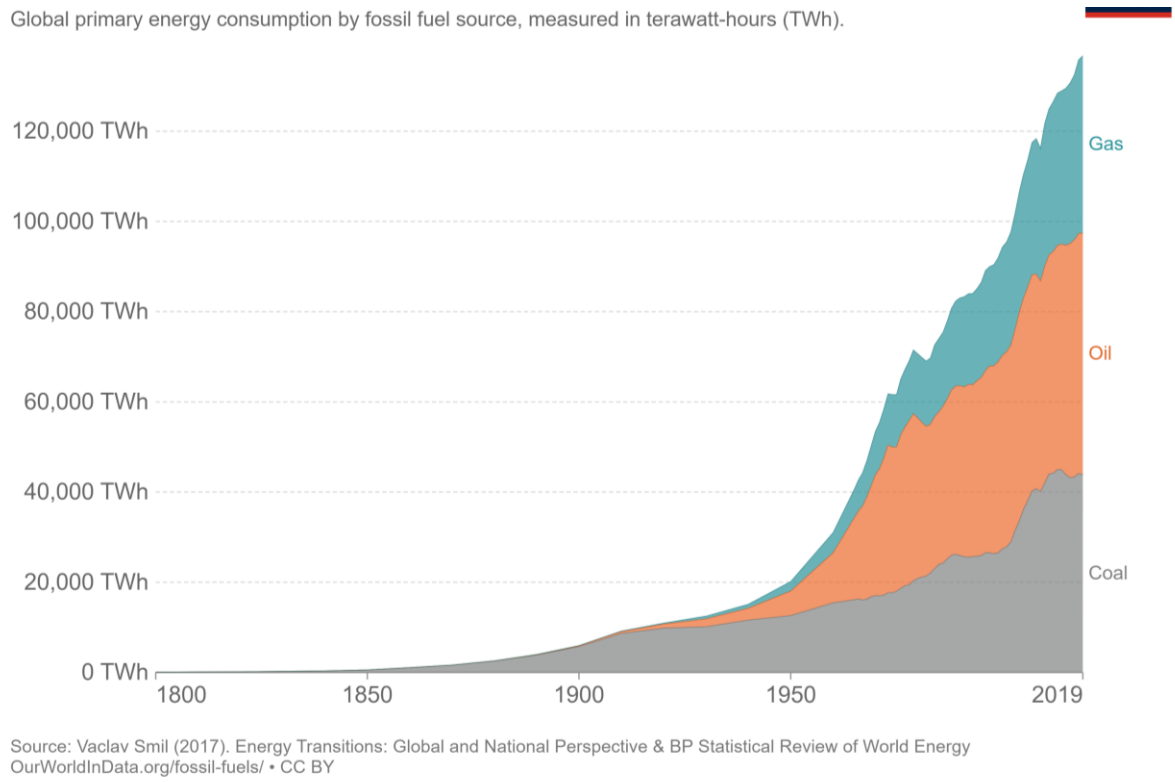

Figure 1.1: Global fossil fuel consumption [1]

In 2017, 54% of the world's energy consumption came from oil and gas. By 2050, it is expected that only 20% of the world's energy supply will come from solar- or wind power. However, there will be about 2.2 billion more people on earth. [2] But we can take a look at the next decade we can understand the significance of oil. This is because oil is not just used in passenger cars but also in heavy-duty transport and some other industries such as petrochemicals and aviation.

Figure 1.2 below shows the change in oil demand between 2020 and 2030 according to respective sectors and regions in three different scenarios. Only in NZE (Net zero-emission) scenario, the change in oil demand for the transport sector goes into negative value. In the current stated policies scenario (STEPS), the oil demand will still increase. Also, there will be a huge demand for oil in developing economies according to STEPS. This chart can be summed up as the global oil market is largely dependent on the change in road transport. Also, due to large increases in the Middle East, India and China oil demand for petrochemicals will increase in all scenarios.

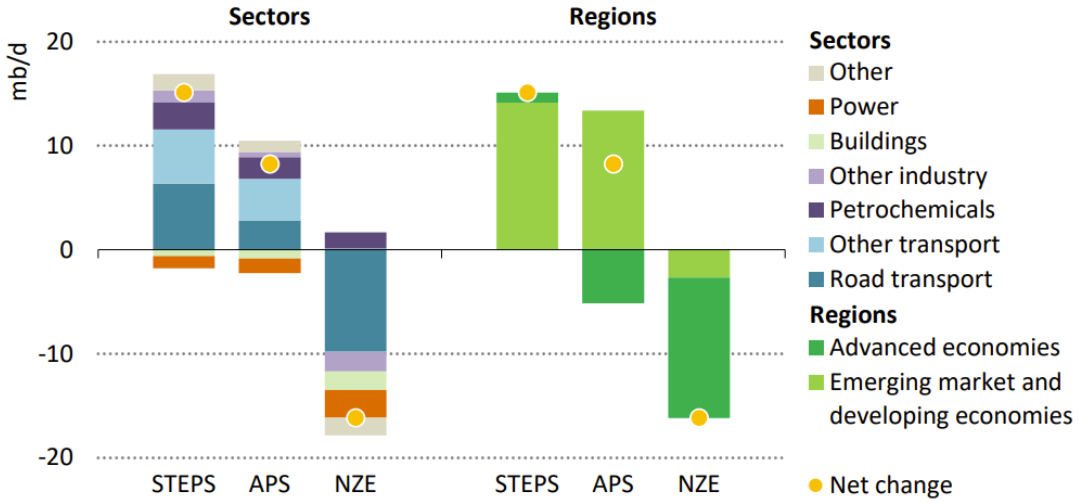

Figure 1.2: Change in oil demand by a scenario from 2020 to 2030. [3]

In the current situation, it is not possible to find a 100 % replacement for the oil. Although, there is a potential to have a more environmentally friendly oil & gas industry. Additionally, 2% of the world's oil production comes from Norway. If Norway stops oil production, it will have a negligible impact on world oil production since other countries will compensate for the difference. [2] Norwegian Continental Shelf (NCS) is one of the most technologically advanced petroleum regions in the world. To ensure that NCS is at the forefront of technological innovations, OG21 (Oil and gas for the 21st century) has come up with a plan to guide research in the field of petroleum technology with an objective of efficient, secure, and environmentally friendly oil and gas production for next generation. Keeping in mind the OG21 strategy, the research project called DigiWell (digital wells for optimal production and drainage) is developed at USN. Along with SINTEF, UiO, ICL, and MIT as the main research partners, this project is funded by the Norwegian Research Council. The main aim of this project is to develop new methods, algorithms, and tools for the prediction of oil production under uncertain conditions to maximize profit margins by minimizing production costs. This thesis is part of this project, and it is of great interest to model and evaluate the performance of advanced wells to improve oil recovery. [4]

1.2 Problem Description

Petroleum reservoirs usually start with a formation pressure high enough to force crude oil into the well and sometimes to the surface through the tubing. This is known as primary recovery.

However, since production is invariably accompanied by a decline in reservoir pressure, “primary recovery” through natural drive soon comes to an end.

When a large part of the crude oil in a reservoir cannot be recovered by primary means, A “secondary recovery” is required to reenergize or “pressure up” the reservoir. This is accomplished by injecting gas or water into the reservoir to replace produced fluids and thus maintain or increase the reservoir pressure. When gas alone is injected, it is usually put into the top of the reservoir, to form a gas cap. The gas injection can be a very effective recovery method in reservoirs where the oil can flow freely to the bottom by gravity.

An even more widely practiced secondary recovery method is waterflooding. After being treated to remove any material that might interfere with its movement in the reservoir, water is injected through some of the wells in an oil field. It then moves through the formation, pushing oil toward the remaining production wells. The wells to be used for injecting water are usually located in a pattern that will best push oil toward the production wells. Water injection often increases oil recovery to twice that expected from primary means alone. [5] This thesis focuses on secondary oil recovery using water flooding.

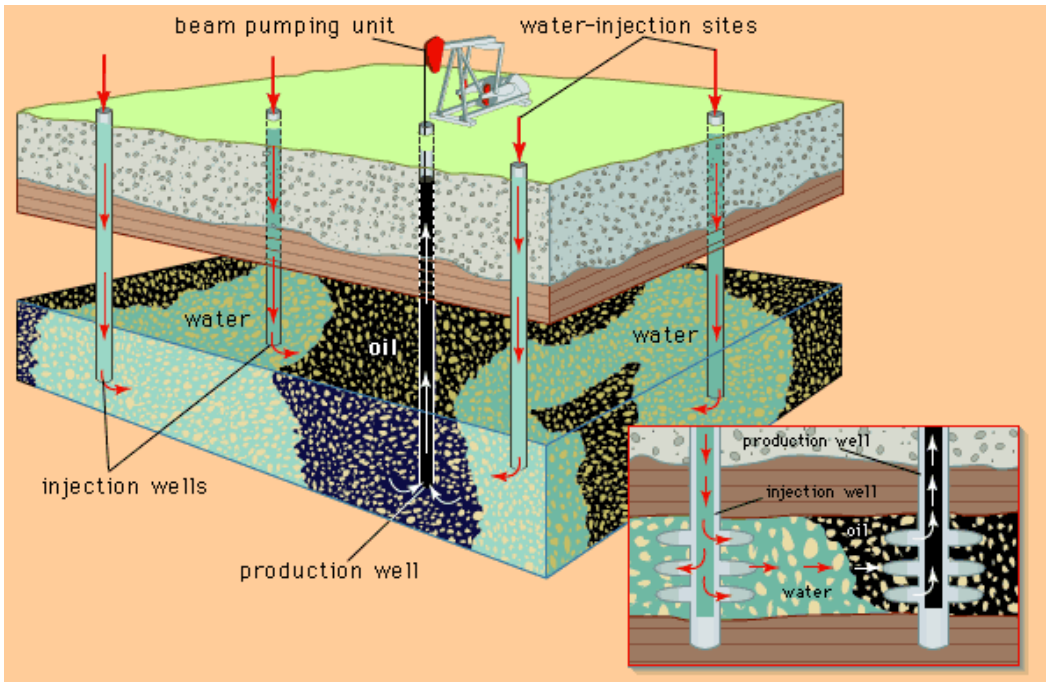

Figure 1.3: Waterflooding technique for oil production. [5]

To achieve cost-effective and efficient oil recovery it is necessary to maximize the well-reservoir contact, and this is achieved using long horizontal wells. Although, this method has its challenges. Due to the heel-toe effect and heterogeneity along with the horizontal wells, early gas and/or water breakthrough is obtained. To tackle this problem, advanced wells are widely used today. Advanced wells are horizontal wells equipped with downhole Flow Control Devices (FCDs), sand screens, zonal isolation as well as monitoring and control systems, etc. FCDs are the key elements of advanced wells. The main types of such devices are passive Inflow Control Devices (ICDs), Autonomous Inflow Control Devices (AICDs), Autonomous Inflow Control Valves (AICVs), and Interval Control Valves (ICVs). To achieve a successful

design of advanced wells, a suitable dynamic model of oil field and advanced wells must be developed. Generally, it is difficult to observe and understand the dynamics of fluid flow in a porous medium and this is one of the main barriers to developing such dynamic models. Also, it is not possible to measure all the parameters that influence the multiphase flow behavior inside a reservoir. Consequently, predicting how a reservoir will produce over time and respond to a different drive and displacement mechanisms. [4]

1.3 Objective

The main objective of this thesis is modeling and simulation of secondary oil recovery with water flooding from a heterogeneous reservoir through advanced wells completed by main types of FCDs. PETREL is commercial software developed by Schlumberger and is used to develop the simulation model.

1. Literature study
   • reservoir rock and fluid properties
   • Improved oil recovery by water flooding
   • Advanced wells
2. Developing the simulation models model using PETREL.
3. Modeling and implementing advanced wells completed by ICDs, AICDs, and AICVs, in Petrel.
4. If time permits, preparing a paper based on the results for the next SIMS conference is highly appreciated.

1.4 Thesis Outline

There is 7 chapter in this thesis. The first chapter focuses on discussing the background of oil production and the problem that this thesis is looking to solve along with the objectives of the thesis. Chapter 2 focuses on the literature review where the previous work in this field is studied which is helpful to meet the objectives of this thesis which includes the study of the water flooding, horizontal wells, and the advanced wells. Chapter 3 continues discussing the necessary theory in the field of petroleum engineering which is crucial to understanding the thesis. Which also includes solving mathematical models for different flow control devices. The simulation software used for the reservoir modeling is Petrel and the next chapter which is the Reservoir Model focuses on different aspects of the reservoir model in Petrel which are the geological model, flow model, well model, and such. At last, the results of the simulation are presented with a detailed discussion of the results in the discussion chapter.

2 Literature Review

2.1 Water flooding

Waterflooding is the most widely used fluid injection process in the world today. Since 1880 it has been recognized that injecting water into the reservoir in certain formations has the potential to improve oil recovery. Although, the current boom in waterflooding begins only in the 1950s. Water injection carried out at a time when the reservoir pressure is at a high level is frequently referred to as a pressure maintenance project. While, if water injection commences at a time when reservoir pressure has declined to a low level due to primary depletion, the injection process is usually referred to as a waterflood. [6] See Figure 1.2 in the introduction chapter.

2.1.1 Water flooding pattern

Many older fields were built with irregular well spacing, improved reservoir mechanics, and conservation principles which have resulted in more uniform well spacing and drilling patterns in recent years. A field is usually completely established when a waterflood begins. Because infill wells are costly to dig and equip, we'll have to make do with the existing well patterns. As a result, a field should be developed on a design that will allow for increased recovery operations in the future. As a result, an awareness of the most typical flood patterns is required. [6]

2.1.1.1 Direct line drive

As previously stated, the only way to achieve a 100% areal sweep at the time of breakthrough is to inject fluid throughout the whole vertical plane. This is not physically viable, but it can be approximated with a layout in which the production and injection wells are directly offset. As the d/a ratio grows, the sweep efficiency of this design improves, where d is the distance between adjacent rows of producers and injectors and a is the distance between adjacent wells in a row as shown in figure 2.1. [6]

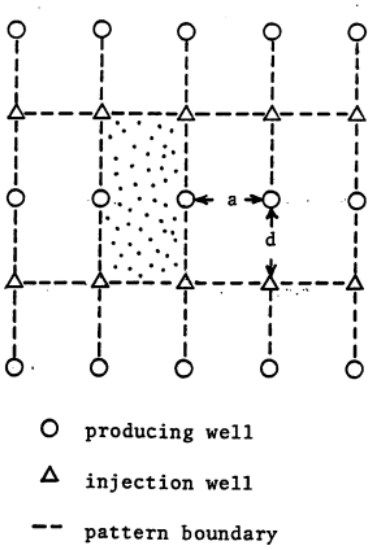

Figure 2.1: Direct inline drive pattern [6]

2.1.1.2 Staggered line drive

As shown in Figure 2.2. The staggered line drive is just a variant of the direct line drive in which rows of producing and injection wells are relocated one-half the inter-well distance between them. This staggering has the effect of greatly increasing breakthrough efficiency when compared to direct line driving, especially for low d/a ratios, as illustrated by the graph in Figure 2.3. As a result, this flood pattern is preferred to the direct line drive if the development pattern allows it. [6]

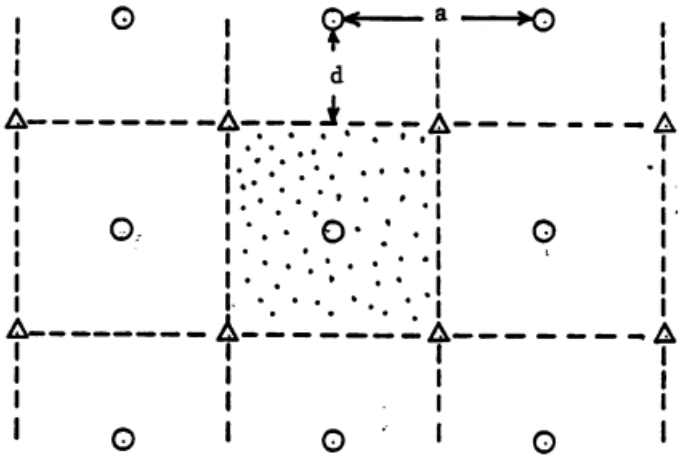

Figure 2.2: Staggered line drive [6]

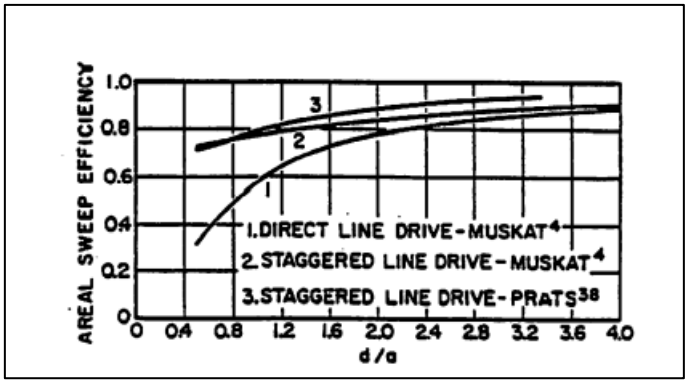

Figure 2.3: Flooding efficiency of direct line (1) and staggered line drive (2 and 3) well networks as a function of d/a. At a mobility ratio of 1. [6]

2.2 Horizontal wells

Horizontal wells are wells that extend horizontally across a reservoir to recover oil. Horizontal wells are divided into two sections: vertical depth and horizontal depth (wellbore). In the horizontal segment, oil flows from the reservoir to the well. The first part of the horizontal section is the heel and the end part is the toe as shown in Figure 2.4. Statoil Company's longest horizontal well in the Statfjord field had a horizontal extension of 7288 meters and a true vertical depth of 2788 meters. [7]

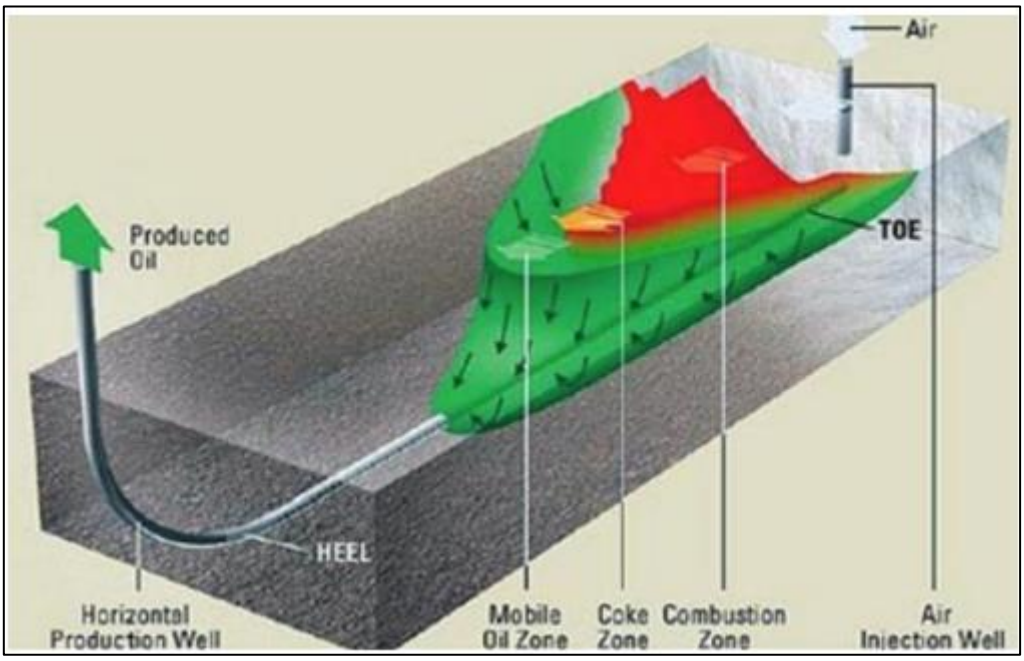

Figure 2.4: Representation of horizontal well. [7]

The advantage of a horizontal well is that it covers a larger area of the reservoir than vertical wells, hence boosting productivity. According to research conducted in Troll Field, the horizontal well's productivity index (J) was 40 times that of the vertical well's productivity index. Horizontal wells also have the advantage of retrieving oil from the field faster, at a lower cost, and with greater efficiency than vertical wells. They also give higher oil recovery from the reservoir, fewer surface disturbances because fewer wellheads may be required, and lower operational costs because fewer wells would be employed. [7]

2.2.1 Heterogeneity in Horizontal well

Figure 2.5 illustrates the impacts that occur in the heterogeneous reservoir. The heterogeneous reservoir is divided into zones, each with its own set of characteristics, including permeability. Different oil inflow in the wellbore can result in early water breakthrough to the zone with high permeability. As a result, total production will originate from select zones with high permeability while oil production to zones with poor permeability will be hindered, resulting in lower overall oil recovery. When the heterogeneous reservoir is influenced by both the heterogeneity and heel-to-toe effects, the heterogeneity effect takes precedence. [7]

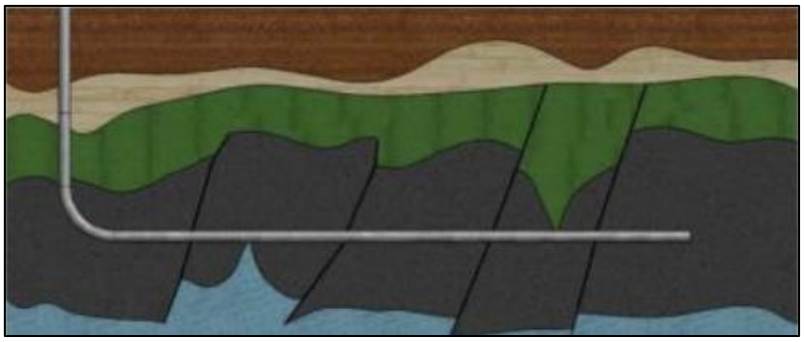

Figure 2.5: Breakthrough of oil and gas in the heterogeneous reservoir. [8]

ICDs help in attaining uniform fluid influx into the wellbore by increasing the pressure drop in the higher permeability zones. Installation of ICDs increases the overall oil recovery. See figure 2.6. [7]

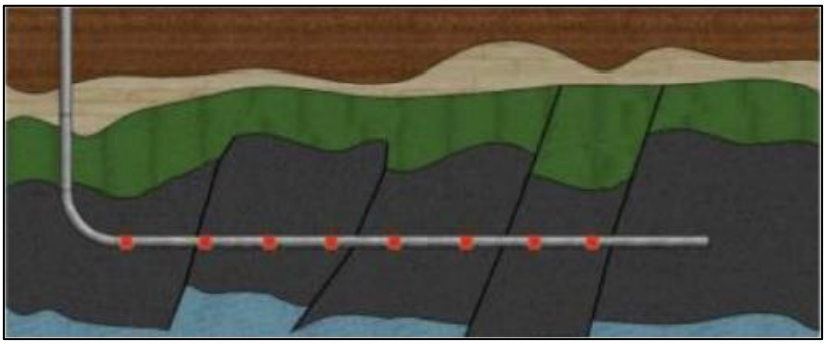

Figure 2.6: Uniform inflow profile after installation of ICD in heterogeneous reservoir [8]

2.2.2 Hill-toe effect

Friction pressure drop along the wellbore causes changes in inflow rates between the heel and toe of the horizontal well, which are caused by friction pressure drop along the wellbore. As demonstrated in figure 2.7, the difference in inflow rates between the heel and the toe might produce earlier water or gas (or both) breakthrough in the wellbore. Figure 2.7 represents a horizontal well perforating an oil reservoir with a gas cap at the top (red color) and an aquifer at the bottom (blue color). Due to higher pressure losses in the wellbore, the inflow rate at the heel will be higher than at the toe, causing WOC to move faster in the heel and, as a result, earlier water or gas breakthrough is obtained which hinders the oil production. [7]

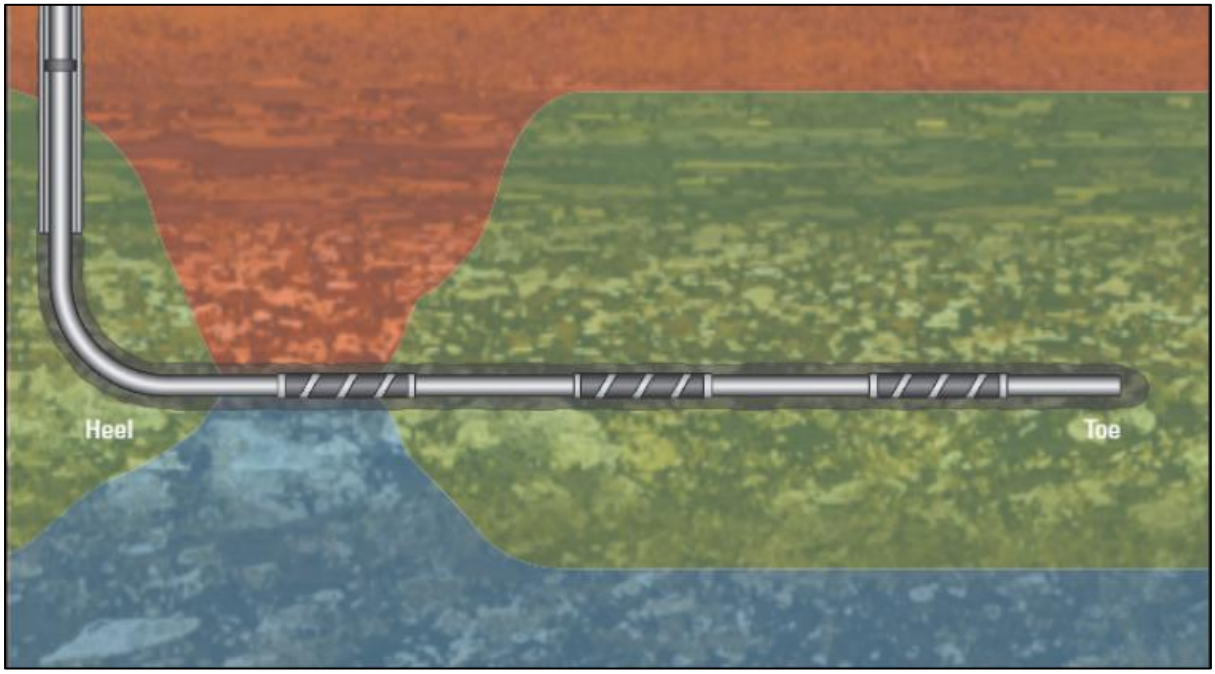

Figure 2.7: Hill toe effect in a horizontal well. [9]

The cumulative oil recovery increases as the horizontal well length increases, but due to the heel-to-toe effect, it will eventually reach a length where cumulative oil output stops increasing, as shown in Figures 2-8. The permeability of the reservoir, the viscosity of the fluid, the wellbore diameter, and the drawdown pressure all have a role in the cumulative oil output with good length, as illustrated in Figure 2.8 for the different permeability scenario. [7]

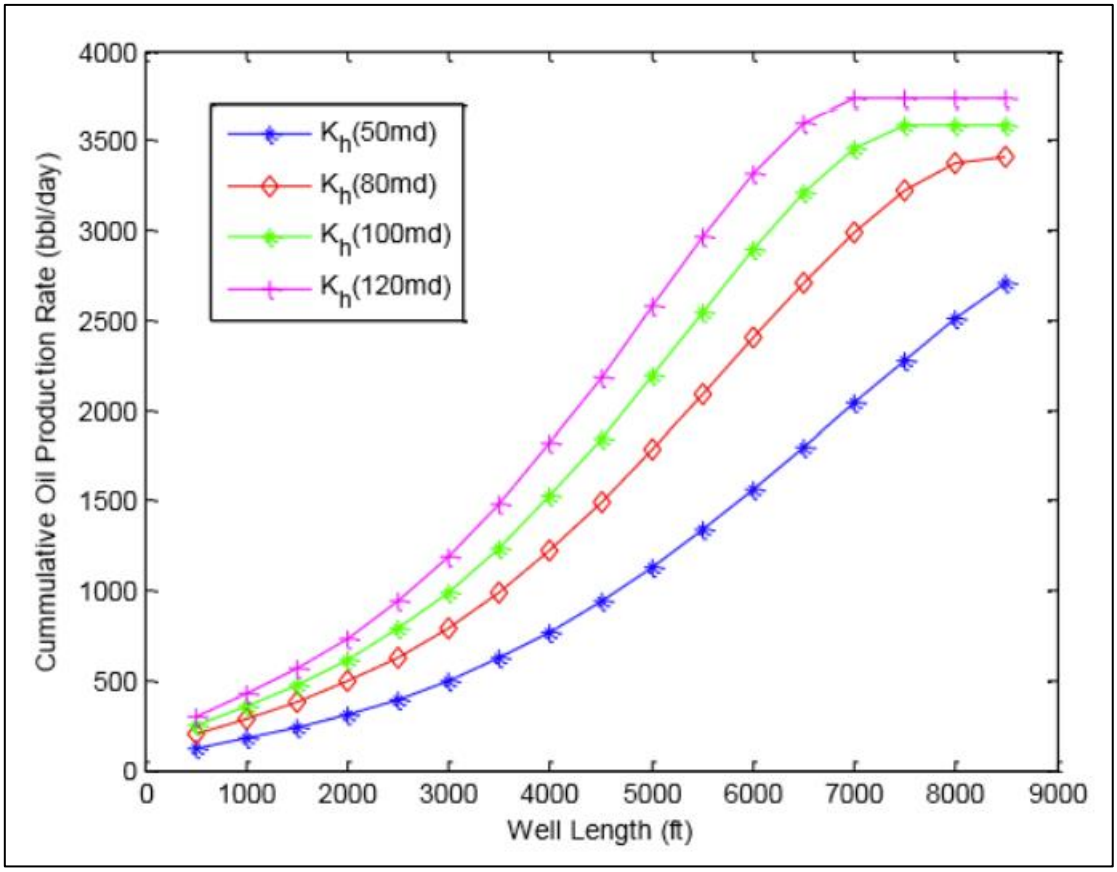

Figure 2.8: The variation of cumulative oil production with the Well length [7]

2.3 Inflow Control Devices

ICDs are devices that are installed in a horizontal well to address the problem of excessive gas, water, or both production that is caused by water/gas breakout, as well as a screen to reduce excessive sand production. As shown in Figure 2.9, the ICDs create fluid restriction or friction as it passes through the channel, nozzle, or orifice, where fluid from the annulus represented by the red arrow flows to the orifice and finally to the production pipe. The fluid pressure drops due to the limiting of fluid delivered by ICDs. ICDs are inserted in well segments with lower pressure drops to add extra pressure drops, balance pressure drops across the wellbore, and finally equalize the inflow along the wellbore. [7]

Because of their inactive flow control nature, ICDs are also known as Passive Flow Control devices. If the type of fluid flowing through the ICD limitation changes, the pressure drop through the ICD will change. However, after the device is put in the wellbore, the ICD restriction cannot be changed. ICDs cannot actively change the volume of fluid produced once an unwanted fluid has congealed at the completion joint. ICDs are therefore termed passive FCDs since they are placed early in the well's life cycle and manage the well's inflow profile before water and/or gas breakout. [10]

An ICD turbulent flow regime results in a quadratic relationship between velocity and pressure drop, which makes ICDs efficient in reducing gas generation. Because the pressure decrease is

related to the square of velocity, gas moving through the ICDs has stronger restrictions than oil or water. [7]

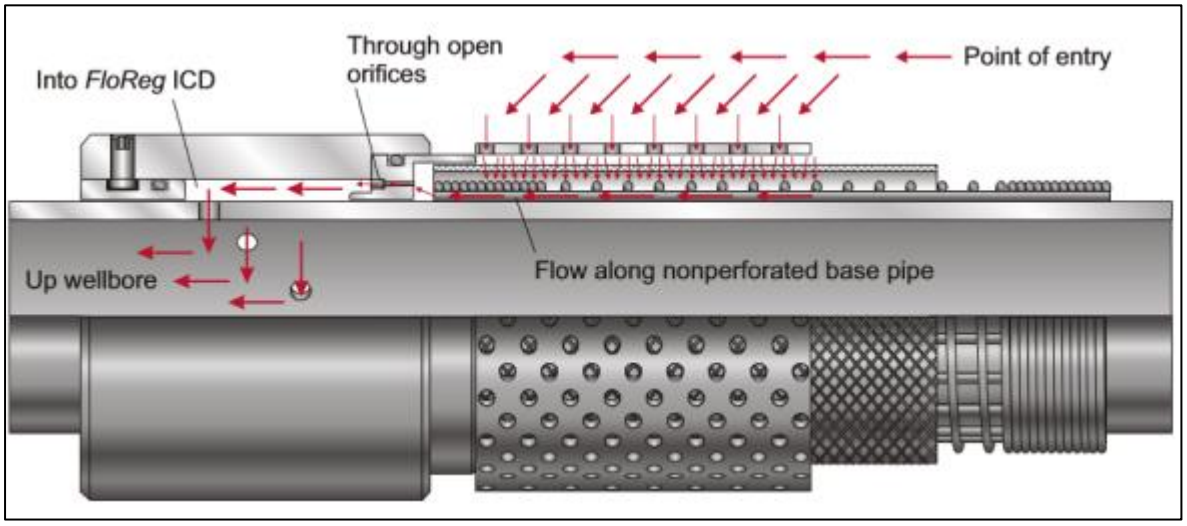

Figure 2.9: Schematic diagram of orifice ICD. [7]

2.3.1 Channel-type (Helical channel) ICD

The ICD shown in Figure 2.10 is a channel-type ICD that generates a pressure drop by using surface friction. The fluid passes through the channel type ICD by traveling via a predetermined length of the channel, then through the opening, and finally into the wellbore. The length of the channel and the diameter of the opening determine the pressure drop in channel-type ICDs. When the fluid passes through these ICDs, it will change direction, causing the pressure loss to be dispersed over a longer channel path. This type of ICD is designed to be long usually 120 inches. enough to provide enough pressure drop. [7]

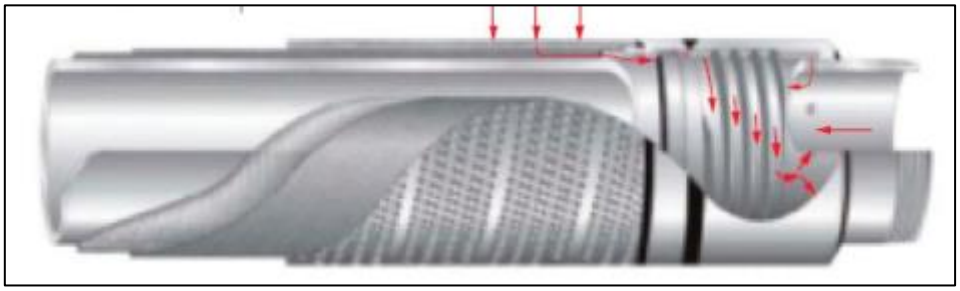

Figure 2.10: Helical channel type ICD. [7]

The performance of channel type ICDs is explained by Poiseuille's law, where the pressure drops of fluid passing through the channel type ICD are proportional to fluid viscosity and velocity as it is shown in Poiseuille's equation. See equation(2.1)

$$\Delta P = \frac{128 \times \mu \times L \times Q}{\pi \times d^4} \tag{2.1}$$

2.3.2 Orifice/Nozzle type ICD

Figure 2.11 shows nozzle-type ICDs that enable fluid limitation to achieve the desired pressure drop. To induce flow resistance, fluid is pushed to pass through small openings (orifices) in a pipe. The pressure drop is caused by the flow resistance that is created. As described by the equation (2.2), these ICDs are sensitive to the density and square of the velocity of the fluid moving through the ICD. [7]

$$\Delta P = \frac{\rho \times v^2}{2} \tag{2.2}$$

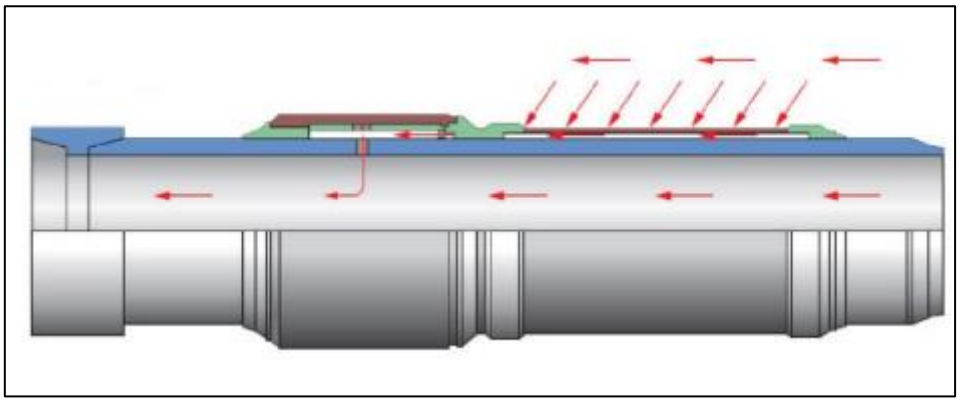

Figure 2.11: Nozzle type ICD. [7]

The advantage of an orifice/nozzle type ICD is that it is easy to construct and may be employed in a reservoir with a wide difference in viscosity between water and oil. It can easily choke water because the pressure drop is independent of viscosity. However, nozzle-type ICDs are dependent on fluid velocity, making them more susceptible to sand particle erosion and less resistant to plugging. [7]

2.4 Autonomous Inflow Control Device (AICD)

After nearly a decade of ICD application, Hydro and Easywell Solutions launched this "Advanced" type of ICDs, which coincided with the development of Inflow Control Valves (ICVs) for intelligent wells. When the water or gas influxes, which has a different density of the fluid mixture, the AICD is triggered by changes in the fluid properties. The device is autonomous and does not require any human or other interaction. The AICD concept was created to address the problem of localized water influx in the North Sea fields of Grane and

Brage, as well as to aid in the control of gas-cap gas ingress in the "thin oil column" area of the Troll field. [10]

The function of AICD is based on the Bernoulli principle by neglecting elevation and compressible effect. And it is expressed by the following equation(2.3). [11]

$$P_1 + \frac{1}{2}\rho V_1^2 = P_2 + \frac{1}{2}\rho V_2^2 + \Delta P_{friction\ loss} \tag{2.3}$$

Where, P_1 is the static pressure, $\frac{1}{2}\rho V_1^2$ is the dynamic pressure, and $\Delta P_{friction\ loss}$ is the frictional pressure loss. This equation states that the static pressure, the dynamic pressure, and the frictional pressure losses along the streamline are constant. [11]

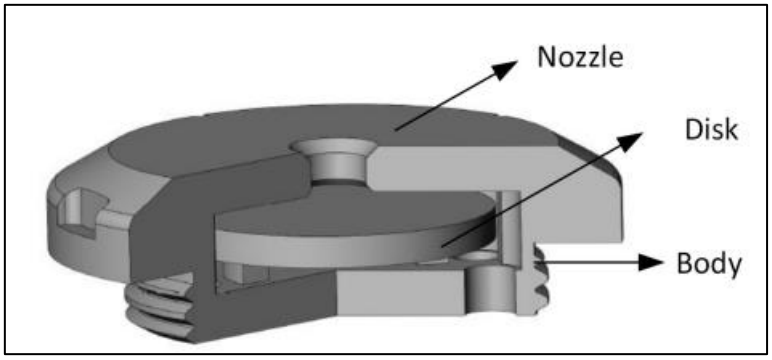

Figure 2.12: AICD design [11]

The AICD is the part of the sand screen joint. The fluids from the reservoir enter the completion through the sand screen filter and flow along the annulus and into the AICD as represented by the red arrows in Figure 2.13. The fluids further flow into the production tubing and then to the surface along with the flow from other AICDs. [11]

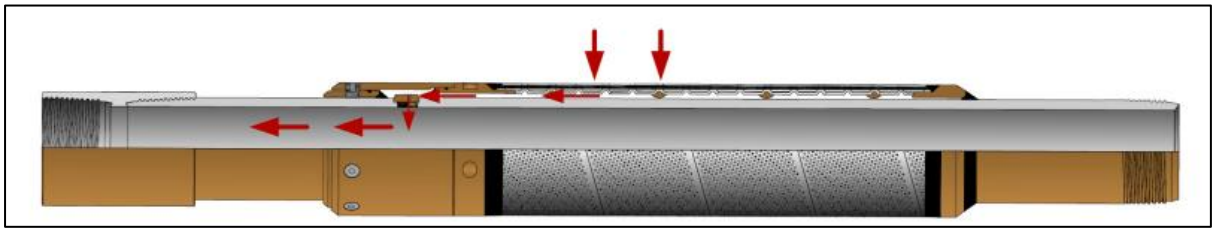

Figure 2.13: AICD flow path and operation. [11]

2.5 Autonomous Inflow Control Valve (AICV)

For high viscous fluids, the AICV opens, while for low viscous fluids, it closes. The functionality is regulated via a minor pilot flow line that runs parallel to the main flow path and carries about 2-5% of the overall flow rate. The minor pilot flow represents the total flow rate through the valve when it is closed. [12]

Figure 2.14 shows the pressure profile in the pilot flow path, with expected pressure at various points along the pilot flow path for oil, water, and gas. P2 is low when the pressure drop through the laminar flow element is high, as it is for oil, and the valve is fully open, producing oil. Low viscous fluids, such as gas/steam, have a lower pressure drop through the laminar restrictor, resulting in a larger P2. The piston will be actuated by the high pressure, which will close the valve. A piston position that restricts or closes low viscosity fluids such as gas/steam is necessary for gas/steam and water choking or shutoff applications. This is accomplished by altering the LFE, TFE, and valve flow areas, resulting in varying P2 pressure, different valve piston positions, and consequently, different net forces acting on the piston. As a result, by adjusting various parts of AICV as in Figure 2.15, oil production can be easily adjusted. [12]

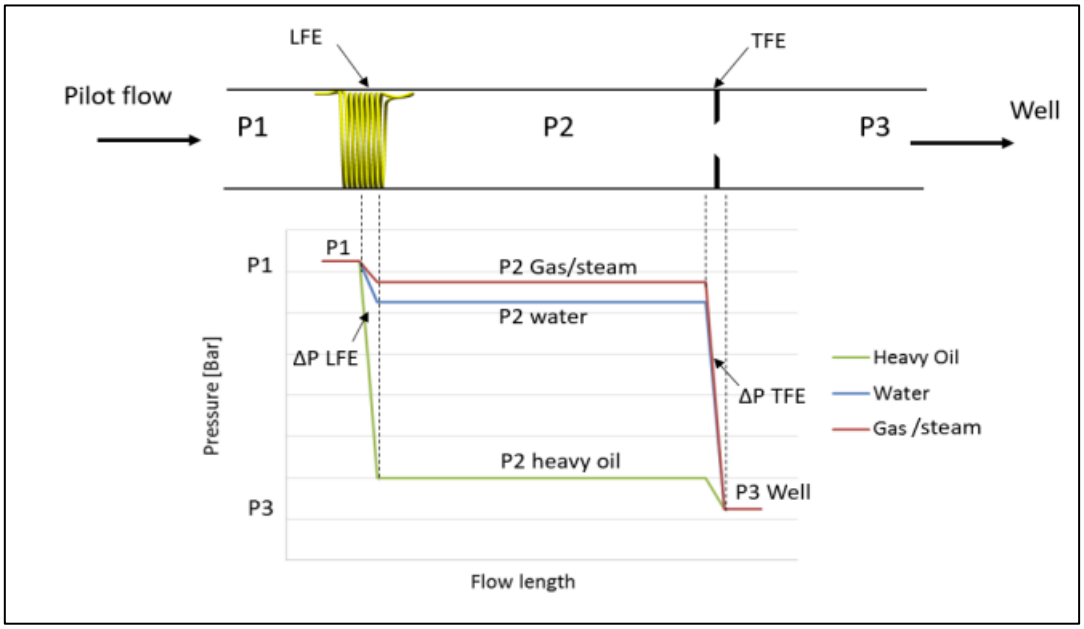

Figure 2.14: AICV pressures. [12]

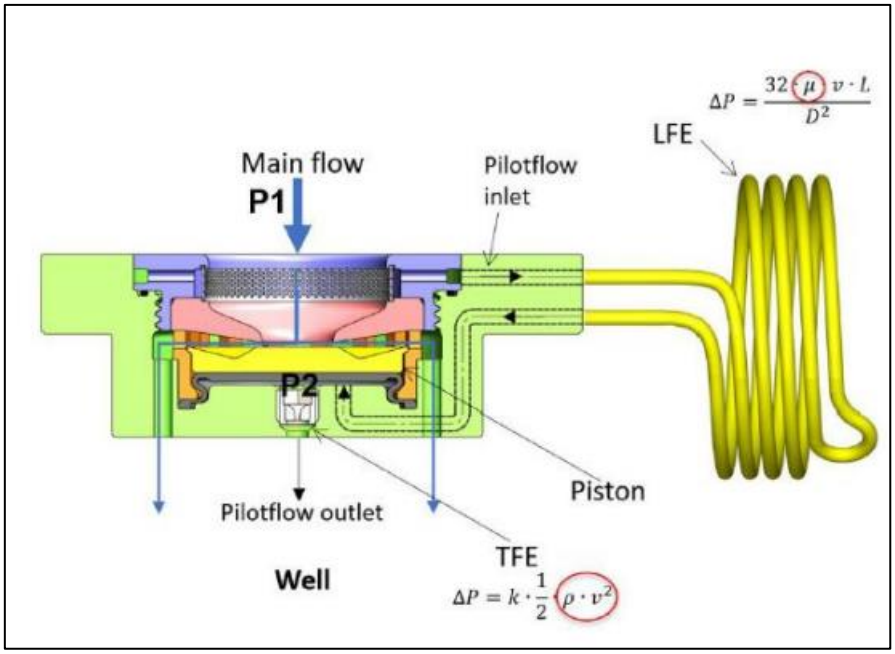

Figure 2.15: AICV components. [12]

2.6 Multi-segmenting

In the standard well model, instantaneous flow inside the well is assumed hence the pressure drop is always hydrostatic. [13] Therefore, the standard well model cannot be used to model the frictional pressure losses, acceleration pressure loss, and pressure drop across the flow control device. To overcome the shortcomings of the standard well model when it deviated to horizontal wells, a more rigorous well model is used which is a multi-segment well model. In this model well is divided into multiple segments. [14] The appropriate number of segments depends on the desired accuracy of the well being modeled. A separate segment can be created for each grid block in which the well is completed. [15] As shown in Figure 2.16 where ICDs are included in individual segments.

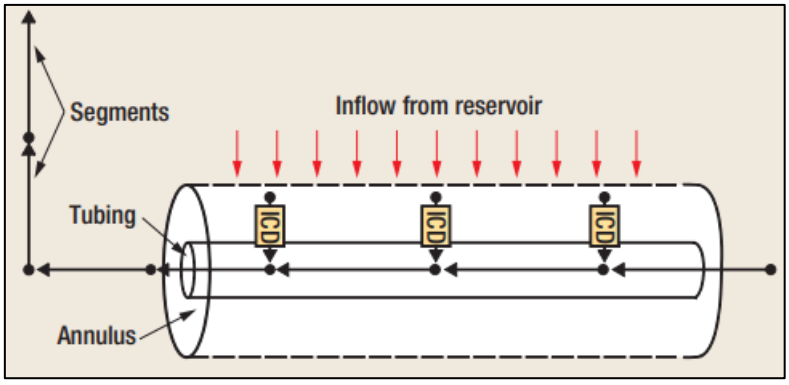

Figure 2.16: ICDs implemented in multisegmented model as individual segments. [16]

Muti-segment well analysis breaks the well into a series of continuous segments with 0, 1, or more connections to the reservoir grid blocks. Each segment will consist of four equations three material balance equations and one pressure drop equation. These equations contain the elements that define hydrostatic, acceleration, and friction effects. These equations are solved pressure, flow rate, and fluid composition in each segment. [16]

The four different primary elements in the well being Q_w, Q_g, Q_o and P. [13] and the well related equations are given in Figure 2.17.

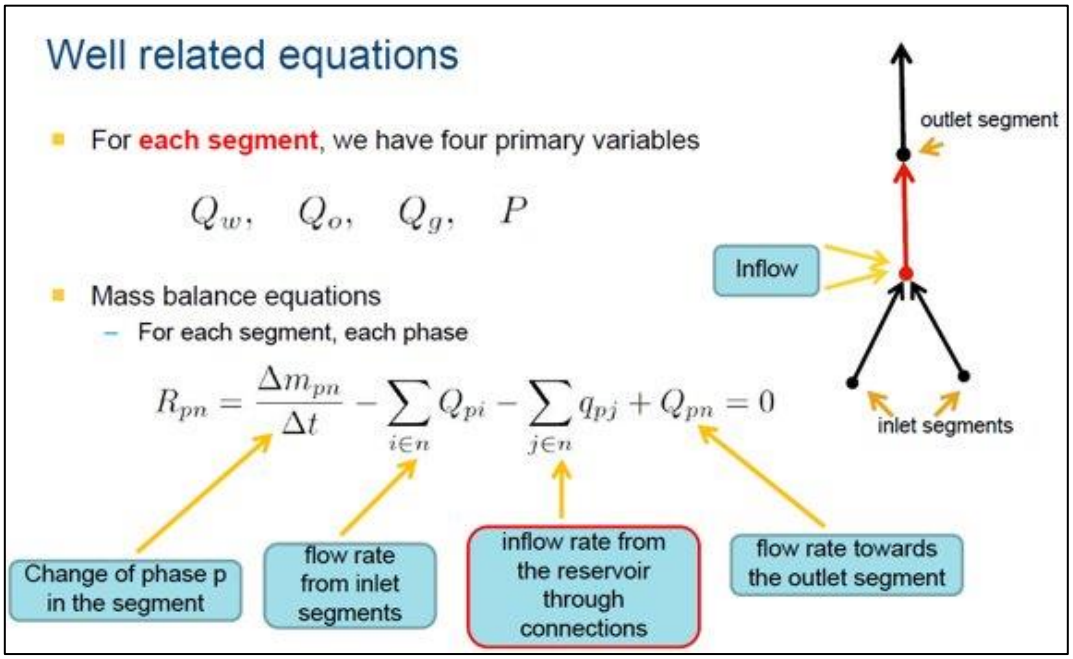

Figure 2.17: Well related equations. [13]

The inflow rate from the reservoir is described by the equation in Figure 2.18.

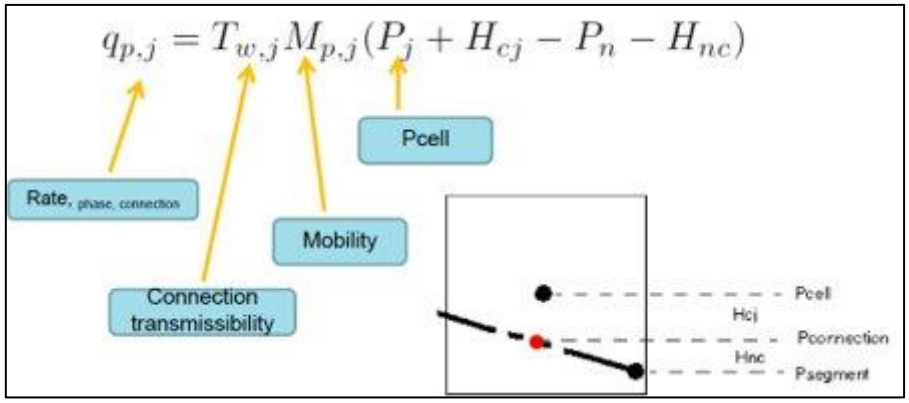

Figure 2.18: Inflow in the segment [13]

The fourth equation which is the pressure equation for each segment defines its pressure drop as a function of the flow rate through its outlet. Applying the steady-state pressure loss relationship gives the equation in Figure 2.19. [15]

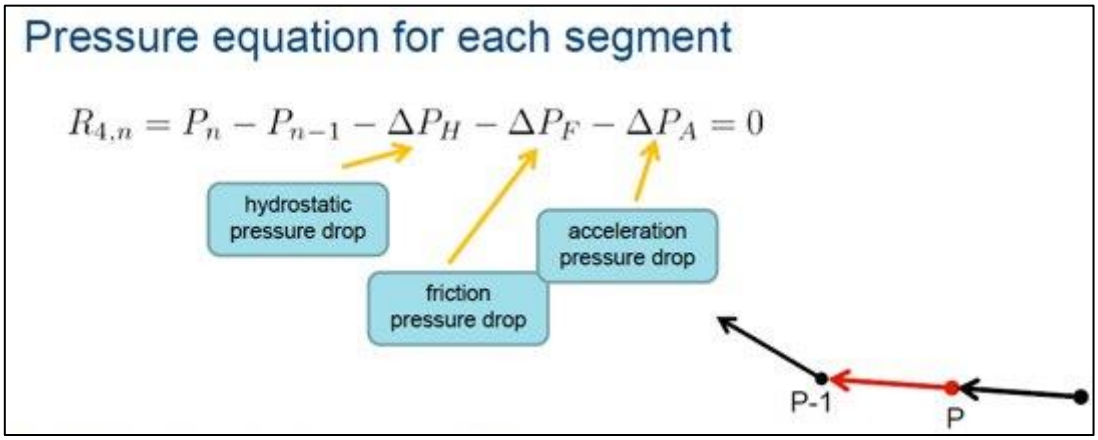

Figure 2.19: Pressure equation for each segment. [13]

3 Theoretical background

3.1 Reservoir Properties

Reservoir rock and fluid properties in the exploration and production of petroleum reservoirs are very important. Therefore, detailed knowledge of reservoir rock and fluid properties is the backbone of almost all exploration and production-related activities such as reservoir engineering, reservoir simulation, well testing, production engineering, enhanced oil recovery (EOR), or improved oil recovery (IOR) methods, and so on. Hence, we will be discussing these properties in this chapter. [17]

3.1.1 Porosity

The petroleum reservoir rocks appear to be solid but are often porous from the inside. The sandstone such as in the figure consists of the sand grain of varying sizes that come together as part of the dispositional process to form the consolidated sandstone rock. These grains in rock have a void space between them which forms the tiny opening in the rock. This opening varies from 20- 200 μm. Hence, just like a sponge soaked in water petroleum reservoir rock stores the fluid in it. And this distinct storage capacity of a reservoir rock is called porosity. Hence, the greater the porosity of rock greater the capacity to store the petroleum fluids.

Figure 3.1: Sandstone sample. [18]

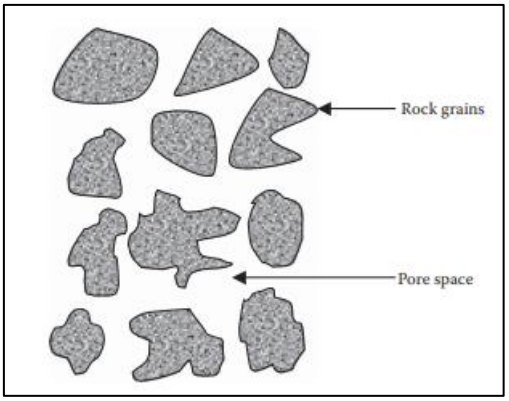

Figure 3.2: Conceptual representation of pore space. [17]

Porosity is denoted by ϕ and is mathematically expressed by the following equation (3.1)

$$\varphi = \frac{Pore\,volume}{Total\,or\,bulk\,volume} \tag{3.1}$$

The pores inside the rock can vary as shown in Figure 3.3 and this leads to the concept of total or absolute porosity.

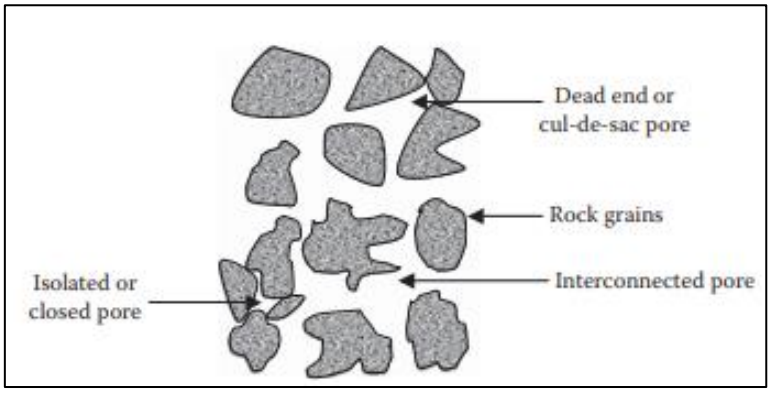

Figure 3.3: Different types of pores. [17]

Total/Absolute Porosity is the ratio of the total void space in the reservoir rock to the total or bulk volume of the rock. And is given by equation (3.2).

$$\varphi = \frac{Volume\,of\ inerconnected\ pores + Volume\,of\ dead\ end\ pores + Volume\,of\ isolated\ pores}{Total\,or\,bulk\,volume} \tag{3.2}$$

Even though a reservoir has very high absolute porosity it is possible that due to a lack of interconnectivity the reservoir fluid remains trapped inside the isolated pores and it becomes unrecoverable. And this leads us to define effective porosity.

Effective porosity is defined as the ratio of the volume of interconnected pores and dead end pores to the total or bulk volume. And is given by equation(3.3).

$$\varphi = \frac{Volume\,of\ interconnected\ pores + Volume\,of\ dead\ end\ pores}{Total\ or\ bulk\ volume} \tag{3.3}$$

3.1.2 Absolute Permeability

If one must compare permeability with the porosity, one can say porosity is the static property of a porous medium while permeability is the dynamic flow property and hence can be only characterized by conducting flow experiments on reservoir rocks. The absolute permeability or simply the permeability can be defined as the ability to flow or transmit the fluids through a rock that is fully saturated with a single-phase fluid. [17]

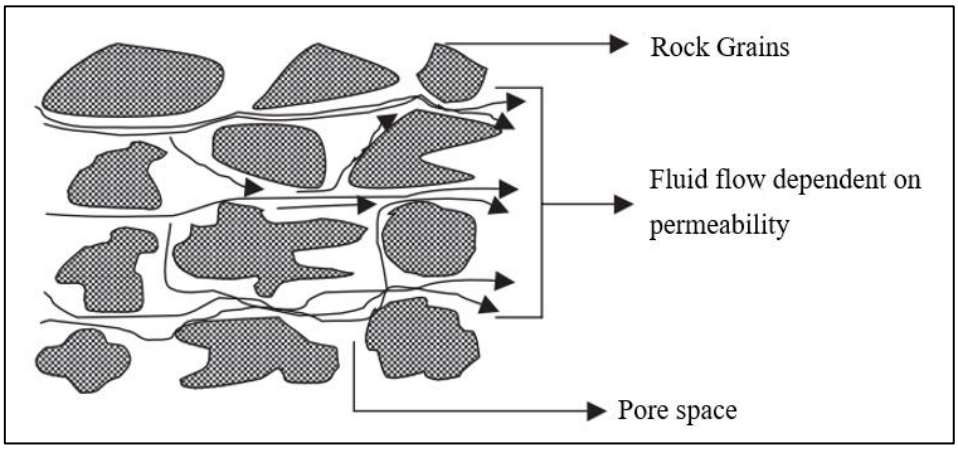

Fig 3.4: Illustration of permeability of a reservoir rock. [17]

Permeability of the porous medium is represented by *k*. Permeability can be mathematically expressed by Darcy's Law.

3.1.2.1 Darcy's Law

It was Henry Darcy, a French civil engineer, who led to the development of mathematical expression which is still used today by the petroleum industry. It allows the calculation of

absolute permeability in the porous medium through flow experiments. [17] Darcy's experiment can be schematically represented in Figure 3.5.

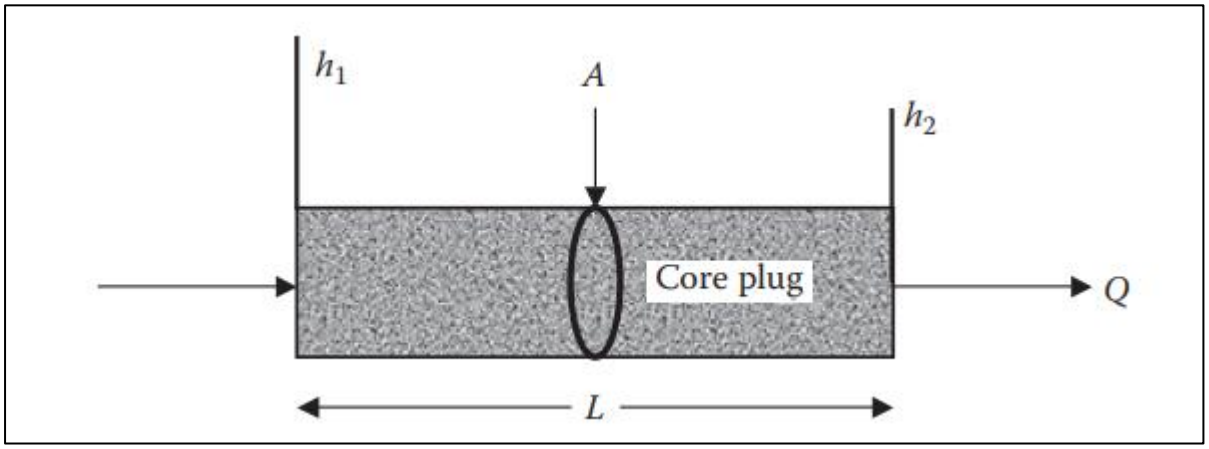

Fig 3.5: Schematic representation of Darcy experiment. [17]

The following equation(3.4) shows the mathematical form of Darcy's flow experiments.

$$Q = KA\frac{(h_1 - h_2)}{L} \tag{3.4}$$

Q is the volumetric flow rate through the core plug (in m^3/s), *K* the proportional constant also defined as hydraulic conductivity (in m/s), A the cross-sectional area of the core plug (in m^2), *L* the length of the core plug (in m or ft), and h_1 and h_2 represent the hydraulic head at inlet and outlet, respectively (in m or ft).

Alternatively, an equation (3.4) can also be expressed in terms of the pressure gradient d*P* over a section d*L* as below.

$$Q = -KA\frac{dP}{dL} \tag{3.5}$$

Where,

$$dP = \Delta h \rho g \tag{3.6}$$

d*P* is the difference between the upstream and downstream pressures (N/m^2), Δh is the difference between the upstream and downstream hydraulic gradients (m), ρ is the fluid density (kg/m^3), and g is the acceleration due to gravity (9.81 m/s^2).

To generalize the equation(3.5) to other fluids, viscosity μ of a given fluid can be incorporated such that *K* is expressed as a ratio of *k*/μ, where. Hence equation(3.5) can be written as an equation(3.7)

$$Q = -\frac{k}{\mu} A \frac{dP}{dL} \tag{3.7}$$

In petroleum reservoir applications, the above equation has to be converted for the radial flow. To do this d*L* in the above equation(3.7) is replaced by the d*r*. Also, area A becomes $2\pi rh$. This gives the below equation(3.8).

$$Q = \frac{k}{\mu} A \frac{dP}{dr} \tag{3.8}$$

In SI unit permeability is measured in m^2. However, given it's a porous medium the value in m^2 can increase to a very high number. Therefore, petroleum industry introduced the unit 'darcy'. [17]

A porous medium is said to have a permeability of one darcy when a single-phase fluid having a viscosity of one centipoise (cP) completely saturates the porous medium and flows through it at a rate of 1 cm^3/s under a viscous flow regime and a pressure gradient of 1 atm/s through a cross-sectional area of 1 cm^2. [17]

$$1 \text{ darcy } = 1\text{D} = \frac{(\text{cm}^3/\text{s})(\text{cP})}{(\text{cm}^2)(\text{atm/cm})}$$

Substituting, the value of 1cP as $1.0 \times 10^{-7}\text{Ns/cm}^2$ and 1atm as 10.1325N/cm^2

$$\begin{aligned} 1\text{D} &= 9.869 \times 10^{-9}\text{cm}^2 \\ &= 9.869 \times 10^{-13}\text{m}^2 \end{aligned}$$

Further, to avoid the use of fractions in describing permeability, the term millidarcy (mD) is used.

$$1\text{mD} = 0.001\text{D}$$

3.1.3 Effective Permeability

Effective permeability is different than absolute permeability in a way that it is applicable when more than one fluid is present in the porous medium. Effective permeability is the permeability to water, oil, or gas (k_w, k_o, k_g) when more than one phase is present. The effective permeability of a phase is dependent on fluid saturation. Effective permeability is used to determine the production (q_o or q_w) or injection (i_w) rates using Darcy's Law. Effective permeability to oil and water is important in waterflood analysis. [6]

Effective Permeability is denoted as k_e and the unit is the same as absolute permeability which is mD or D

3.1.4 Relative Permeability

In a reservoir, there are two or sometimes three phases are present, that is oil, water, and sometimes gas. Hence, due to interaction with other phases, one would expect the permeability of either fluid to be lower than that of the single fluid since it occupies only part of the pore space. This situation is addressed by the concept of relative permeability. [19]

The relative permeability to oil is given as See equation (3.9).

$$k_{ro} = \frac{k_{eo}}{k} = \frac{effective\,oil\ permeability}{base\ permeability} \tag{3.9}$$

Similarly, the relative permeability of water is given as. See equation (3.10).

$$k_{rw} = \frac{k_{ew}}{k} = \frac{effective\,water\ permeability}{base\ permeability} \tag{3.10}$$

When a porous medium saturated with more than one fluid phase is considered, for instance, an oil-water system, the saturations may vary from, for example, 20% oil and 80% water to 80% oil and 20% water. Therefore, multiple values of relative permeability exist, with respect to a given saturation value. And hence, relative permeability is plotted as k_r values at different saturations for a given fluid phase, for example, as different k_{ro} values at oil saturations of 40%, 50%, 60%, and so forth. [17]

3.1.4.1 Effect of Wettability on relative permeability.

Wettability affects the fluid distribution inside the reservoir rock and, thus, has a very significant effect on relative permeability. Figure 3.4 compares data for water-wet and oil-wet systems. [6]

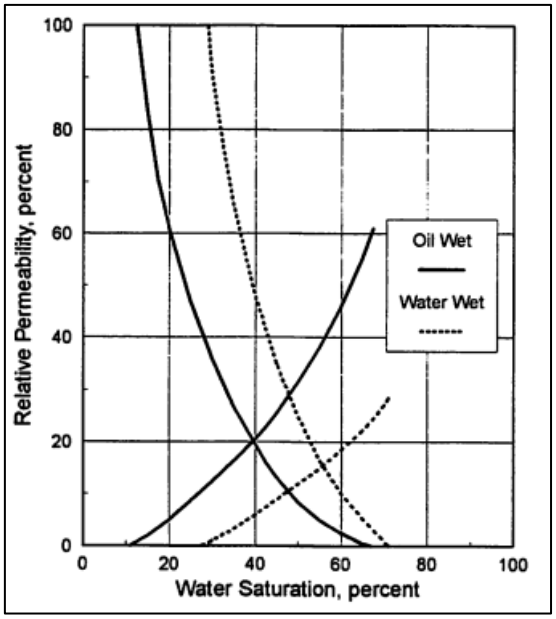

Figure 3.4: Effect of wettability on relative permeability data. [6]

a. In the water-wet system, the water saturation at which oil and water permeabilities are equal (intersection of two curves) is usually greater than 50% while it is less than 50% for the oil-wet system. [6]
b. For the water-wet system, the connate water saturation is usually greater than 20%. While, for oil-wet systems, it usually is less than 15%. [6]
c. For water-wet systems, the relative permeability to water at maximum water saturation (residual oil saturation) will be less than about 0.3 but for the oil-wet system, it will be greater than 0.5. [6]

   Most of the time the reservoirs can be at an intermediate wettability state and in such cases, the above observations may not hold to be true. Nevertheless, Figure 3.4 gives an indication of the wettability of a reservoir for moderate to low levels of permeability. (100mD) [6]

3.1.5 Wettability

In a reservoir, wettability can be defined as the tendency of a fluid to preferentially adhere to, or wet, the surface of a rock in the presence of other immiscible fluids. In the waterflooding case, the wetting phases can be oil or water. In the case of water-wet rock, water occupies the small pores and contacts the rock surface in the large pores while the oil is in the middle of the large pores. On the other hand, an oil-wet system is partially different from the water-wet system in a way that, the water usually continues to fill the very small pores but oil contacts most of the rock surface in the large pores. The water in the middle of the large pores does not contact the large pore throat surface and is usually present in small amounts. The reason oil does not enter the small pores in the oil-wet system is due to capillary forces and hence, the wettability of the small pores does not change. [6]

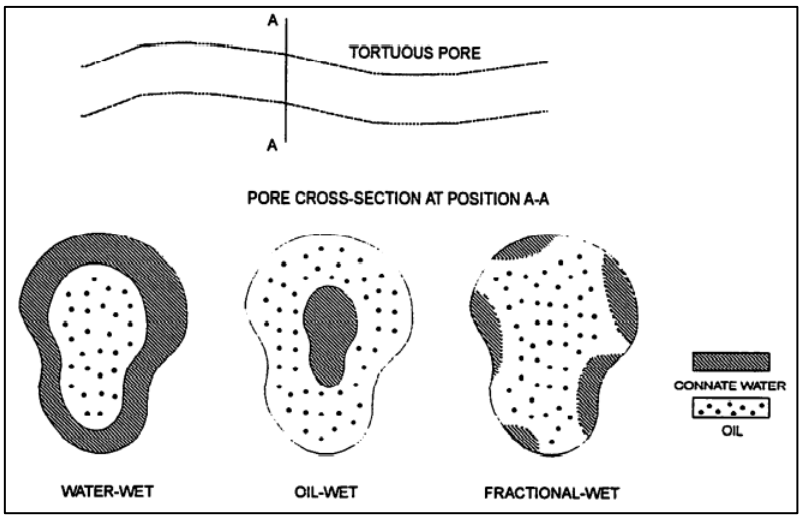

Fig: plane view, cross-section view, and fluid distribution in a hypothetical water-wet, oil-wet, and fractional-wet pore [6]

Wettability is not a parameter that is used directly in the computation of waterflood performance. However, wettability can have a significant impact on parameters such as relative permeability, connate water saturation, capillary pressure, and residual oil saturation which directly affect waterflood performance. [6]

3.1.6 Capillary Pressure

Reservoir rock typically contains oil, water, and gas which are at the immiscible phases. The capillary forces are the forces that hold these fluids in equilibrium with each other. During waterflooding, these forces and the frictional force may resist the flow of oil. Therefore, it is the point of interest to understand the nature of these capillary forces. [20]

Capillary pressure is the pressure difference existing across the interface separating two immiscible fluids. [20]

If the wettability of the system is known, then the capillary is defined as the difference between the pressures in the non-wetting and wetting phases. See Equation (3.11) [20]

$$P_c = P_{nw} - P_w \tag{3.11}$$

Hence, for the water wet system,

$$P_c = P_o - P_w \tag{3.12}$$

3.2 Models and Calculation

3.2.1 The horizontal well production mechanism

The flow related to oil production is pressure-driven. This means that flow goes from high pressure (toe) to low pressure (heel). The higher the pressure drop from the reservoir to the production well, the higher the flow rates from the reservoir to the well. However, the fluids in the production will need to be transported to the surface. Thus, the higher the pressure drops from the production pipe to the surface, the higher the flow rate to the surface. But, if the production well pressure is too low, we may have high production from the reservoir, but not sufficient pressure to lift and produce oil on the surface. Hence, the pressure in the production well must satisfy these two requirements. The pressure in the production well must overcome the hydrostatic pressure from the weight of the petroleum fluids in the pipes towards the surface, as well as the pressure drop due to friction, and possible pressure variations due to acceleration of the fluids. To counter these pressures, it is required to maintain the pressure at the heel of the production pipe. This pressure will be controlled by manipulating a choke valve at the surface which governs the rate of production from the well. Also, the bottom hole pressure at the heel must be above a certain value, but not be too high, as this may block efficient production by damaging the formation in the reservoir. Typically, the pressure drop from the reservoir to the heel of the production pipe is in the order of 10–20 bar. [21]

When a well is producing oil from the reservoir, the bottom hole pressure (Pwf) can be found by the Inflow Performance Relationship (IPR) equation (3.13), where P_{r} is the reservoir pressure, J is the productivity index and q_o is the flowing rate at surface conditions, the equation is expressed in SI units. [22]

$$P_{wf} = P_r - \frac{1}{J} q_o \tag{3.13}$$

The resistance of the fluid flow depends on the rate of the fluid flow and a productivity index (J). The high fluid rate causes higher pressure to drop in the reservoir, further causing much higher energy loss when the reservoir is produced at higher rates. Higher J will result in a lower pressure drop and hence lower energy losses in the reservoir. [22]

The productivity index (J) depends on the fluid and reservoir properties such as viscosity, permeability, formation volume factor, and geometry of the reservoir. The productivity index is inversely proportional to viscosity and directly proportional to the permeability, hence an increase in permeability of reservoir rock increases the fluid productivity and reduces the loss in pressure, on the other hand, an increase in fluid viscosity reduces the productivity index and increases the pressure losses and the vice versa. Since a high permeable zone provides lower pressure loss, the reservoir zones with high permeability produce more fluid than the zone with low permeability. [22]

3.2.2 Modeling of Nozzle ICDs

The Figure 3.5: Flow-through nozzle ICD in well. Figure 3.5 shows the nozzle ICD completion where the fluid path is shown by red arrows. The reservoir fluid flows into the well through the annulus via sand screen and then through the nozzle ICD. As stated in the equation (3.14), when the fluid flows through the small nozzle, the pressure drop is generated as a function of fluid density, viscosity squared, and geometry of ICD. Also, in the case of nozzle ICD, this pressure drop is almost not dependent on the fluid viscosity. The nozzle size and the pressure drop for a specific fluid are set for the nozzle ICD before the installation. [23]

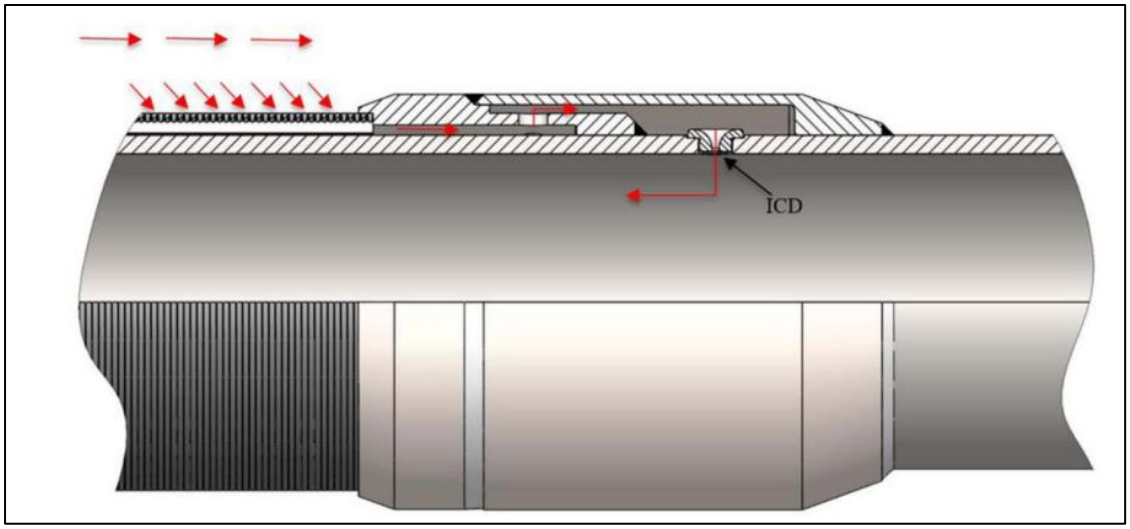

Figure 3.5: Flow-through nozzle ICD in well. [23]

$$\Delta P = C\frac{1}{2}\rho v^2 \tag{3.14}$$

Where,

$$v = \frac{q}{A} \tag{3.15}$$

Here, q is the volume flow rate of oil, gas, or water depending on the fluid being referred. ΔP is the pressure drop. C is the geometrical constant, ρ is the density of fluid referred to, v and is the velocity of the fluid through the nozzle.

Figure 3.6 shows the flow performance curves for oil with a density of 900 kg/m^3, water with a density of 1000 kg/m^3, and gas with a density of kg/m^3 for nozzle ICD. Since the cross-sectional area of the ICD is fixed and due to the density difference of the fluids flowing through it, the flow rate for the gas is significantly higher and for oil and water, there is a slight difference given the density difference is not very significant. [23]

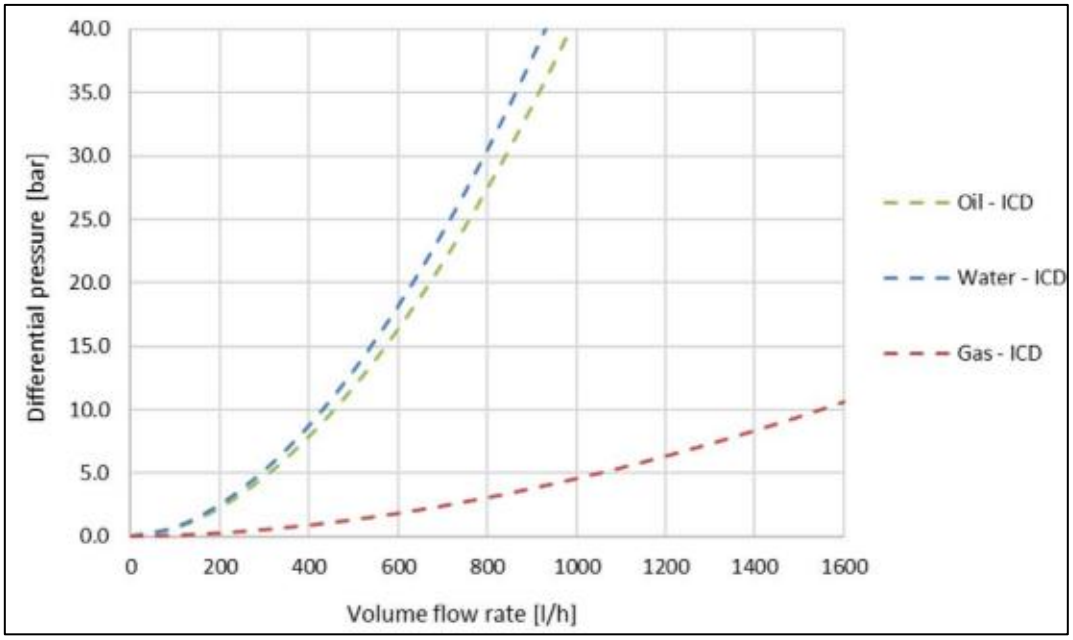

Figure 3.6: Performance curves for nozzle ICD for oil, water, and gas. [23]

3.2.2.1 Calculating the cross-sectional area of the nozzle ICD.

Using the volume flow rate and differential pressure for oil from Figure 3.6 in equation(3.14) and equation(3.15) the value of cross-sectional area (A) can be found. Here the volume flow rate at a differential pressure of 15 bar is used because the oil curve of ICD intersects the oil curve of AICD at 15 bar (See Figure 3.8). This is necessary to directly compare the ICD with AICD in the same case. The value of the geometrical constant (C) is 0.85.

Substituting all these values in the equation(3.14) and equation(3.15) the value of cross-sectional area (A) for ICD is found to be 3.3653×10^{-6} m^2. That is, the diameter of the opening is 2.07 mm. The calculation is in Appendix B.

3.2.3 Modeling of AICDs

The Autonomous Inflow Control Device developed by Statoil is the Rate Control Production (RCP) valve. This valve helps to delay the gas and water breakthrough and autonomously stops the flow of low viscous fluids after there is a breakthrough of fluids. The RCP consists of a movable disc that can change the flow area depending on fluid properties and flow conditions. See Figure 3.7. This helps to keep the drawdown low by restricting the flow of a low viscous fluid like water in our case while maintaining the oil production from other zones. [23]

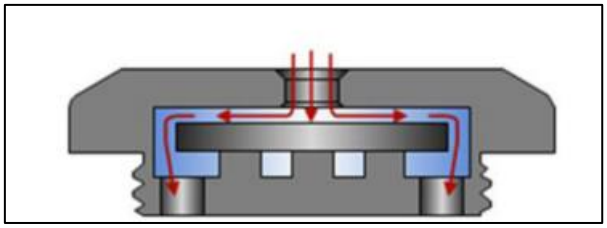

Figure 3.7: AICD flow path. [23]

Figure 3.8 shows the performance of the RCP compared to the performance of the nozzle ICD. For both the devices the flow rate of the oil is equal. The flow rate for the gas and water is seen to be less for the ICD compared to RCP because the flow area is varying in RCP. The flow rate for the low viscous fluid gas flow rate is significantly lower than the ICD.

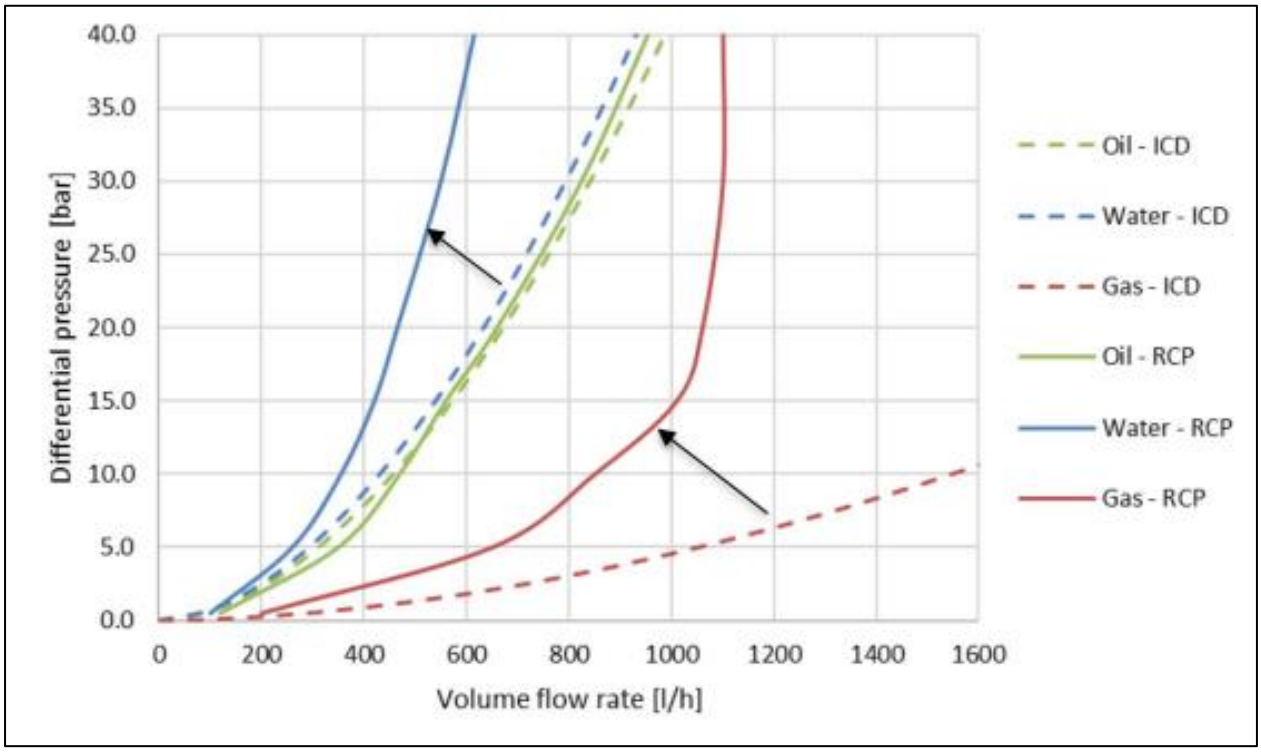

Figure 3.8: Performance curve of ICD and RCP for oil, water, and gas. [23]

3.2.3.1 Mathematical modeling of the AICD.

The mathematical function in the equation(3.16) is used in the reservoir simulation. The pressure drop across the AICD varies with the density and viscosity of the fluid flowing through the device according to this equation. [11]

$$\Delta P = (\frac{\rho_{mix}}{\rho_{cal}}).(\frac{\mu_{cal}}{\mu_{mix}})^{y}.\rho_{mix}.a_{AICD}.q^{x} \tag{3.16}$$

Eclipse uses this equation as the equation(3.17).

$$\Delta P = (\frac{\rho_{mix}}{\rho_{cal}}).(\frac{\mu_{cal}}{\mu_{mix}})^{y}.\rho_{mix}.a_{AICD}.(\frac{q}{q_{cal}})^{x-2}q^{2} \quad (3.17)$$

Here, a_{AICD}, x, y is the input strength parameters based on the size of the nozzle where x is the volume flow rate exponent and y is the viscosity function exponent, q is the volumetric mixture flow rate, and ρ_{cal} μ_{cal} are the calibration density and viscosity respectively. While, ρ_{mix} and μ_{mix} are the flowing mixture density and viscosity at the downhole conditions. And are given by the following equation (3.18) and equation (3.19).

$$\rho_{mix} = \alpha_{oil}^{a}\rho_{oil} + \alpha_{gas}^{b}\rho_{gas} + \alpha_{water}^{c}\rho_{water} \quad (3.19)$$

$$\mu_{mix} = \alpha_{oil}^{d}\mu_{oil} + \alpha_{gas}^{e}\mu_{gas} + \alpha_{water}^{f}\mu_{water} \quad (3.20)$$

To keep the approach simple *a,b,c,d,e,f* are been kept 1.

Figure 3.9 shows the predicted and test results at Troll conditions. These experimental results are obtained based on testing of the TR7 RCP valve performance for single-phase flow of oil.

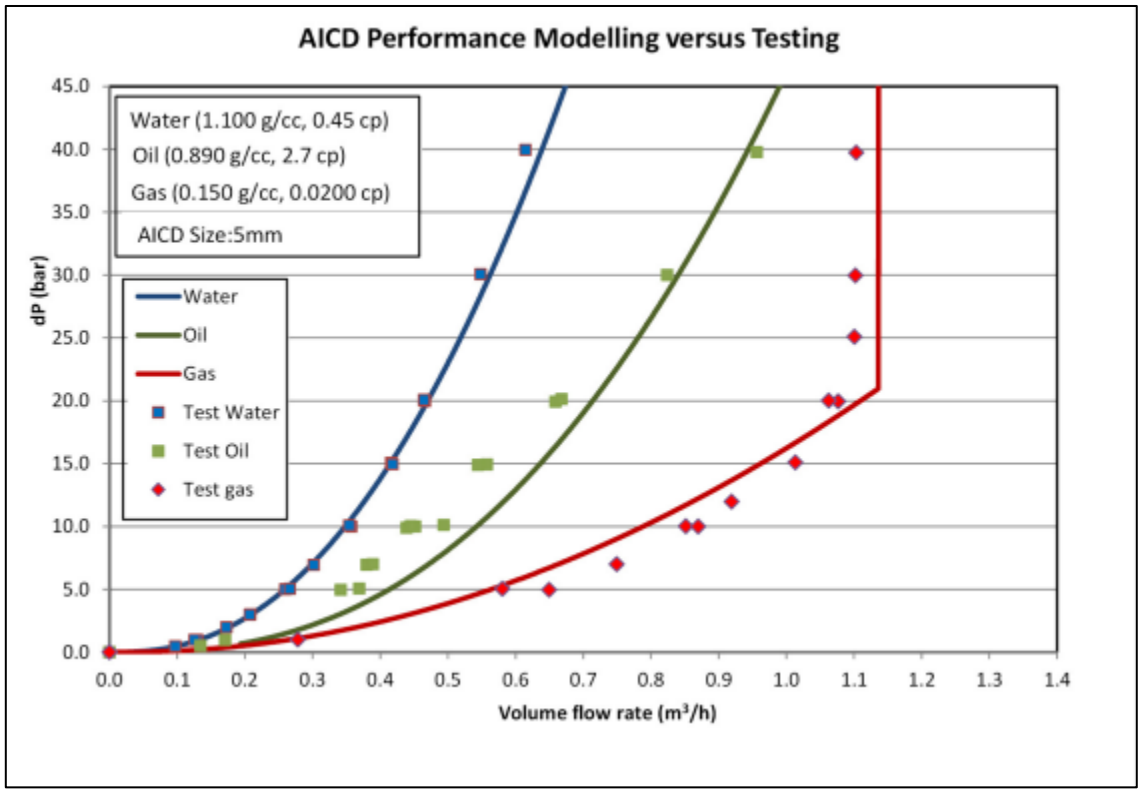

Figure 3.9: AICD performance modeling versus testing. [11]

The AICD, in this case, is modeled at the oil viscosity of 2.7cP, oil density of 890 kg/m3, water with the viscosity of 0.45 cP and water density of 1100 kg/m^3, as well as a gas with a viscosity of 0.02 cP and a density of 1.5 kg/m^3 based on the testing of the TR7 RCP. [11] The graph in Figure 3.9 model is very much in line with the graph in Figure 3.8. Thus, the fluid properties mentioned in Figure 3.9 can be used for the Figure 3.8.

The data point of the graph from Figure 3.8 is extracted using web plot digitizer. And the screen snip is given in Appendix C. Table 3.1 shows the values of pressure differential and the flow rate obtained from the AICD curves for water and oil.

Table 3.1: Extracted results for AICD from Figure 3.8.

Experimental results for oil		Experimental results for water	
q (l/h)	dP (bar)	q (l/h)	dP (bar)
120.40	0.45	101.39	0.45
174.26	1.45	126.73	1.12
231.29	2.45	167.92	2.23
288.32	3.57	218.61	3.57
345.35	4.80	262.97	5.02
402.38	6.69	300.99	6.69
449.90	8.93	324.75	8.03
494.26	11.16	370.69	10.93
541.78	13.84	403.96	13.39
592.48	16.51	430.89	15.84
646.34	19.19	446.73	17.74
689.11	21.65	462.57	19.64
738.22	24.44	491.09	22.76
780.99	27.11	518.02	25.89
814.26	29.23	551.29	29.90
845.94	31.46	560.79	31.46
876.04	33.70	573.47	33.03
910.89	36.37	586.14	35.26
933.07	38.27	603.56	38.05
955.25	39.94	616.24	40.00

To be able to use the AICD in the simulation case the values of a_{AICD}, x, y, ρ_{cal}, and μ_{cal} must be determined based on the data points in

Table 3.1. The values of the above coefficients are found by curve fitting and multi variable non-linear regression using MATLAB. See Figure 3.10.

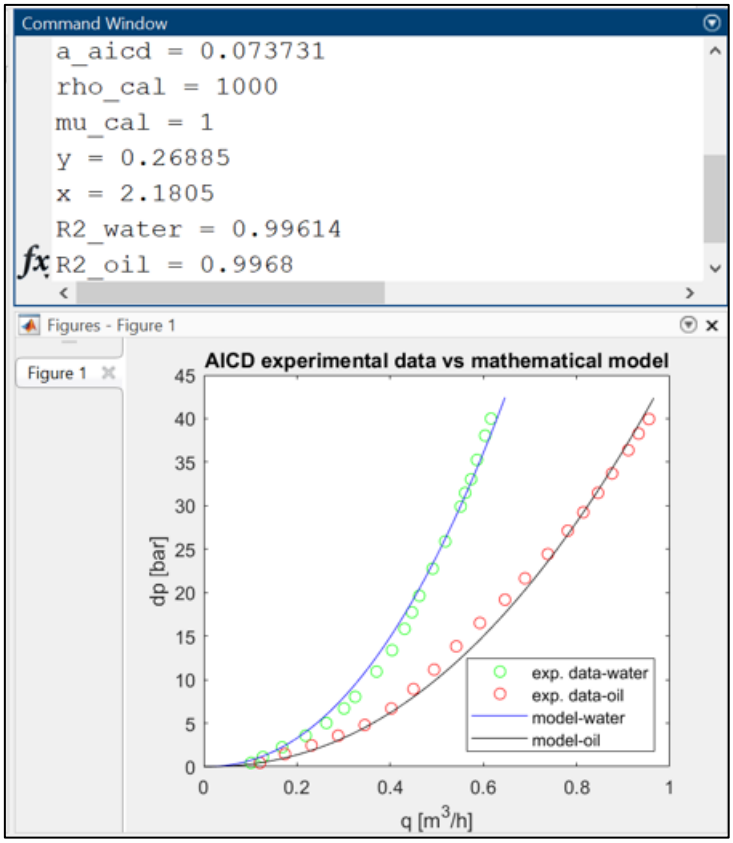

Figure 3.10: Multi variable non-linear regression for AICD curve.

The values of these coefficients for AICD are given in Table 3.2.

The unit of a_{AICD} in Petrel must be in bars/((kg/m^3)(m^3/day)^2)) but the unit of a_{AICD} is in bars/((kg/m^3)(m^3/h)^2)) the above mentioned model, so you should divide those values by 24^2 = 576 to be in bars/((kg/m^3)(m^3/day)^2)) as it is in Petrel.

Table 3.2: Coefficients of AICD.

AICD Coefficients				
a_{AICD}	x	y	ρ_{cal}	μ_{cal}
1.28×10^{-4}	0.1805	0.26885	1000	1

3.2.4 Modeling of AICVs

The autonomous Inflow Control Valve (AICV) can close completely for unwanted fluids. AICV can completely regulate itself and does not need to be regulated electronically. AICV can distinguish between the fluids based on fluid properties such as density and viscosity. It is designed to allow the flow of high viscous fluid such as oil and restrict the flow of low viscous fluids such as water or gas. The disc that blocks the flow of fluid is controlled by a minor pilot flow parallel to the main flow. Around 2% of the total flow rate is the minor flow. When the valve is closed, this minor flow is the total flow of the valve. [23] The operation of AICV is shown in Figure 3.11.

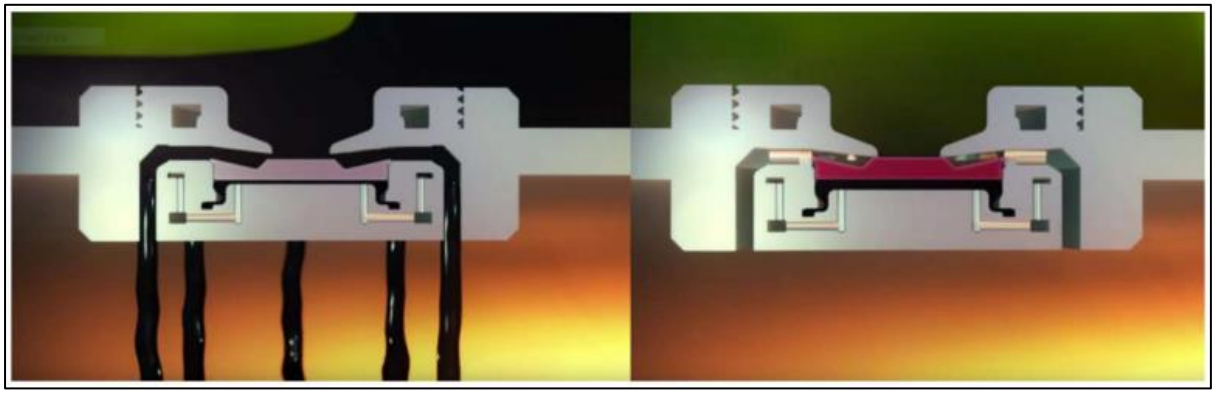

Figure 3.11: Open AICV (left) and Closed AICV (right) [23]

The figure shows the performance curves for oil, water, and gas of the AICV compared to the nozzle ICD. For the same strength of the AICV and ICD, the performance of the oil in AICV is almost in line with the ICD. When there is a breakthrough of the low viscous fluids such as water and gas the AICV closes and allows the flow of these fluids through the pilot flow which is a very minor flow. Hence, the flow rate of water and gas is considerably lower than in ICD. The black arrow in the Figure 3.12 shows the flow of water and gas in AICV compared to the ICD. This shows that the AICV technology is very improved than the ICD. [23]

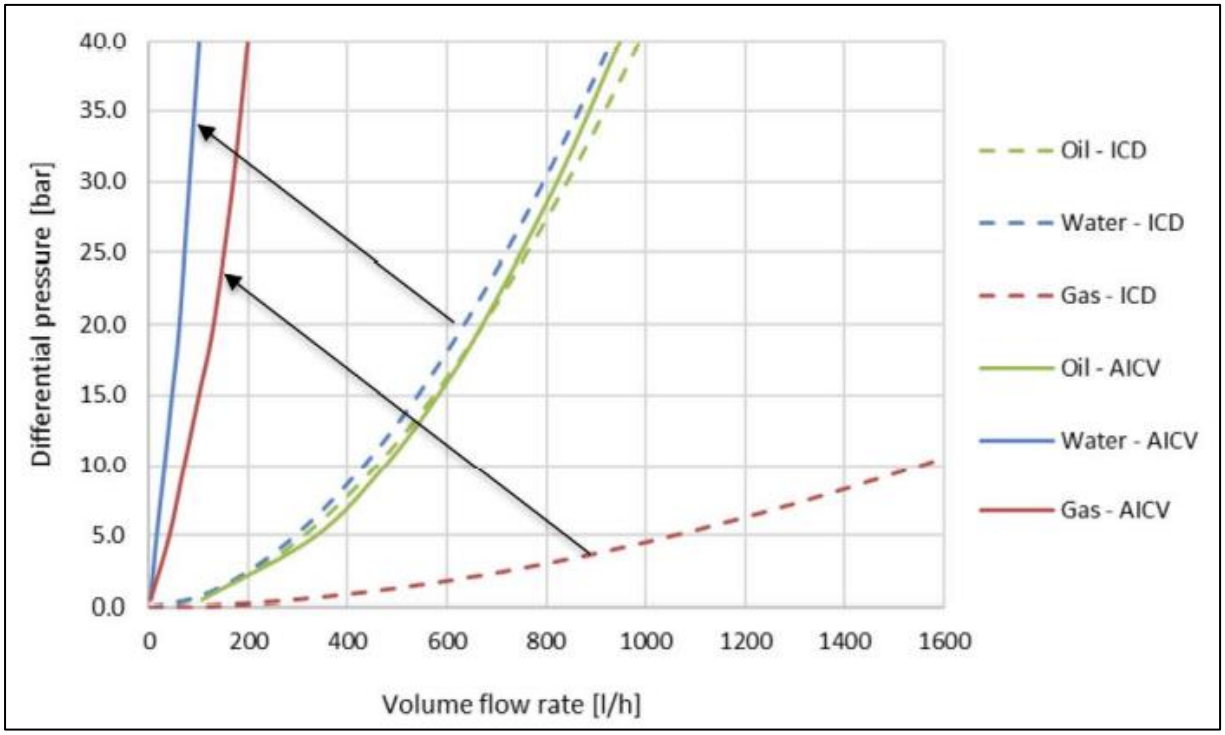

Figure 3.12: Performance curve of AICV and ICD for oil, water, and gas. [23]

3.2.4.1 Mathematical modeling of the AICV.

The AICV can be modeled using the same formulae as the AICD. Refer to the equation(3.16) ,(3.19) and (3.20). The AICD, in this case, is modeled at the oil viscosity of 2.7cP, oil density of 890 kg/m3, water with a viscosity of 0.45 cP and water density of 1100 kg/m^3, as well as a gas with a viscosity of 0.02 cP and a density of 1.5 kg/m^3 which are same as in case of AICD modeling.

The data point of the graph from Figure 3.12 above is extracted using a web plot digitizer. Just like in the AICD case. The

Table 3.1 shows the values of pressure differential and the flow rate obtained from the AICV curves for water and oil.

Table 3.3: Extracted results for AICV from Figure 3.12.

Experimental results for oil		Experimental results for water	
q (l/h)	dP (bar)	q (l/h)	dP (bar)
107.63	0.45	3.21	0.68
163.86	1.47	9.64	2.61
234.54	2.83	14.46	4.31
295.58	3.97	20.88	6.23
356.63	5.55	27.31	8.73
404.82	7.14	33.73	10.76
459.44	9.29	43.37	13.60
502.81	11.10	49.80	15.98
546.18	13.26	57.83	18.36
587.95	15.30	62.65	20.17
631.33	17.56	65.86	21.98
661.85	19.49	70.68	23.80
706.83	22.21	73.90	26.06
751.81	25.27	78.71	28.16
803.21	28.67	83.53	30.93
833.73	30.82	88.35	33.20
873.90	33.88	91.57	35.18
906.02	36.60	96.39	36.94
926.91	38.30	99.60	38.53
947.79	39.89	101.20	39.89

To model the AICV, The values coefficients such as $a_{AICD}\, x,\ y, \rho_{cal}$, and μ_{cal} must be determined based on the data points in

Table 3.1. The values of the above coefficients are found by curve fitting and multi variable non-linear regression using MATLAB. See Figure 3.13.

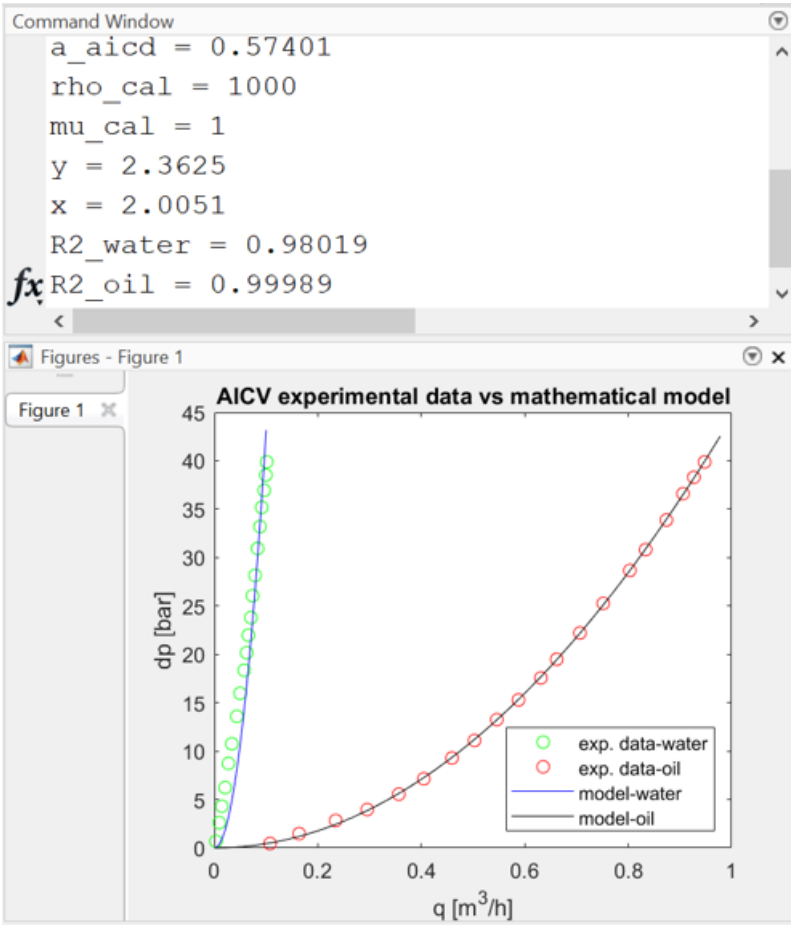

Figure 3.13: Multi variable non-linear regression for AICD curve.

The values of these coefficients for AICD are given in Table 3.4.

The unit of a_{AICD} in Petrel must be in bars/((kg/m^3)(m^3/day)^2)) but the unit of a_{AICD} is in bars/((kg/m^3)(m^3/h)^2)) the above mentioned model, so you should divide those values by 24^2 = 576 to be in bars/((kg/m^3)(m^3/day)^2)) as it is in Petrel.

Table 3.4: Coefficients of AICV.

AICV Coefficients				
a_{AICV}	x	y	ρ_{cal}	μ_{cal}
9.9654×10^{-4}	0.00051	2.3625	1000	1

4 Reservoir Model

4.1 Geological Model

In this reservoir simulation case, the ‘Egg Model’ was developed in Petrel 2021. This Egg model has a staggered line drive pattern as discussed in Chapter 2.1.1.2. The model is further enlarged to create an ‘Enlarge Egg Model’ to form a more realistic case. Finally, to see the effects of Advance Flow control devices a simplified model with one producer and one Injector was created from the Egg Model.

4.1.1 Egg Model

The geological model used in this simulation case is the Egg Model. The ‘Egg Model’ is a synthetic reservoir model consisting of small three-dimensional realizations of an oil reservoir produced under water flooding conditions with eight water injectors and four oil producers. This model has been used to demonstrate a variety of aspects related to water flooding simulations. [24]

The model consists of a reservoir with discrete permeability fields modeled with 60×60×7 = 25,200 grid cells of which 18,553 cells are active. The non-active cells are all at the outside of the model, which leaves an egg-shaped model of active cells. The expanse of the Egg Model is 480 m in the X and Y direction, while the height is 28 m with 7 layers.

The reservoir model is presented in Figure 4.1 [24]

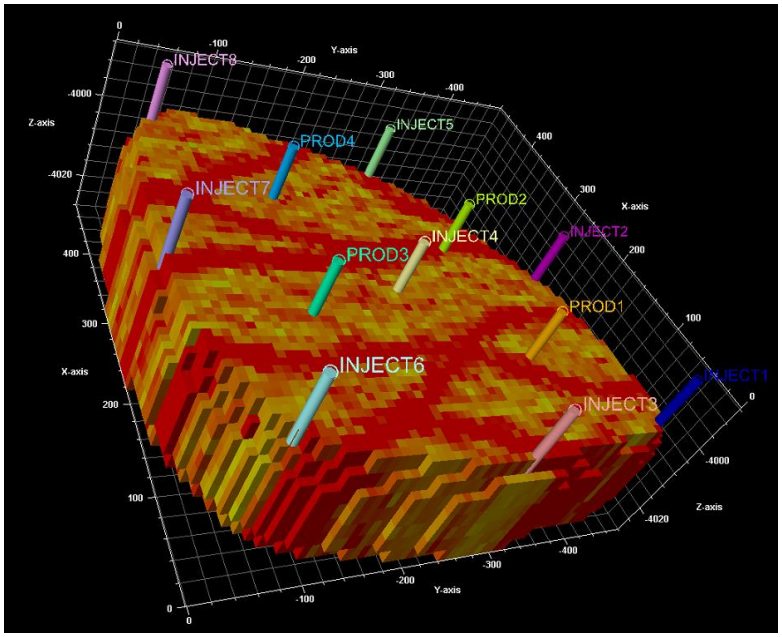

Figure 4.1: Egg model of the reservoir showing 8 injectors and 4 producers. [24]

The model is used for two-phase (oil-water) flow. The model has no aquifer and no gas cap, primary production is almost negligible, and the production mechanism is water flooding with the aid of eight injection wells and four production wells. [24]

The reservoir properties are used from the problem statement provided in Appendix D.

The reservoir model is homogeneous with Permeability in the x-direction equal to the permeability in the y-direction. And permeability in the z-direction is 10 % of the permeability in the X/Y direction.

Permx = Permy = 500 mD,

Permz = 0.1×Permx = 50 mD

Where Permx is the Permeability in the X direction, Permy is the permeability in the Y direction, and Permz is the permeability in the Z direction.

A number of grids: 15 x 15 x 7. And the Image showing the properties of the model created in petrel is shown in Appendix E

The dimensions of the grid block and the input parameters for the model are given in Figure 4.2.

Symbol	Variable	Value	SI units
h	Grid-block height	4	m
Δx, Δy	Grid-block length/width	8	m
ϕ	Porosity	0.2	–
c_o	Oil compressibility	1.0×10^{-10}	Pa^{-1}
c_r	Rock compressibility	0	Pa^{-1}
c_w	Water compressibility	1.0×10^{-10}	Pa^{-1}
μ_o	Oil dynamic viscosity	5.0×10^{-3}	Pa s
μ_w	Water dynamic viscosity	1.0×10^{-3}	Pa s
k_{ro}^0	End-point relative permeability, oil	0.8	–
k_{rw}^0	End-point relative permeability, water	0.75	–
n_o	Corey exponent, oil	4.0	–
n_w	Corey exponent, water	3.0	–
S_{or}	Residual-oil saturation	0.1	–
S_{wc}	Connate-water saturation	0.2	–
p_c	Capillary pressure	0.0	Pa
p_R	Initial reservoir pressure (top layer)	40×10^6	Pa
$S_{w,0}$	Initial water saturation	0.1	–
q_{wi}	Water injection rates, per well	79.5	m^3/day
p_{bh}	Production well bottom-hole pressures	39.5×10^6	Pa
r_{well}	Well-bore radius	0.1	m
T	Simulation time	3600	day

Figure 4.2: Input properties of the simulation case.

4.1.2 Simple model with one producer and one injector.

The Egg model discussed in the above section can be simplified based on the pattern observed in Figure 4.3. The injector injects in the last three layers and the producer is in the first three layers. The simple model has been created in petrel to implement ICDs, AICDs, and AICVs in a single producer. Figure 4.4 shows the screenshot of the model created in Petrel.

The dimension of each grid block is the same as the egg model with a length and width of 8 m and a height of 4m. The dimensions of the whole reservoir block are 120 m in X and Y directions with a height of 28 m with 7 layers.

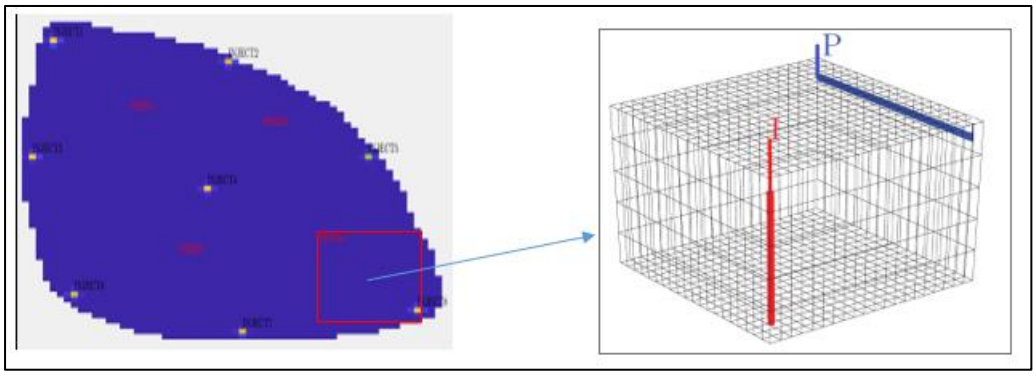

Figure 4.3: Staggered line drive pattern of egg model.

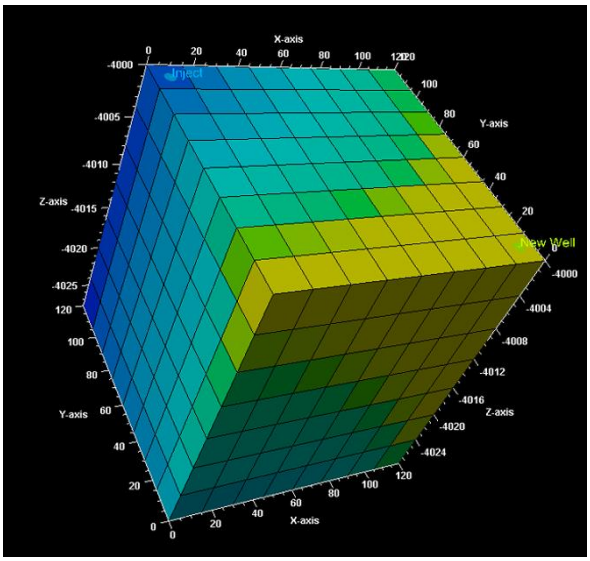

Figure 4.4: Simple reservoir model.

4.1.3 Enlarged Egg Model

In this model, the width and the length of a single grid block are increased 5 times and the height of the block is doubled. Hence, the total number of grid cells is the same as in Egg Model, which is 25200 grid cells. Other properties of the reservoir are kept as in the case of the Egg Model. Figure 4.5 shows the enlarged egg model of the reservoir with four vertical producers and 8 vertical injectors.

The expanse of the Enlarged Egg Model is 2400 m in the X and Y direction, while the height is 56 m with 7 layers. The Figure shows the model description and the model.

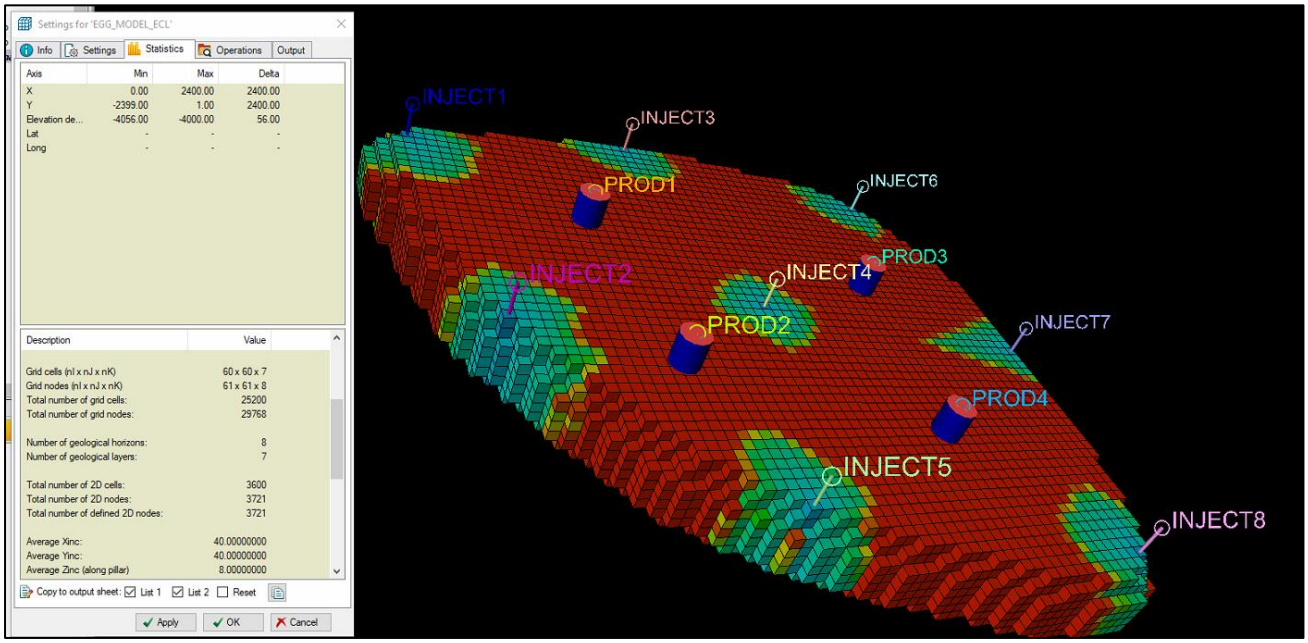

Figure 4.5: Model description and the model.

4.1.4 Fluid Contacts

The oil-water or gas-water contact is the lowest elevation at which mobile hydrocarbons are obtained. The transition zone is the elevation range in which water is coproduced with oil. The gas-oil contact is the elevation above which gas is produced. [25]

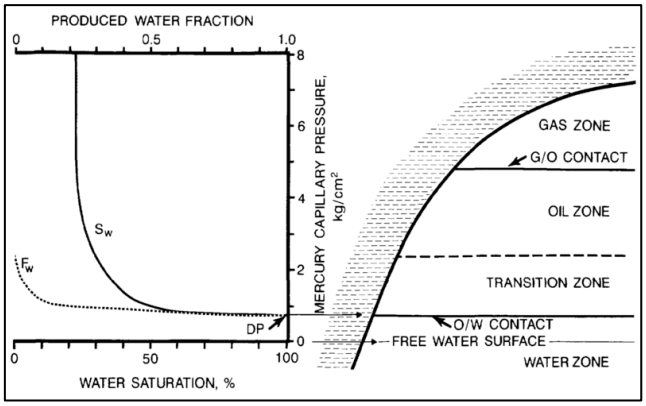

Figure 4.6: Relationship of contacts in a pool (right) to reservoir capillary pressure and fluid production curves (left). [25]

4.1.4.1 Gas-oil contact

The gas-oil contact in this simulation case is set at -4000 m i.e at the datum of the reservoir. This is because in the simulation case the gas phase is not encountered, and it is just oil and water. Hence the gas-oil contact is kept at the topmost surface indicated by the green color as shown in Figure 4.7.

4.1.4.2 Water-oil contact

The water-oil contact in this simulation case is set at -5000 m. This is because it is considered that, initially the saturation of oil in the reservoir is very high and there is no significant water present in the reservoir. The water contact at -5000 m can be seen in Figure 4.7 indicated by the blue color.

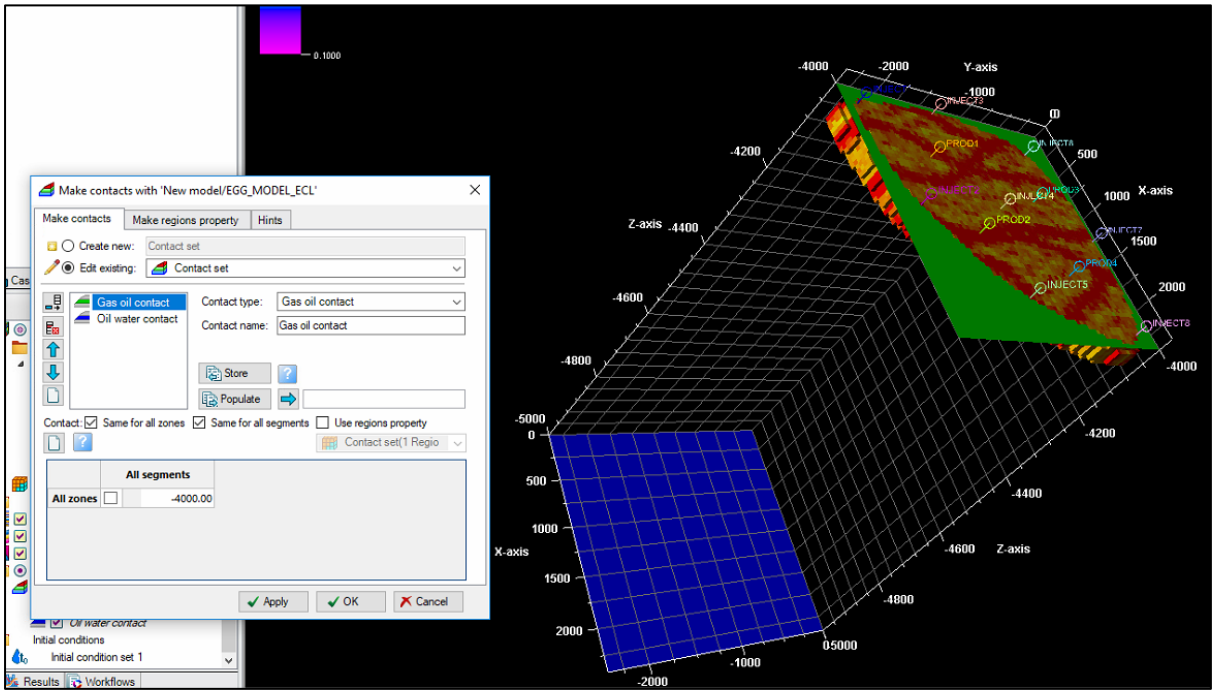

Figure 4.7: Gas-oil contact (Green) & water-oil contact(Blue).

4.2 Fluid Model

The fluid used in this simulation model is the dead oil and the water. There is no gas in the reservoir. Hence it makes a two-phase flow simulation.

4.2.1 Reservoir conditions

The minimum pressure inside the reservoir is maintained at 395 bar based on the bottom hole pressure of the production well while the maximum pressure is maintained at 405 bar based on the bottom hole pressure of the injection well. The temperature inside the reservoir is 76.85°C. The setting of the reservoir conditions in the Petrel Software is shown in Figure 4.8.

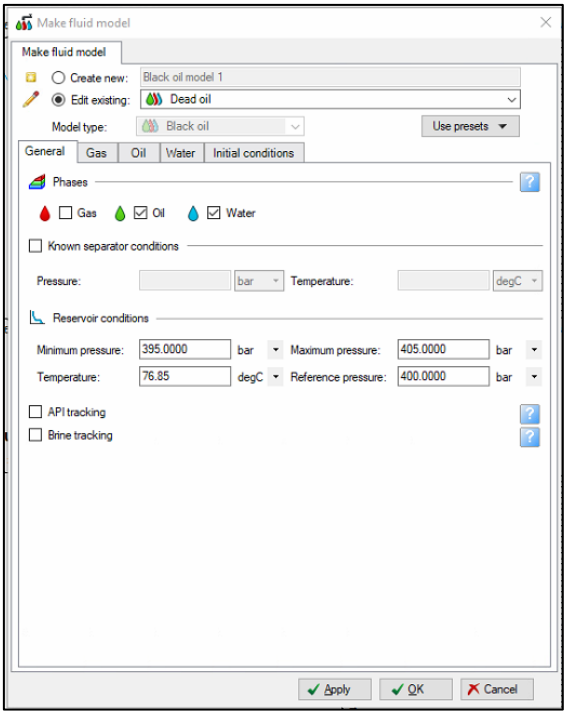

Figure 4.8: Make a fluid model tab in the Petrel.

4.2.2 Oil

Oil Crude oil contains natural gases and volatile components. If all these gases and volatile components have been stripped off the crude oil thanks to pressure and temperature after reaching the surface during production, the remaining oil is referred to as dead oil. Furthermore, oil in a dead state will be difficult to extract from a reservoir under regular reservoir conditions. [26] The density of the oil is set to be 900 kg/m^3.

Figure 4.9: Dead oil [26]

4.2.3 Water

The density of water is 1000 kg/m^3. The compressibility from the given conditions are 1×10^{-10} 1/Pa. The viscosity of water is 1×10^{-3} Pa.s. Figure 4.11 shows the make fluid model tab for water in Petrel.

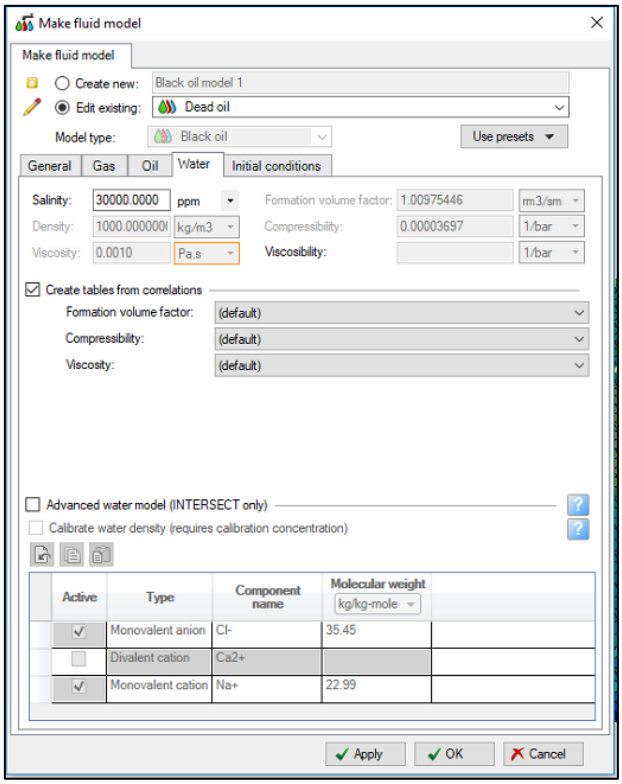

Figure 4.10: Make a fluid model tab for water in the Petrel.

4.2.4 Rock Physics

4.2.4.1 Relative permeability

The relative permeability is set according to the input parameters given in Figure 4.2. The input for relative permeability in the Petrel is shown in Figure 4.11. Also, the relative permeability curve is shown in Figure 4.12.

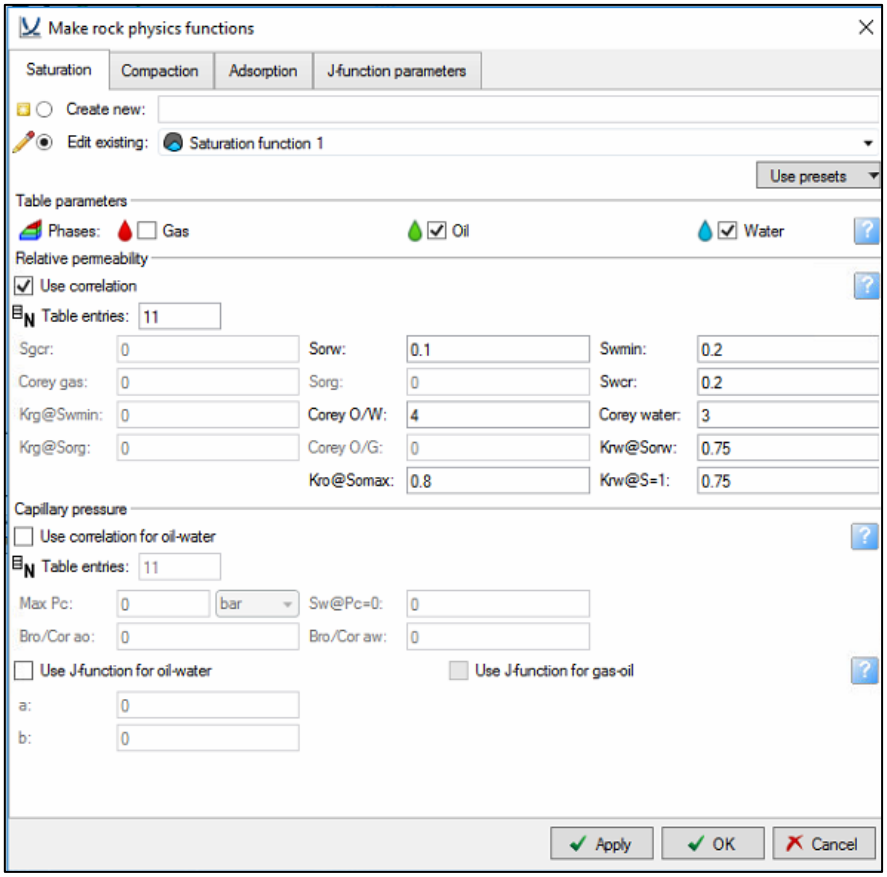

Figure 4.11: Relative permeability values.

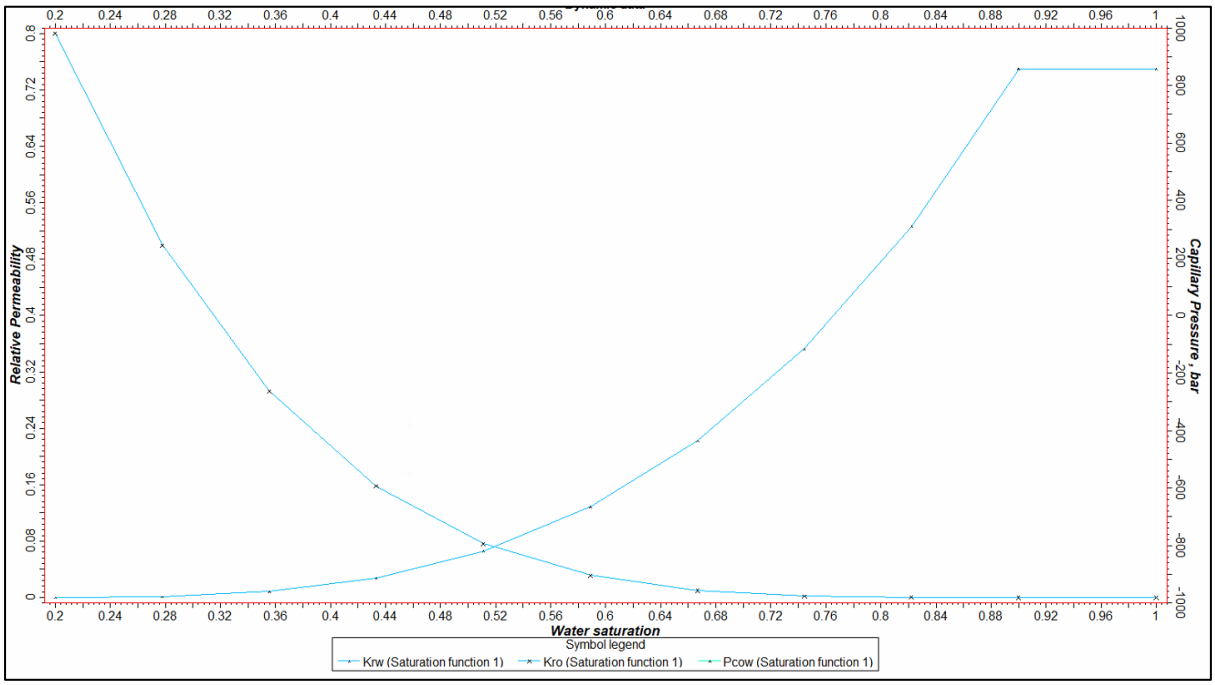

Figure 4.12: Relative permeability curve obtained from data in Figure 4.11.

4.3 Well Model

This sub-chapter discusses the vertical production and injection wells, their lengths, and the position of the wells. Further, the vertical wells are converted into horizontal wells in the enlarged egg model. These horizontal well in the simple case is then equipped with the completions such as ICD, AICD, and AICV. Lastly, the development strategy for the injectors and the producers is discussed.

4.3.1 Well, Design.

This section discus various design parameters of the vertical and horizontal wells in different simulation cases.

4.3.1.1 Vertical wells of Egg Model.

The Egg Model is equipped with 8 vertical injectors and 4 vertical producers as discussed in the Staggered line drive pattern. The position of the vertical wells can be seen in Figure 4.13.

Each well is 40 m in length vertically with the well head at -3988 m up to the base of the reservoir at -4028m. The open hole diameter of the well is 8 inches which can be set in the global completion tab.

The spreadsheet for the injector 1 is shown in Image 1 in Appendix F

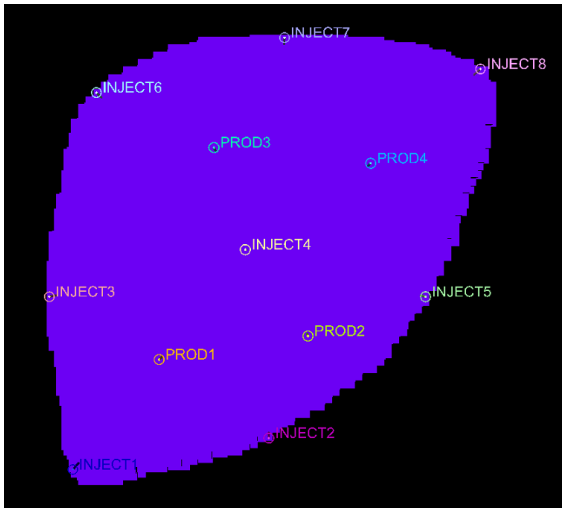

Figure 4.13: Pattern of injectors and producers in egg model.

4.3.1.2 Vertical wells of Enlarged Egg Model.

The vertical wells in the enlarged egg model are at the same location as in the case of the egg model as seen in Figure 4.14. This is because the model is just the enlarged version of the previous enlarged model. The only difference is that the measured depth MD is increased from 40 m to 80 m with well head at -3976 m and the bottom of the well at -4056 m at the bottom surface of the reservoir.

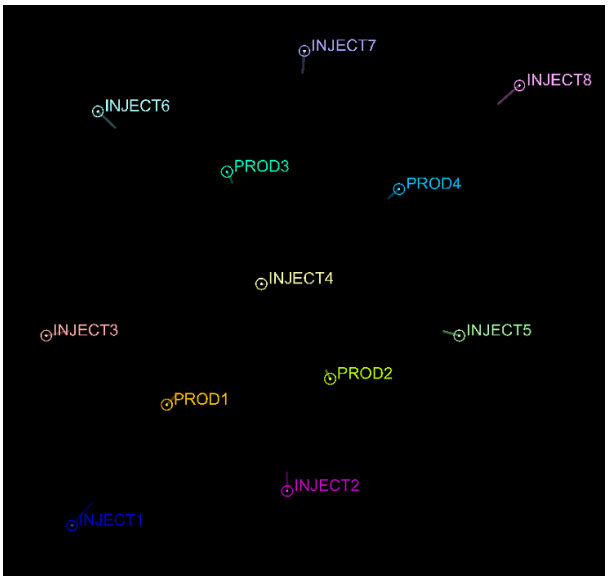

Figure 4.14: Top view of the enlarged egg model showing the wells

4.3.1.3 Horizontal producer wells of Enlarged Egg Model.

The vertical wells of the Enlarged Egg Model are converted into horizontal wells using the good template tab in the Well Engineering section. The template used to plan the well is J well plan and the good coordinates are as shown in Image 2 and Image 3 in Appendix F respectively. The position of the well is such that the well is placed in the middle of the injectors so that the oil is swept right towards the wells. Also, high and low permeability zones play an avital role in horizontal wells. See Figure 5.13 which shows the horizontal wells on the left and the permeability of the reservoir on right. This also avoids the early breakthrough of the water. Different positions and directions of the well were tried before coming to the final will positions. The length of all the wells is kept around 500 m to 600 m.

Also, the length of producer 1 (PROD 1) was kept at around 500 m and then later it was changed to around 1000 m to observe the effect of length on well production. The detailed dimensions and the positions of the producers are given in Image 4 Appendix F.

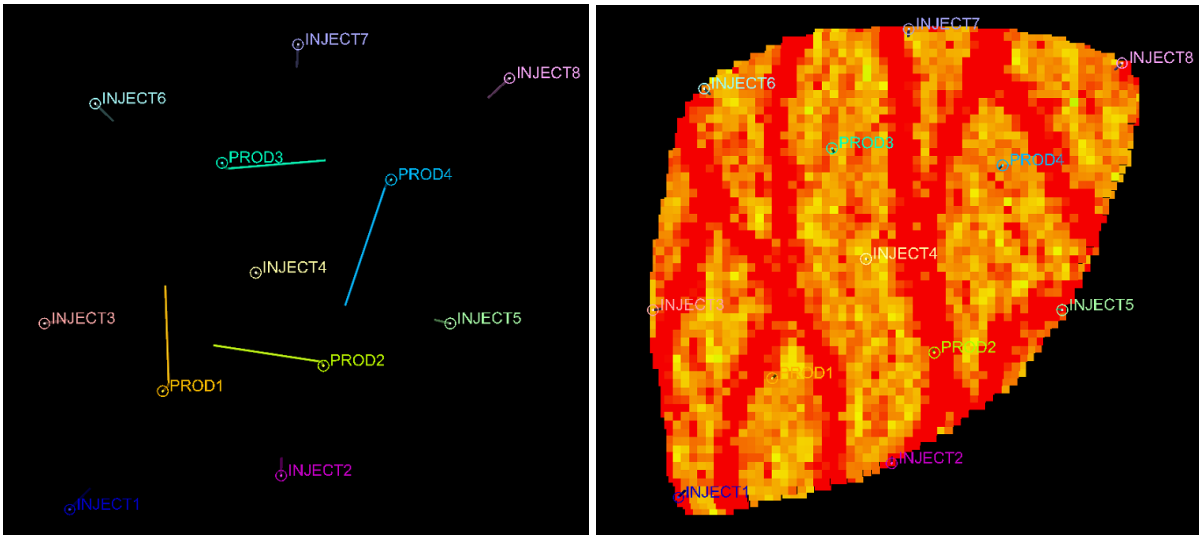

Figure 4.15: Top view of the reservoir showing horizontal good directions (left) and high permeability zones (Right).

4.3.1.4 Horizontal producer wells of Simple Model with single injector and producer.

The length of the vertical injector well in the simple model is 40 m which is the same as the egg model. But the producer, in this case, is horizontal with a total length of 107 m and it lies in the first three layers of the reservoir. The diameter of the open hole is kept at 8 inches. Figure 4.16 shows the horizontal well created in simple cases.

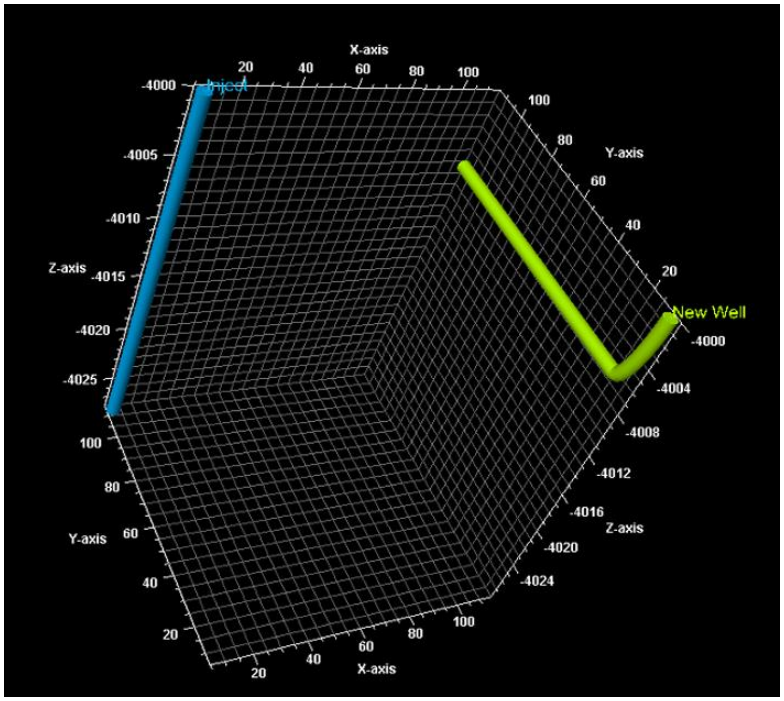

Figure 4.16: Horizontal producer and vertical injector in a simple model.

4.3.2 Well Completion

The well completions are implemented in the simple model with a single injector and producer. It is done so using the Automated design tab in the Well engineering section in Petrel. Petrel has several options to create the completions automatically which are Creating simple completions, Creating ICD/FCV completions, Modifying completion attributes, and as shown in Image 1 in Appendix G. All these functions are used to create the advanced well with completion.

4.3.2.1 Creating the tubing and casing.

To create the casing and tubing the option called Creating simple completion is used in the Advance design tool. The diameter of the casing is 7 inches for the open hole of 8 inches and the diameter of the tubing is 5.5 inches which rest inside the casing. The outer diameter of the casing is 7 inches while the outer diameter of the tubing is 5.5 inches. It is important that the casing is partially submerged in the upper surface so that it can hold the tubing.

4.3.2.2 Implementing the ICD.

The ICD can be implemented using the Creating ICD/FCV option in the Automated design tool just like for tubing. It is possible to set the compartment length and the desired number of ICDs in one compartment. One compartment is formed by the distance between two packers. See Image 1 in Appendix G.

The ICD in this case has a cross-sectional area of 3.3653×10^{-6} m^2 as calculated in section 3.2.2.1. In Petrel, the attribute for the cross-sectional area is the Channel x-sect area. And the Geometrical constant is given by the flow coefficient. The attributes for all the ICDs implemented can be changed by using the function called Modify equipment attribute in the Automated design tool. Figure 4.17 shows all the attributes of the ICDs in this case.

Name	Value	Unit
Depth		
Bottom from	Well datum	
Bottom MD	5.30	m
Bottom offset	5.30	m
Bottom SSTVD	4004.61	m
Top from	Well datum	
Top MD	0.30	m
Top offset	0.30	m
Top SSTVD	4000.31	m
Device		
Channel roughness	0.00060	in
Channel x-sect area	0.000003	m2
Flow coefficient	0.85	
Physical valves equivale	1	
VFP table	Undef	
Diameters		
Coupling outer diameter		in
Drift diameter		in
Inner diameter	5.00000	in
Outer diameter	5.50000	in
General		
Category	Devices	
Completion length	5.00	m
End date		
Equipment ID	NICD-5.50/4x4.0	
Name	Nozzle ICD 1	
Start date	01/01/2022 00:00:00	
Type	Nozzle ICD	
UWI		
Well folder	Wells	
Well name	New Well	
Material		
Inner roughness	0.000600	in
Outer roughness	0.000600	in
Tubular		
Collapse resistance		bar

Figure 4.17: ICD attributes.

4.3.2.3 Implementing the AICD and AICV.

The procedure to implement the AICD and AICV is exactly like that of ICD. The input attributes calculated in section 3.2.3.1 Table 3.2 for AICD and section 3.2.4.1 Table 3.4 for AICV are implemented using the function Modify equipment attribute in the Automated design tool. The attributes of AICD and AICV are shown in Figure 4.18.

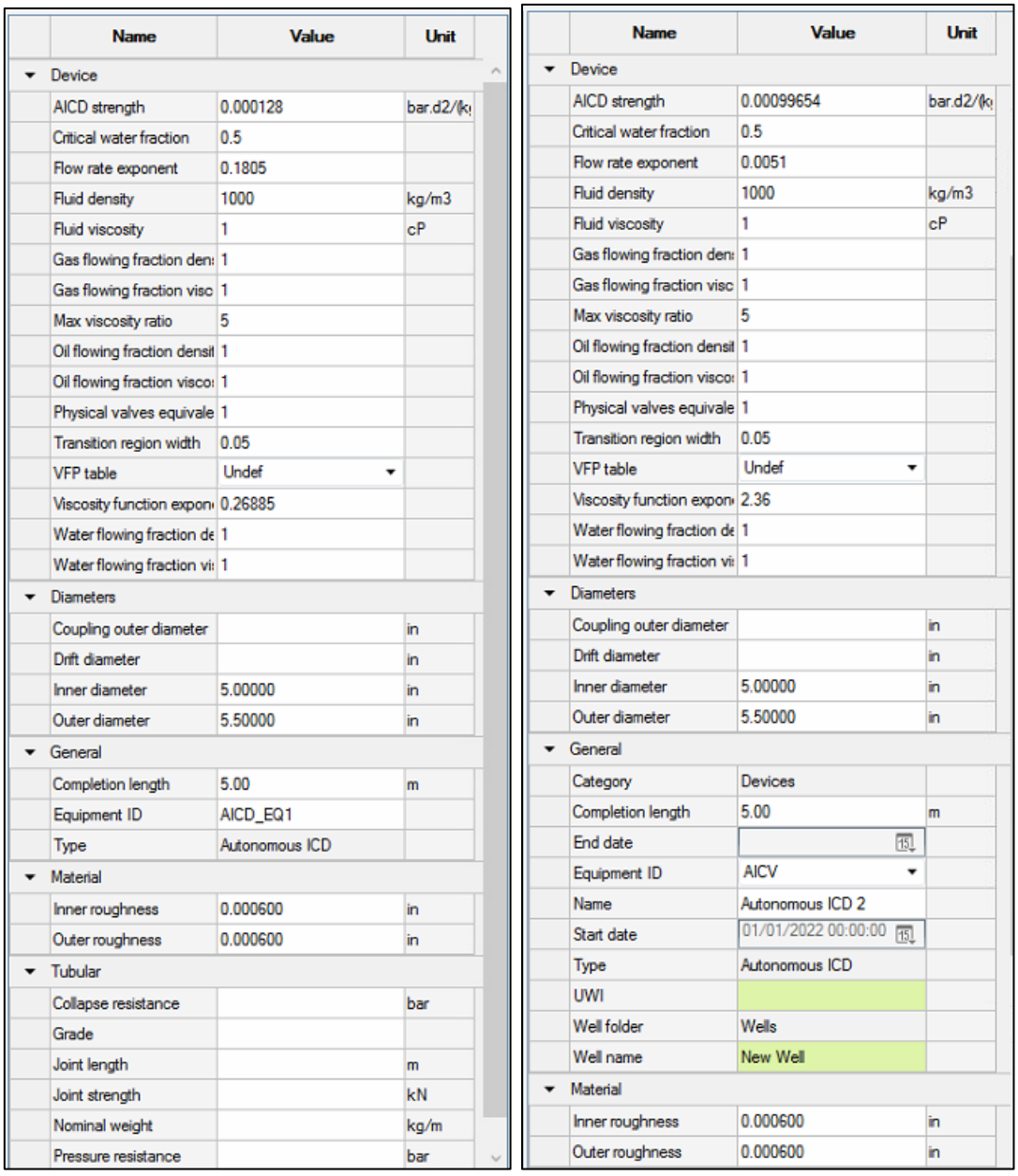

Name	Value	Unit
Device		
AICD strength	0.000128	bar.d2/(k
Critical water fraction	0.5	
Flow rate exponent	0.1805	
Fluid density	1000	kg/m3
Fluid viscosity	1	cP
Gas flowing fraction den	1	
Gas flowing fraction visc	1	
Max viscosity ratio	5	
Oil flowing fraction densit	1	
Oil flowing fraction visco	1	
Physical valves equivale	1	
Transition region width	0.05	
VFP table	Undef	
Viscosity function expon	0.26885	
Water flowing fraction de	1	
Water flowing fraction vi	1	
Diameters		
Coupling outer diameter		in
Drift diameter		in
Inner diameter	5.00000	in
Outer diameter	5.50000	in
General		
Completion length	5.00	m
Equipment ID	AICD_EQ1	
Type	Autonomous ICD	
Material		
Inner roughness	0.000600	in
Outer roughness	0.000600	in
Tubular		
Collapse resistance		bar
Grade		
Joint length		m
Joint strength		kN
Nominal weight		kg/m
Pressure resistance		bar

Name	Value	Unit
Device		
AICD strength	0.00099654	bar.d2/(k
Critical water fraction	0.5	
Flow rate exponent	0.0051	
Fluid density	1000	kg/m3
Fluid viscosity	1	cP
Gas flowing fraction den	1	
Gas flowing fraction visc	1	
Max viscosity ratio	5	
Oil flowing fraction densit	1	
Oil flowing fraction visco	1	
Physical valves equivale	1	
Transition region width	0.05	
VFP table	Undef	
Viscosity function expon	2.36	
Water flowing fraction de	1	
Water flowing fraction vi	1	
Diameters		
Coupling outer diameter		in
Drift diameter		in
Inner diameter	5.00000	in
Outer diameter	5.50000	in
General		
Category	Devices	
Completion length	5.00	m
End date		
Equipment ID	AICV	
Name	Autonomous ICD 2	
Start date	01/01/2022 00:00:00	
Type	Autonomous ICD	
UWI		
Well folder	Wells	
Well name	New Well	
Material		
Inner roughness	0.000600	in
Outer roughness	0.000600	in

Figure 4.18: AICD attributes (Left) and AICV attributes (Right)

4.3.3 Development Strategy

Development strategies are used to tell the simulator how a field will be developed – that is, which wells will produce or inject, what rates and pressures they will flow at, what operations will be carried out on the wells over time, and so on. Development strategies make it easy to keep track of how the control of a field evolves with time: for instance, the new wells can be added to the field, wells are converted from producer to injector, and new platforms can be created at the specified time are added.

Development strategies make it easy to apply the same constraint to many wells, using well folders, or to apply different values of a particular constraint to individual wells. This gives so much flexibility for setting a simulation case.

Petrel has a few preset development strategies readily available to use. One of them is the prediction waterflooding strategy. The strategy used in all the cases of simulation is waterflooding strategy. In this case, the reservoir production is controlled by the surface injection rate and the bottom hole pressure of the producer. See Figure 4.19. The reservoir production is controlled by the following two rules. All the parameters except for the injection rate and simulation time are the same in all the cases.

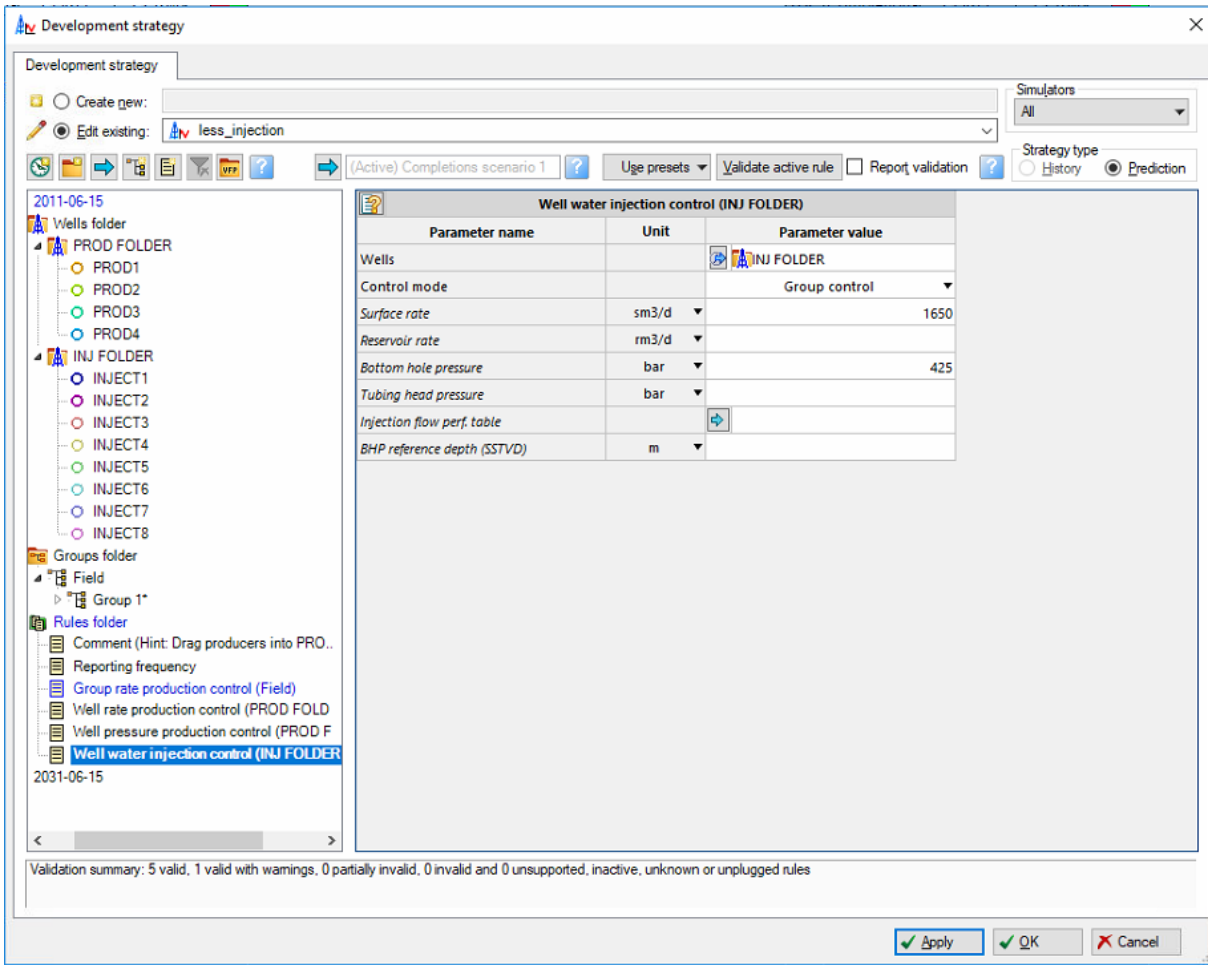

Figure 4.19: Development strategy for waterflooding in the Petrel software.

4.3.3.1 Well water Injection control.

The water injection rate for the Egg model and the simple case with a single producer and injector is 79 m^3/day as per the input parameters from Figure 4.2. The water injection rate for the Enlarged Egg model is kept at 1650 m^3/day since the simulation time is doubled and the size of the model is also larger.

Also, during the simulation run, there were some issues. And I was found that it is important to set the bottom hole pressure if the injectors higher than the maximum reservoir pressure to avoid the extrapolation of PVT values. Hence the Bottom hole pressure (BHP) of the injector is set to be 425 bar in all the simulation cases.

4.3.3.2 Well oil production control

The oil production is controlled by the bottom hole pressure. The bottom hole pressure of the production well is kept at 395 bar.

4.3.3.3 Simulation time.

The simulation time for the Egg Model and the simple model is 10 years starting from 15th June 2011 to 15th June 2021. In the case of the Enlarged Egg Model, the simulation time is 20 years starting from 15th June 2011 to 15th June 2031.

5 Simulation Result

This chapter displays the results of the different models created in Petrel 2021 software. Starting with analyzing the results of the Egg Model developed in Petrel. Further the results of the Enlarged Egg Model are presented which primarily shows the results for vertical and horizontal wells and then also goes on to compare the oil production of Producer 1 at different lengths. At last, the 3D results of the Enlarged Egg model are shown.

5.1 Analyzing Egg model in Petrel.

The results of all the four producers of the Egg Model created in Petrel are compared to the results model with the results of the egg model developed in eclipse and MRST as presented in the Geoscience Data Journal [24]. Figure 5.1 to Figure 5.4 shows the comparative result of Petrel and Eclipse for all four producers. The green oil production is represented by the green color and the water production is represented by the blue color. The result of the eclipse model is shown by the solid line while the result of the Petrel model is shown by the dotted line.

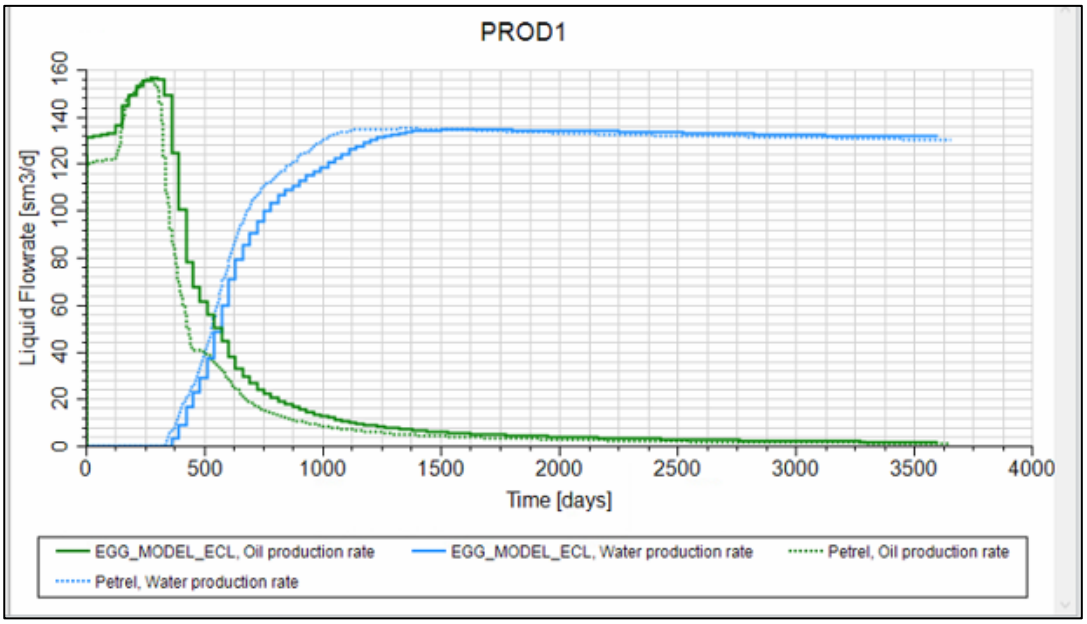

Figure 5.1: Oil and water production of producer 1.

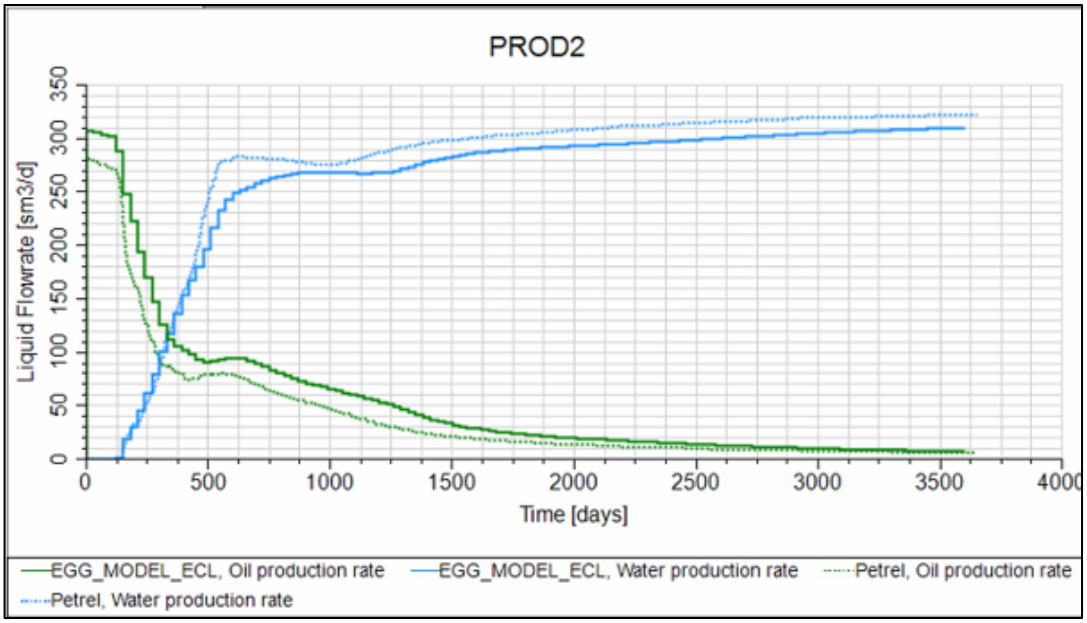

Figure 5.2: Oil and water production of producer 2.

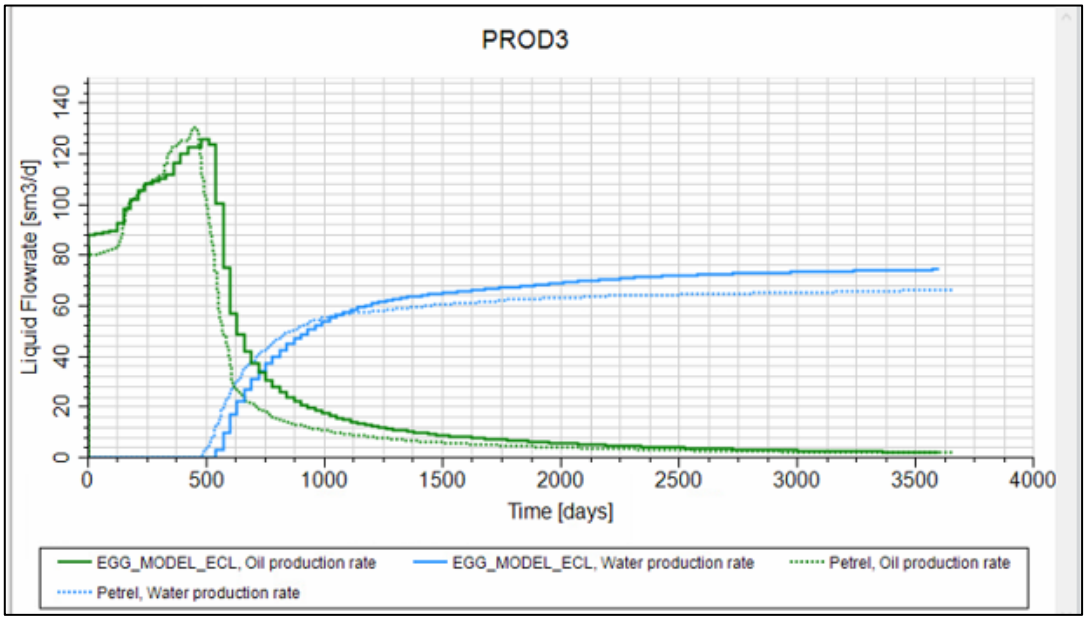

Figure 5.3: Oil and water production of producer 3

.

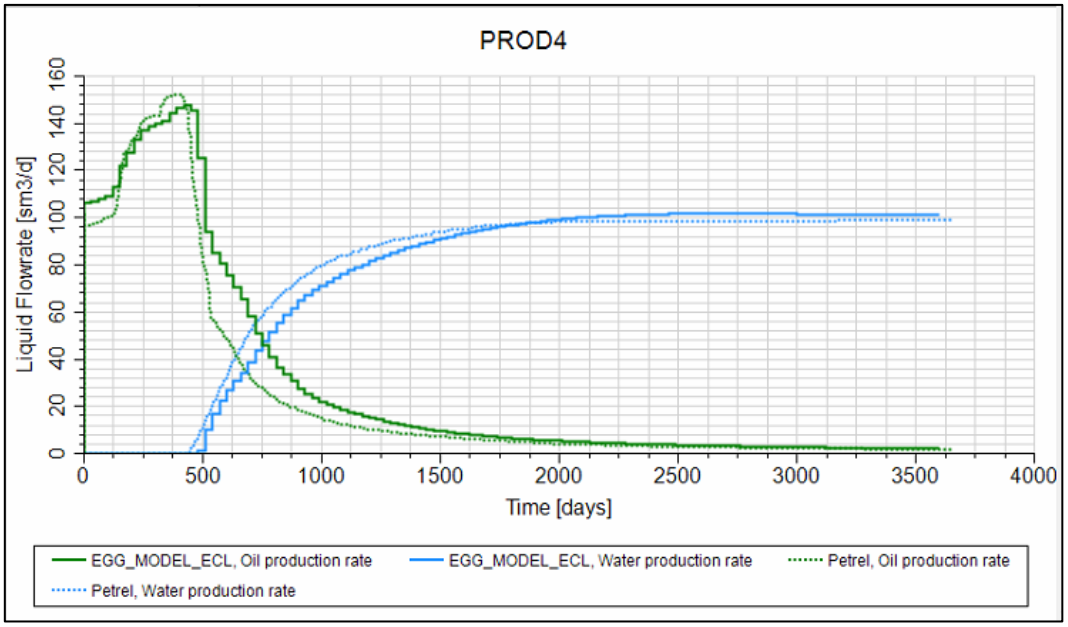

Figure 5.4: Oil and water production of producer 4.

5.2 Vertical open hole production vs Horizontal open hole production of reservoir.

After the Egg model is modified to the Enlarged Egg Model, the wells are vertical as described in the subchapter54 4.3.1.2. Then the vertical wells are converted to the horizontal wells as mentioned in subchapter 4.3.1.3. All the injectors are injecting water at the constant rate of 1650 m^3/day. The results of oil production for vertical wells with the horizontal wells for all four producers. Also, the production rate of the whole field with horizontal wells is compared with the field of a vertical well. In all the graphs green color represent oil and the blue color represents water. The horizontal well production is represented by sold line while the vertical well production is represented by the dotted line.

5.2.1 Producer 1

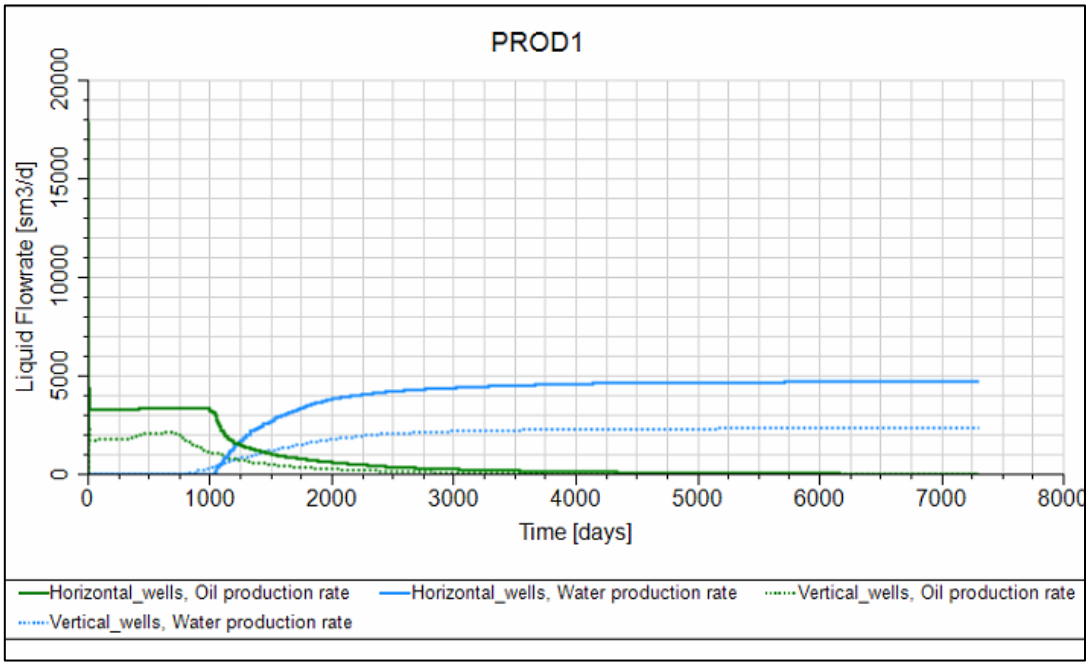

Figure 5.5: Horizontal vs Vertical well production of Producer 1.

5.2.2 Producer 2

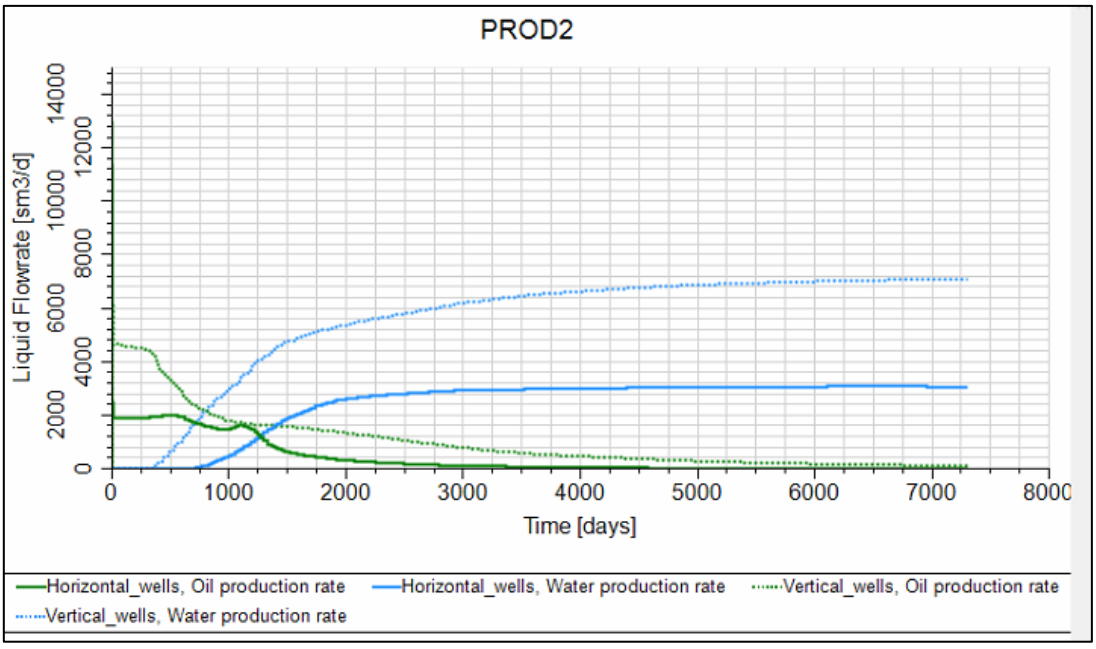

Figure 5.6: Horizontal vs Vertical well production of Producer 2.

Figure 5.7 shows the oil saturation result of the Enlarged Egg Model with vertical well w.r.t time. The red circle describes the position of producer two on the field. And the location of Injector 7 and injector 2 is shown.

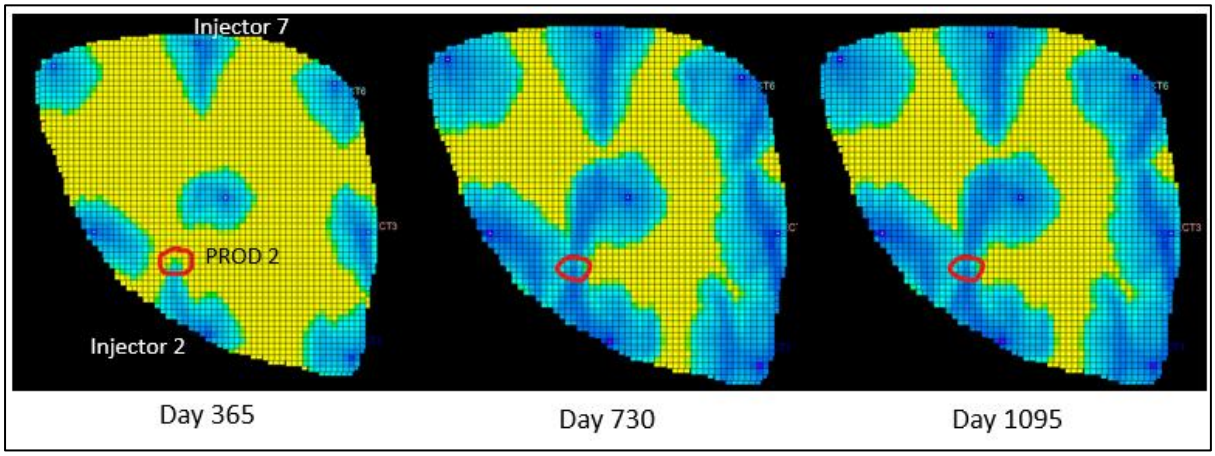

Figure 5.7: Oil saturation w.r.t time of Enlarged Egg Model with vertical well

5.2.3 Producer 3

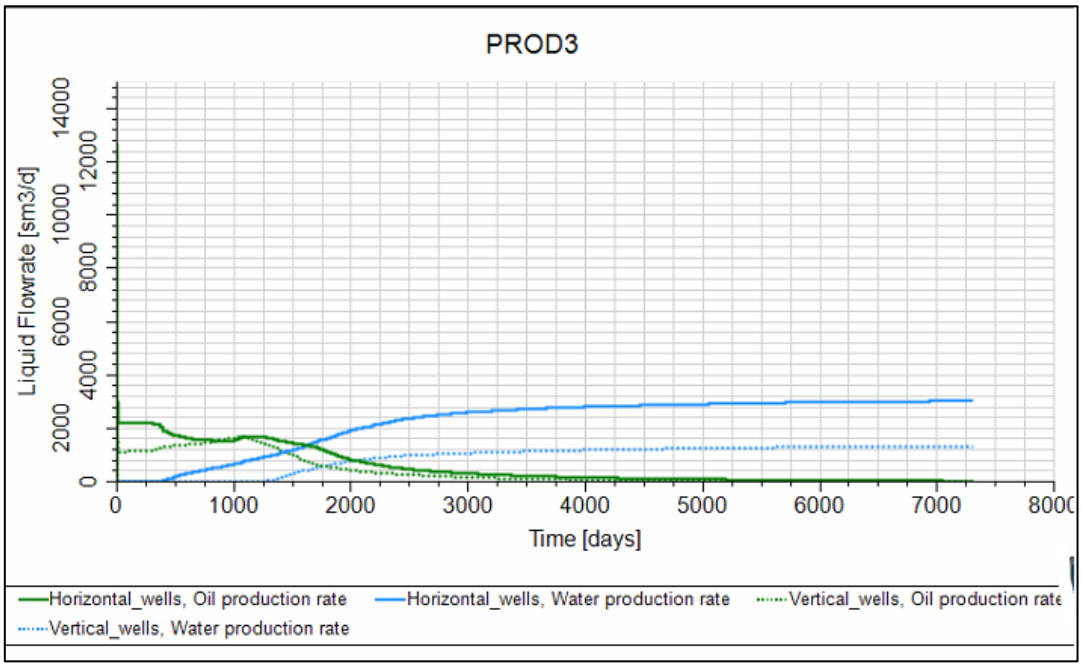

Figure 5.8: Horizontal vs Vertical well production of Producer 3.

Figure 5.9 shows the oil saturation results of horizontal wells after 1 year.

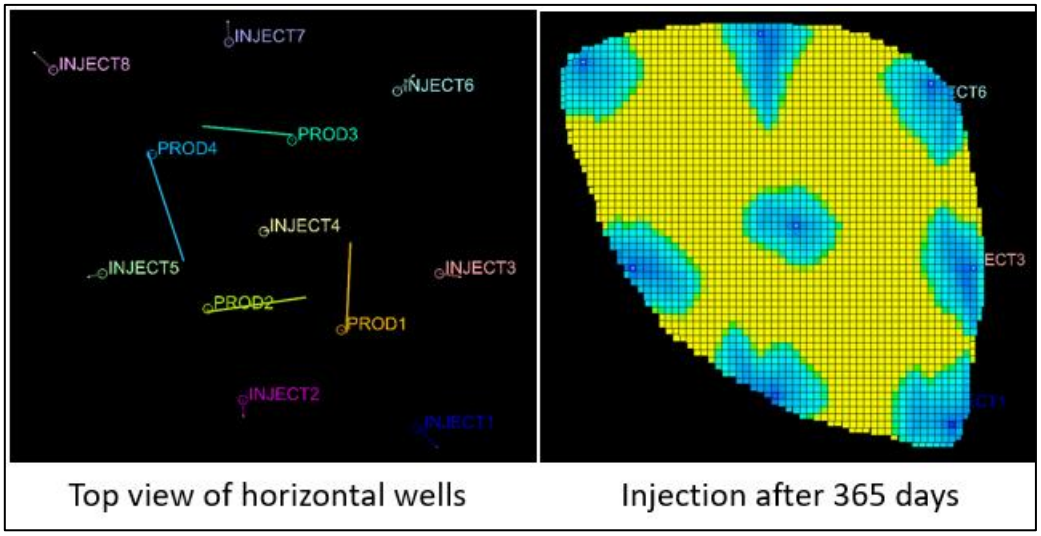

Figure 5.9: Oil saturation results of horizontal well case after 365 days.

5.2.4 Producer 4

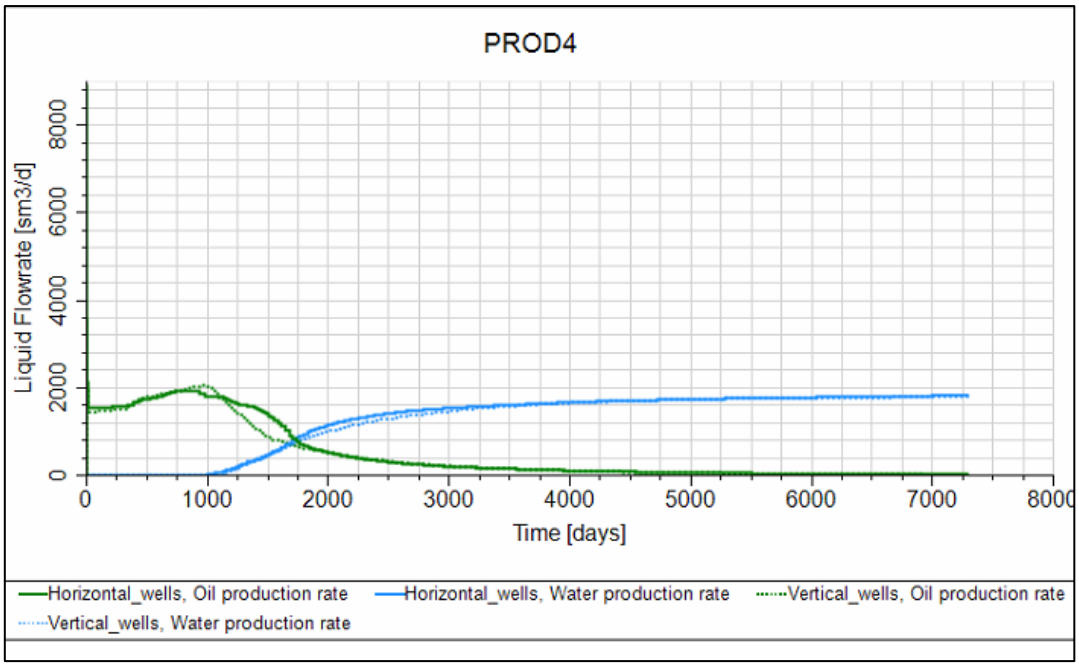

Figure 5.10: Horizontal vs Vertical well production of Producer 4.

5.2.5 Cumulative field production rate.

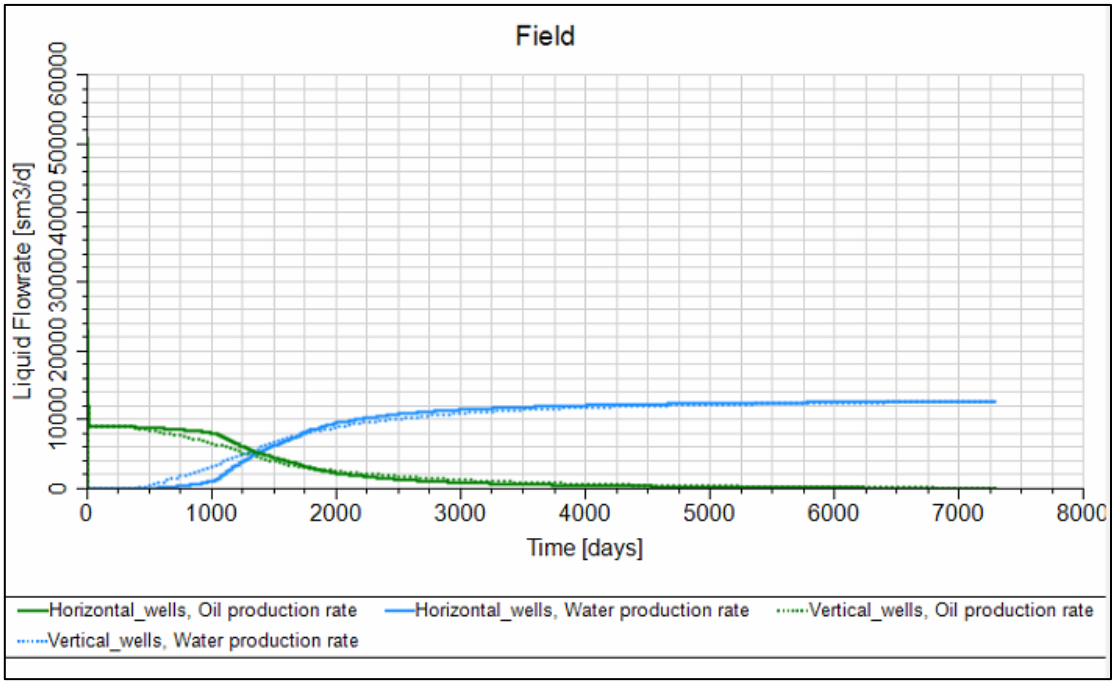

Figure 5.11: Cumulative production rate of horizontal vs vertical wells.

5.3 Impact of horizontal well length on production.

The horizontal Producer 1 (PROD1) is tested at two different lengths. First at 533 m (533-meter) and then at 1133 m (1133-meter). The green and blue color represent oil and water respectively while the solid line represents 1133m well and the dotted line represents 533 m long length.

5.3.1 Production rate.

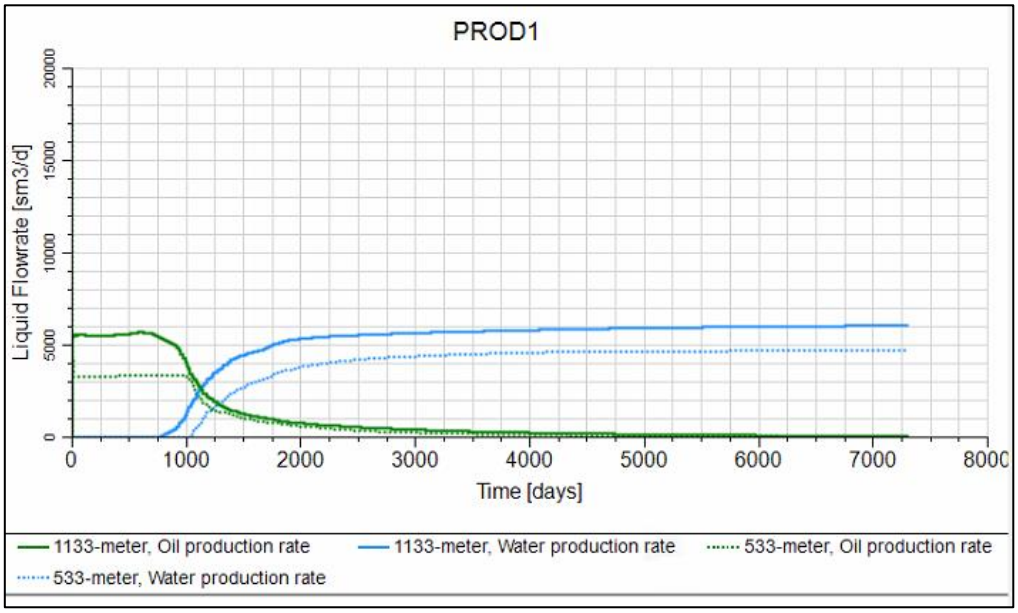

Figure 5.12: Oil and water production for PROD1.

5.3.2 Water-oil ratio.

The water-oil ratio of the 533m long well (533-meter) is given by a dotted line and the 1133m long well (1133-meter) is given by a solid line.

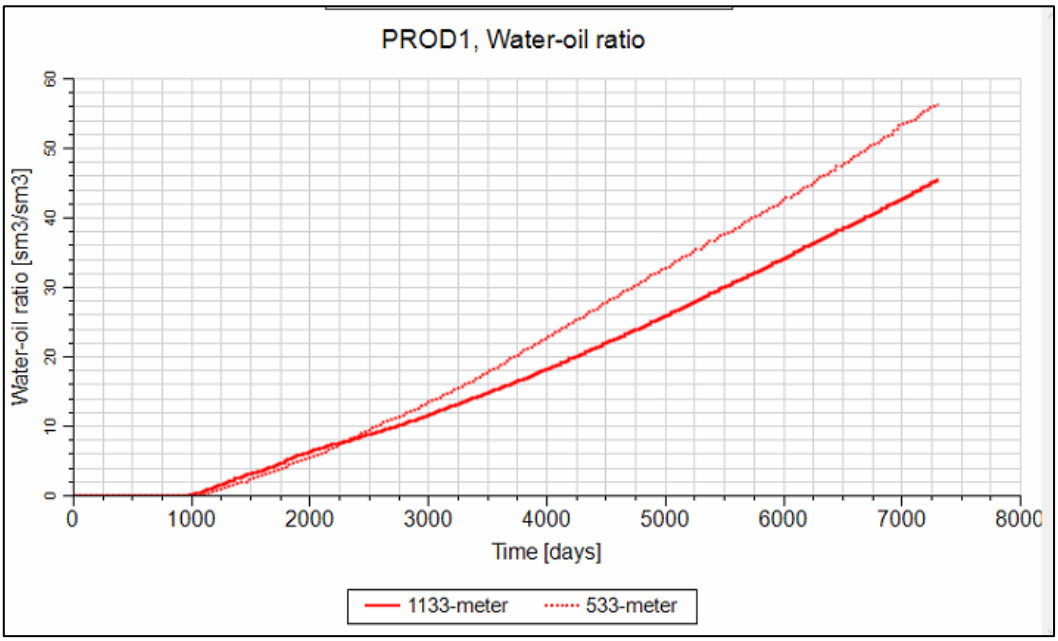

Figure 5.13: Water-oil ration of PROD1 at varying length.

5.4 3D simulation results of Oil Saturation.

Figure 5.14 shows the 3D oil saturation simulation result of the Enlarged Egg model with horizontal producers. The simulation is run for 20 years, and the images are taken at the interval of every four years.

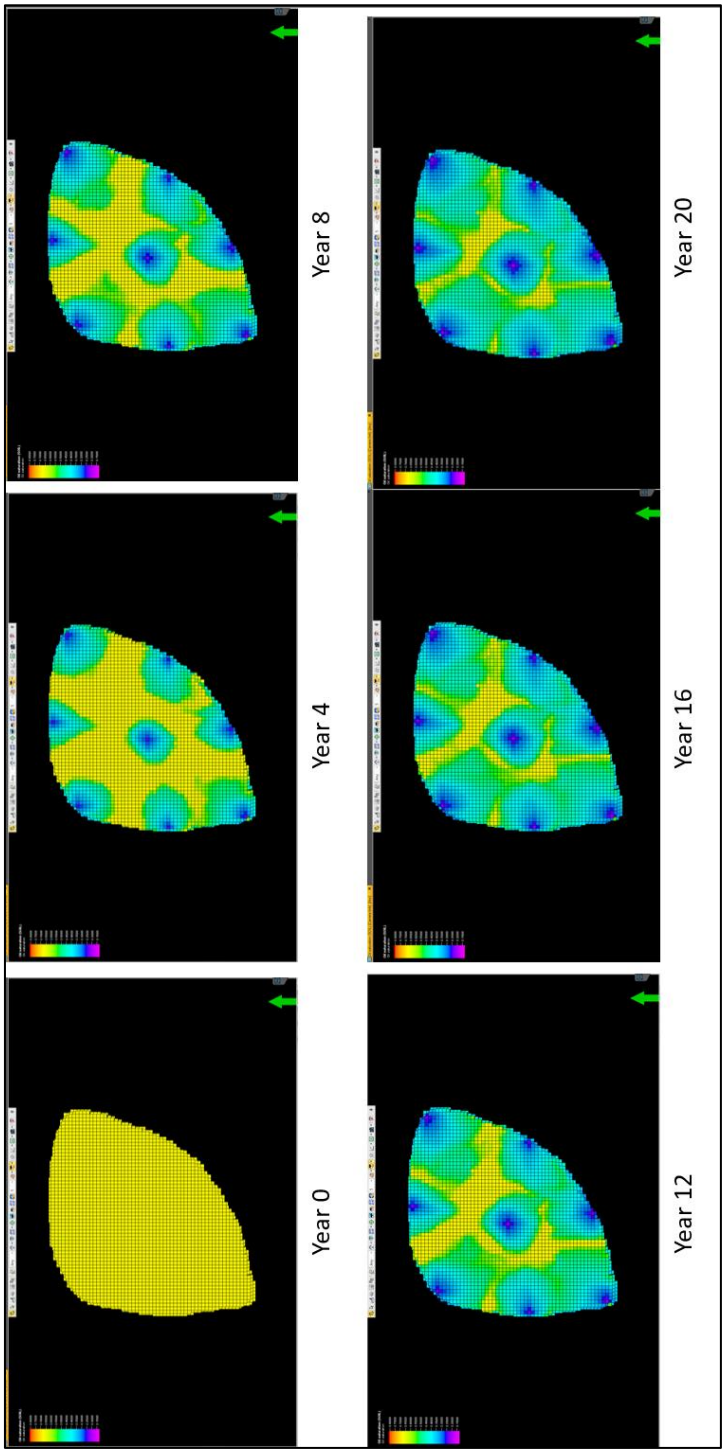

Figure 5.14: 3D simulation results at the interval of 4 years.

6 Discussion

6.1 Egg Model

The grid and well data of the egg model developed in eclipse were imported in the Petrel and were further developed by assigning the right porosity, permeability, contact sets, fluid models, rock properties, and development strategies. The simulation result of this case developed in petrel is then compared with the MSRT/eclipse results presented in the reference [24]. Figure 5.1, Figure 5.2, Figure 5.3, and Figure 5.4 shows the simulation result of Petrel (Dotted) vs Eclipse (Solid). In both cases, the bottom hole pressure for the production well is set at 395 bar and the rate of water injection at the surface is 79.5 m^3/day. The oil and water production was simulated for 10 years in both cases. It can be observed that the result of both the cases in all the four plots follows a similar trend of oil and water production. The simulation result of Petrel in all four producers is not exactly in line with the simulation result of Eclipse and MRST as presented in the reference [24]. This is because Petrel is a highly advanced modeling software and has a library of preset data for the fluid model. This can lead to some variation in the simulation results. Since the trend of production for both oil and water is the same, the results of Petrel are considered acceptable.

6.2 Oil production in vertical vs horizontal wells.

The Enlarged Egg Model was developed for vertical and horizontal wells to compare the oil production in these two different scenarios. All the reservoir conditions were maintained exactly similarly in both scenarios.

The plot for oil and water production of PROD1 is given in Figure 5.5. It is clear from the plot that the production of a horizontal well is significantly higher than a vertical well for both oil and water production. The water breakthrough for the vertical PROD1 is earlier compared to the horizontal well. After observing the 3D simulations, it was observed that the water spreads in the lower part of the reservoir first given its higher density, and then it moves towards the upper layers pushing oil towards the top surface. And this explains the early breakthrough of water in vertical wells as the horizontal wells are situated in the first three layers of the reservoir.

Figure 5.6 shows the result for PROD2. Just as in the case of PROD1 the water breakthrough is earlier in vertical PROD2 which is around day 350 compared to day 750 in the case of a horizontal well. But the production of the vertical well is higher compared to the horizontal well since the location of the well also plays a vital role. This can be seen in the case of PROD2. Figure 4.15 shows the high permeability pattern in the reservoir which shows that the PROD2 sits exactly on top of this zone. Also, Figure 5.7 shows that the PROD2, INJECT2, and INJECT7 are in the same high permeability zone of the reservoir model. Due to this, the oil is swept rapidly towards the PROD2. Also, in a high permeability zone, the pressure drop is low, and this increases the production rate. In Figure 5.7 the PROD2 is marked with the red circle and the first image on the left verifies the water breakthrough on day 365. In the case of a

horizontal well, the production is comparatively low because the horizontal well lies in the low permeability zone completely.

The production of PROD3 is plotted in Figure 5.8. The production of the horizontal well is higher compared to the vertical well in PROD 3. But the water breakthrough, in this case, is significantly higher. This can be explained in Figure 5.9 where the oil saturation plot shows that the water reaches the horizontal well (water breakthrough) after 365 days.

The production of oil and water in the PROD4 is almost in line with the vertical as seen in the plot of Figure 5.10. The rate of oil production in the horizontal well is almost like that of PROD2 and PROD 3 which is around 2000 m^3/day. In this case, since the vertical PROD4 lies very close to the high permeability zone (See Figure 4.15), the production of the vertical well gets higher reaching close to the production of a horizontal well.

The cumulative production rate of all the producers i.e., the rate of production of the field is plotted in **Error! Reference source not found.**. The rate of oil production is seen as higher in the case of the horizontal well compared to the vertical well. Also, the water breakthrough in vertical wells happens earlier than in horizontal wells given the fact that water first spreads in a lower layer of the field. Due to this, the rate of production of oil is higher in the first 2000 days and the rate of water production is lower. After this point, most of the oil is produced and the production of water rises.

6.3 Effect of horizontal well length on reservoir production.

The increasing length of the horizontal well has a positive impact on the rate of oil production. As shown by the plot in Figure 5.12. In this simulation case, the oil production is nearly 3200 m^3/day for a 533m long well compared to 5500 m^3/day for an 1133 m. The production of oil increased by 70 %. This increase in production can also be validated from the figure Figure 2.8 in Chapter 2. The water breakthrough is early in longer well. 3D water saturation results show that the water reaches the longer well first and this explains the early breakthrough of water.

The plot in Figure 5.13 shows the water-oil ratio. The water-oil ratio is zero until the water breakthrough. For the longer well the water breakthrough is higher initially. This is because there is an early water breakthrough in the longer well. Then the water-oil ratio of the shorter well starts increasing. After 20 years, the water-oil ratio of the shorter well is higher than the longer well. This shows that the longer well produced more oil and less water.

6.4 Observation from the 3D plots with respect to time.

Timely simulation results help to better understand the oil sweeping efficiency of the pattern of injectors. This simulation results can be used to optimize the reservoir production by better locating the wells. This way wells can be directed in a better direction at a better inclination. Also, these timely simulation results help to locate the high permeability zones which shows the flow of fluid flow. These simulation results were used in this thesis to set the direction of horizontal wells such that the wells avoid the early water breakthrough in the Enlarged Egg Model.

7 Conclusion

This master's thesis has been conducted to develop a simulation model for secondary oil recovery and to achieve cost-effective and efficient oil recovery. The method used to achieve this was by studying and creating horizontal wells. To achieve the main objective of the thesis along with reservoir rock and fluid properties, different methods of water flooding were studied. Also, as a part of the literature review, horizontal wells and their challenges were examined in addition to the operation and working principles of the flow-controlled devices.

The challenging part however was learning a new reservoir modeling software. This was challenging given the fact that Petrel was never used before and there was very little study material available to study the software and create the reservoir model. Hence this was the most extensive part of this thesis. Overcoming this challenge, the Egg Model was developed in the Petrel and its results were compared with the other reservoir modeling software such as Eclipse and MRST. It was concluded that the results of a model developed in Petrel are very similar to the results from MRST and eclipse.

Through the comparative analysis of the vertical vs horizontal well, it can be concluded that it is possible to delay the water breakthrough in the horizontal well by using the appropriate pattern of producer wells. They also can increase the well's productivity since they help to increase the surface area of the well. Once the vertical well establishes contact with high permeability water channels they keep producing water and it becomes difficult to extract oil from the low permeability zones. This problem can be overcome by horizontal wells by implementing them in the low permeability zones which can help to improve the oil production by achieving better drainage patterns.

The length of the horizontal well also can significantly increase the production rate of the well. And this can help to achieve cost-effective oil production since it can reduce the number of offshore platforms and equipment. This in turn has a positive impact since the carbon footprint is also reduced.

The downside to the horizontal well is that it can have a heel-toe effect and the heterogeneity effect which can lead to the early water breakthrough which in turn leads to a significant drop in oil production. This phenomenon was also observed in the Enlarged Egg Model simulation for a horizontal well.

Also, the visual dynamic results of the simulations helped to better develop the pattern for producers and injectors and hence was useful to optimize the oil production. It was also easy to compare the different scenarios side by side to better understand and develop the reservoir model in Petrel.

Advanced flow control devices such as ICD, AICD, and AICV were also developed as a part of this thesis. They were also implemented in the Petrel software. However, their functionality was not analyzed given the time constraint. Literature review of the horizontal wells and the flow control devices show that they should help reduce the early breakthrough of water and enhance oil production. This can work as a base for future work.

8 References

[1] M. R. a. P. R. Hannah Ritchie, "Energy," 2020. [Online]. Available: https://ourworldindata.org/energy.

[2] "ELDOR," [Online]. Available: https://www.eldor.no/blog/will-the-oil-and-gas-industry-be-sustainable-in-the-future.

[3] I. E. Agency, "Exploring multiple futures fuels, Liquid fuels," in *2021, Energy Outlook*, iea, 2021, pp. 213-223.

[4] P. Description, "FMH&=&Master's Thesis 2022," University of South-Eastern Norway.

[5] P. G. M. T. E. o. E. B. Ben H. Caudle, "petroleum production - Recovery of oil and gas | Britannica," Britannica, [Online]. Available: https://www.britannica.com/technology/petroleum-production/Recovery-of-oil-and-gas.

[6] W. M. C. James T. Smith, " Review of Rock Properties and Fluid Flow," in *Waterflooding*, 17th Dec 1997, pp. 2-1.

[7] M. Mgimba, "Numerical Study on Autonomous Inflow Control Devices: Their Performance and Effects on the Production from Horizontal Oil Wells with an Underlying Aquifer," Norwegian University of Science and Technology, Department of Geoscience and Petroleum, August 2018.

[8] L. F. Olafsson, "Experimental study on thermal effects on well components," Faculty of Science and Technology, University of Stavanger., 2018.

[9] G. G. Alpay Erkal, "Inflow Control Devices- Rising Profiles," *Oilfield Review Winter* , 2019/2010.

[10] F. T. M. Al-Khelaiwi, "A Comprehensive Approach to the Design of Advanced Well, Volume 1," Institute of Petroleum Engineering, Heriot-Watt University, Edinburgh – Scotland, UK, 2013.

[11] M. ,. M. M. ,. V. M. M. ,. I. M. I. ,. a. A. G. Halvorsen, "Enhanced Oil Recovery On Troll Field By Implementing Autonomous Inflow Control Device.," in *SPE Bergen One Day Seminar*, Grieghallen, Bergen, Norway, April 2016.

[12] M. H. M. Abd El-Fattah, "Case Study: Utilizing of Autonomous Inflow Control Valves Helps to have Better Fahud Wells Production Performance," in *Mediterranean Offshore Conference & Exhibition*, Alexandria, Egypt, 2019.

[13] A. Moradi, *DigiWell Project, WP1, Multisegment Well Model*, Porsgrunn: University of South-Eastern Norway, 7th March 2022.

[14] Schlumberger, "Reservoir Engineering," 2010.

[15] S. G. T. B. S. N. H. A. a. 0. L. S. S. J.A. Holmes, "Application of a Multisegment Well Model to Simulate Flow in Advanced Wells," *Society of Petroleum Engineers.,* p. 2, 2o-22 October 1998.

[16] K. N. a. J. H. S. Bryony Youngs, "Multisegment well modeling optimizes inflow control devices," *World Oil,* no. May 2010, pp. 37-42.

[17] A. Y. Dandekar, Petroleum Reservoir Rock and Fluid Properties, CRC Press, 2013.

[18] A. M. Pantami, "Factors affecting the quality of sandstone reservoir rocks," *Research Gate,* June 2021.

[19] P. G. Dr, "Relative Permeability," in *Formation Evaluation MSc Course Notes, University of Leads*, pp. 104-118.

[20] [Online]. Available: https://web.mst.edu/~numbere/cp/chapter%203.htm.

[21] B. Lie, "Project, FM1015 Modelling of Dynamic Systems," 17 Sept 2021.

[22] M. Mgimba, "Numerical Study on Autonomous Inflow," Norwegian University of Science and Technology, Department of Geoscience and Petroleum, Aug 2018.

[23] H. A. a. V. M. I. Anita B. Elverhøy, "Autonomous Inflow Control for Reduced Water Cut and/or Gas Oil Ratio," *Offshore Technology Conference,* 30 April-3 May 2018.

[24] R. M. F. S. K. M. M. S. G. M. V. E. a. P. M. J. V. d. H. J. D. Jansen1, "Thee egg model – a geological ensemble for reservoir simulation," *Royal Meteorological Society,* 15th October 2014.

[25] [Online]. Available: https://wiki.aapg.org/Fluid_contacts#:~:text=The%20hydrocarbon%2Dwater%20(oil%2D,is%20the%20produced%20hydrocarbon%20phase..

[26] O. Team, "Dead Oil (dead crude)," 04 March 2018. [Online]. Available: https://oilfieldteam.com/en/a/learning/dead-crude-030418. [Accessed 28 May 2022].

[27] D. K. a. A. S. O. Babu, "Productivity of a Horizontal Well.," *SPE Reservoir Engineering,* pp. 417-421, 1989.

Appendices

Appendix A

University of South-Eastern Norway

Faculty of Technology, Natural Sciences and Maritime Sciences, Campus Porsgrunn

FMH606 Master's Thesis

Title: Modeling and analysis of secondary oil recovery through advanced wells

USN supervisor: Prof. Britt M. E. Moldestad, Associate Prof. Amaranath S. Kumara, and Ali Moradi

External partner: Equinor and SINTEF

Task background:
According to DNV's Energy Transition Outlook 2021, oil and gas will remain the most important source of energy for the foreseeable future and there is an urgent need to improve oil and gas recovery with less carbon footprint to meet the future energy demands. Norway has a great potential to supply petroleum to the global market, and the Norwegian Continental Shelf (NCS) is one of the most technologically advanced petroleum regions in the world. To secure the competitiveness of the NCS in the international market and to ensure that NCS is at the forefront of adopting the latest technological innovations, OG21 (Oil and gas for the 21st century) has developed a national technology strategy for guiding research efforts in the field of petroleum technology. The main strategic objective of OG21 is to obtain efficient, secure, and environmentally friendly value creation from the Norwegian oil and gas resources for several generations.

In line with the OG21 strategy, there is an ongoing research project called *DigiWell* (*digital wells for optimal production and drainage*) at USN, funded by the Norwegian Research Council, as well as Equinor. In addition, SINTEF, UiO, ICL, and MIT are the main research partners of this project. The project aims at developing new methods, algorithms, and tools for the prediction of oil production under uncertain conditions in order to maximize the profit margins by minimizing the production cost. As part of this project, it is of great interest to model and evaluate the performance of advanced wells with the goal of improving oil recovery.

A hydrocarbon reservoir can be considered as a rigid sponge that is confined inside an insulating material and has all its pores filled with hydrocarbons, which may appear in the form of a liquid oleic and a gaseous phase. Extraction of oil from a reservoir starts by drilling a well into the oil zone. If the initial pressure inside the reservoir is sufficiently high, it will push oil up to the surface which is referred as primary production, see Figure 1 for further details. As the oleic phase is produced, the pressure inside the reservoir will decline. Therefore, other mechanisms like gas and/or water injection are used for maintaining pressure and producing more oil from the reservoir. This production system is called secondary production, see Figure 2 for further details.

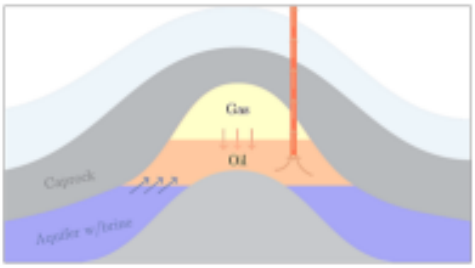

Figure 1. Primary oil production

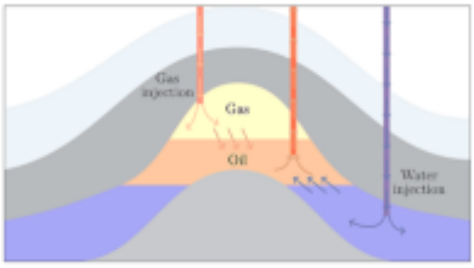

Figure 2. Secondary oil production

One of the main principles to achieve cost-effective and efficient oil recovery is maximizing the well-reservoir contact by using long horizontal wells. One of the main challenges of using such wells is early gas and/or water breakthrough due to the heel-toe effect and heterogeneity along the horizontal wells. To tackle this problem, advanced (smart or intelligent) wells are widely applied today. Advanced wells are horizontal wells equipped with downhole Flow Control Devices (FCDs), sand screens, zonal isolation as well as monitoring and control systems, etc. FCDs are the key elements of advanced wells. The main types of such devices are passive Inflow Control Devices (ICDs), Autonomous Inflow Control Devices (AICDs), Autonomous Inflow Control Valves (AICVs), and Interval Control Valves (ICVs). In order to achieve a successful design of advanced wells, a suitable dynamic model of oil field and advanced wells must be developed. One of the main barriers for developing such dynamic models is that generally, it is difficult to observe and understand the dynamics of fluid flow in a porous medium. Besides, measuring all the parameters that influence the multiphase flow behavior inside a reservoir is not possible. Consequently, predicting how a reservoir will produce over time and respond to different drive and displacement mechanisms has a large degree of uncertainty attached.

The main objective of this thesis is modeling and simulation of secondary oil recovery with water flooding from a heterogeneous reservoir through advanced wells completed by main types of FCDs. The simulation models can be developed either by free open source or commercial software.

Task description:

The objectives of this research project can be achieved by completing the following tasks:

1. Literature study
   - Reservoir rock and fluid properties
   - Improved oil recovery by water flooding
   - Advanced wells
2. Developing the simulation models
   - MATLAB Reservoir Simulation Toolbox (MRST, developed by SINTEF) is a free open-source software for reservoir modeling and simulation and it is a robust tool for this purpose, but commercial reservoir simulators like OLGA in combination with ROCX, and PETREL can also be used.
3. Evaluating the performance of advanced wells in secondary oil recovery
   - The performance of advanced wells completed by ICDs, AICDs, AICVs, and ICVs as well as zonal isolations in a heterogeneous reservoir with water flooding should be analyzed.
4. If time permits, preparing a paper based on the results for the next SIMS conference is highly appreciated.

Student category: EET and PT students

Is the task suitable for online students (not present at the campus)? No

Practical arrangements: Necessary software will be provided by USN.

Supervision:
As a general rule, the student is entitled to 15-20 hours of supervision. This includes necessary time for the supervisor to prepare for supervision meetings (reading material to be discussed, etc).

Signatures:

Supervisor (date and signature):

Student (write clearly in all capitalized letters):

Student (date and signature): Onkar Bhujange

Appendix B

ICD modelling calculations

$$\Delta P = C\frac{1}{2}\rho v^2$$

Where,

$$v = \frac{q}{A}$$

Therefore,

$$q = C.A\sqrt{\frac{2\Delta P}{\rho}}$$

$$A = \frac{q}{C\sqrt{\frac{2\Delta P}{\rho}}}$$

$$A = \frac{0.6/3600\ m^3/s}{0.85\sqrt{\frac{2\times 15\times 10^5\ Pa}{890\ Kg/m^3}}}$$

$$A = 3.3653\times 10^{-6}\ m^2$$

Appendix C

Web Plot Digitizer SS

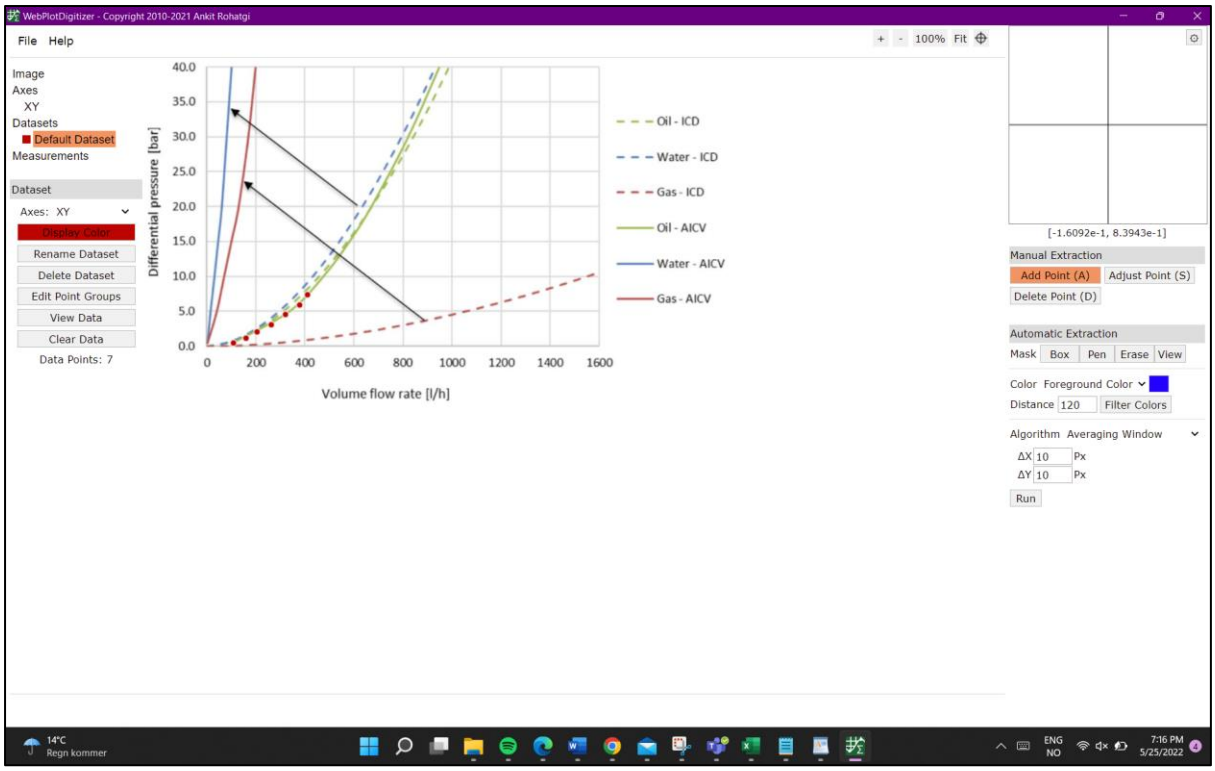

Appendix D

Input Parameters

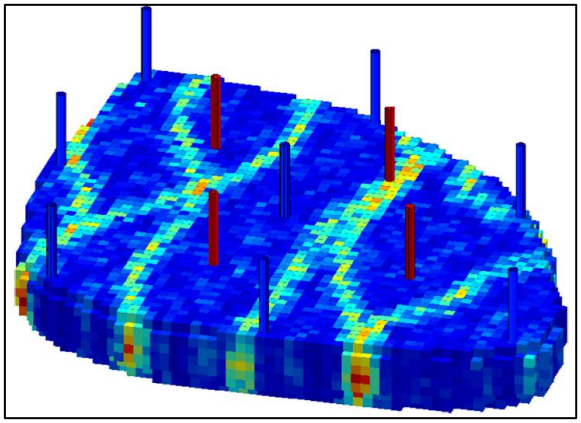

Two-phase (oil-water) flow. The model has no aquifer and no gas cap, primary production is almost negligible, and the production mechanism is water flooding with the aid of eight injection wells and four production wells.

Assume the injection wells are located in the last three vertical layers and the production wells are located in the first three layers

Assume Hemogenous reservoir with Permx = Permy = 500 mD, Permz = 0.1 x Permx = 50 mD

Number of grids: 15 x 15 x 7

Symbol	Variable	Value	SI units
h	Grid-block height	4	m
Δx, Δy	Grid-block length/width	8	m
ϕ	Porosity	0.2	–
c_o	Oil compressibility	1.0×10^{-10}	Pa^{-1}
c_r	Rock compressibility	0	Pa^{-1}
c_w	Water compressibility	1.0×10^{-10}	Pa^{-1}
μ_o	Oil dynamic viscosity	5.0×10^{-3}	Pa s
μ_w	Water dynamic viscosity	1.0×10^{-3}	Pa s
k_{ro}^0	End-point relative permeability, oil	0.8	–
k_{rw}^0	End-point relative permeability, water	0.75	–
n_o	Corey exponent, oil	4.0	–
n_w	Corey exponent, water	3.0	–
S_{or}	Residual-oil saturation	0.1	–
S_{wc}	Connate-water saturation	0.2	–
p_c	Capillary pressure	0.0	Pa
p_R	Initial reservoir pressure (top layer)	40×10^6	Pa
$S_{w,0}$	Initial water saturation	0.1	–
q_{wi}	Water injection rates, per well	79.5	m^3/day
p_{bh}	Production well bottom-hole pressures	39.5×10^6	Pa
r_{well}	Well-bore radius	0.1	m
T	Simulation time	3600	day

Inject one pore volume of water

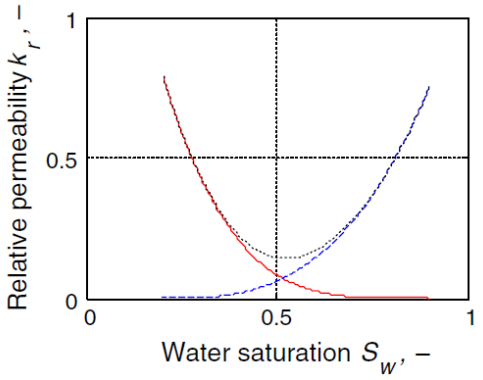

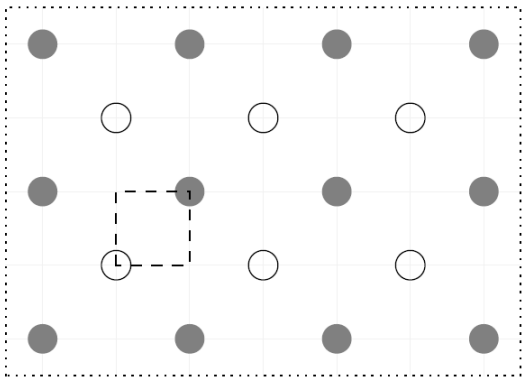

Producer

Injector

Quarter five-spot

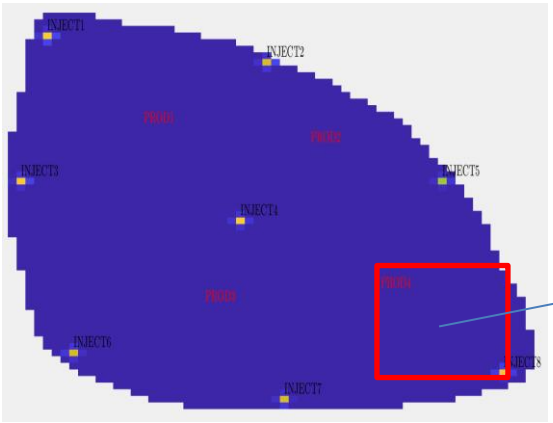

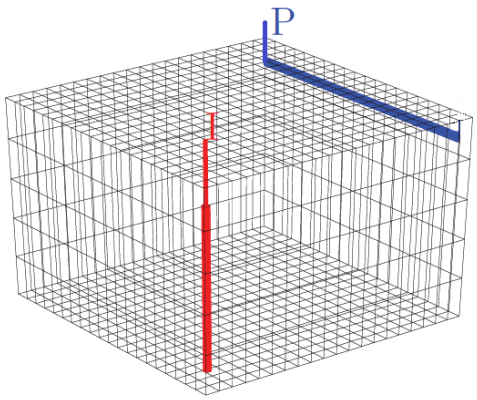

Appendix E

Vertical Wells of Egg Model

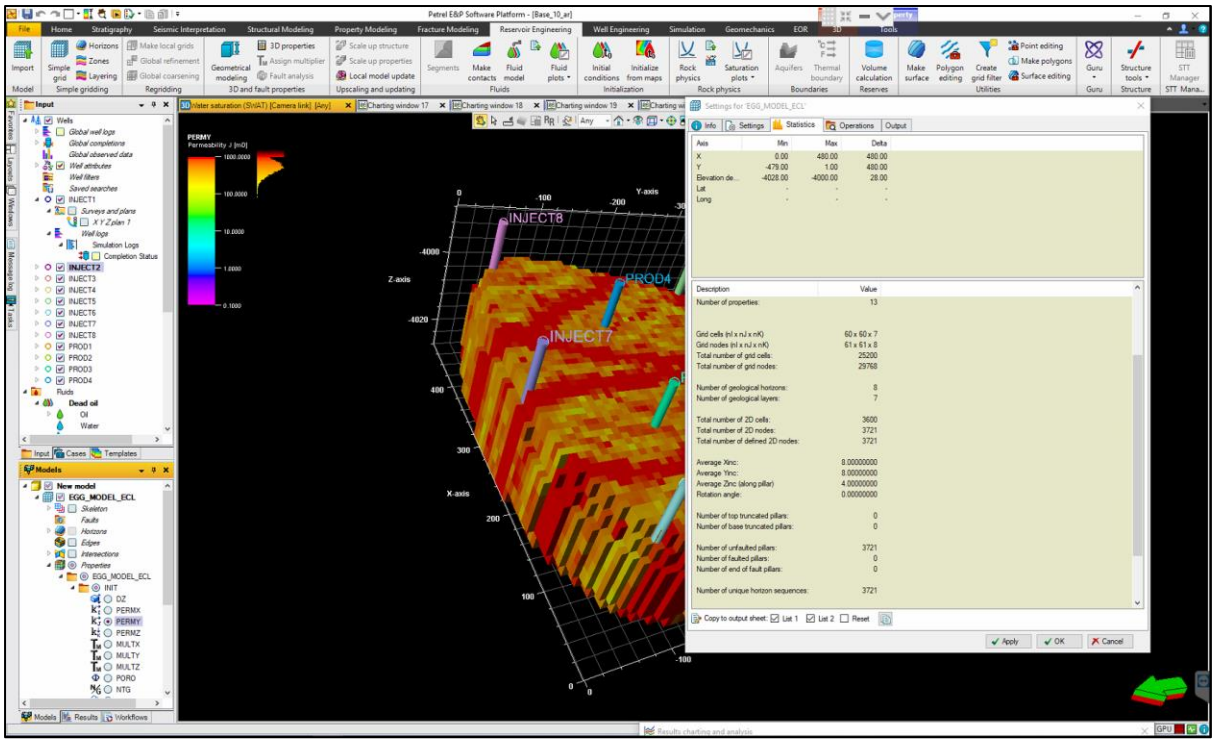

Appendix F

Well Modelling SS

Trajectory spreadsheet for 'X Y Z plan 1'

First MD: 0.00 m

Show calculated result

Show

	X m	Y m	Z m	MD m	Inclination deg	Azimuth deg	DX m	DY m	TVD (Well datum) m	TWT ms	DLS deg/30m
1	36.00	-451.00	-3988.00	3988.00	0.00	0.00	0.00	0.00	3988.00		0.00
2	36.00	-451.00	-4002.00	4002.00	0.00	0.00	0.00	0.00	4002.00		0.00
3	36.00	-451.00	-4006.00	4006.00	0.00	0.00	0.00	0.00	4006.00		0.00
4	36.00	-451.00	-4010.00	4010.00	0.00	0.00	0.00	0.00	4010.00		0.00
5	36.00	-451.00	-4014.00	4014.00	0.00	0.00	0.00	0.00	4014.00		0.00
6	36.00	-451.00	-4018.00	4018.00	0.00	0.00	0.00	0.00	4018.00		0.00
7	36.00	-451.00	-4022.00	4022.00	0.00	0.00	0.00	0.00	4022.00		0.00
8	36.00	-451.00	-4026.00	4026.00	0.00	0.00	0.00	0.00	4026.00		0.00
9	36.00	-451.00	-4028.00	4028.00	0.00	0.00	0.00	0.00	4028.00		0.00

Image 1

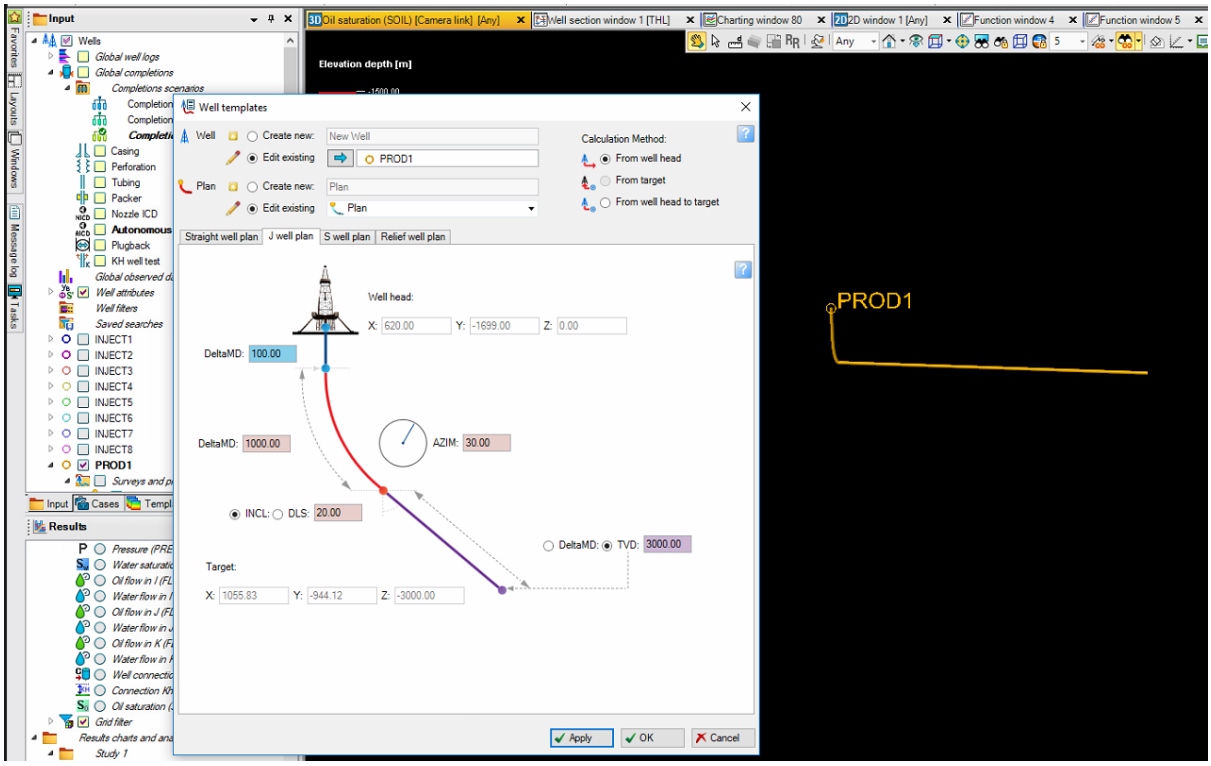

Image 2

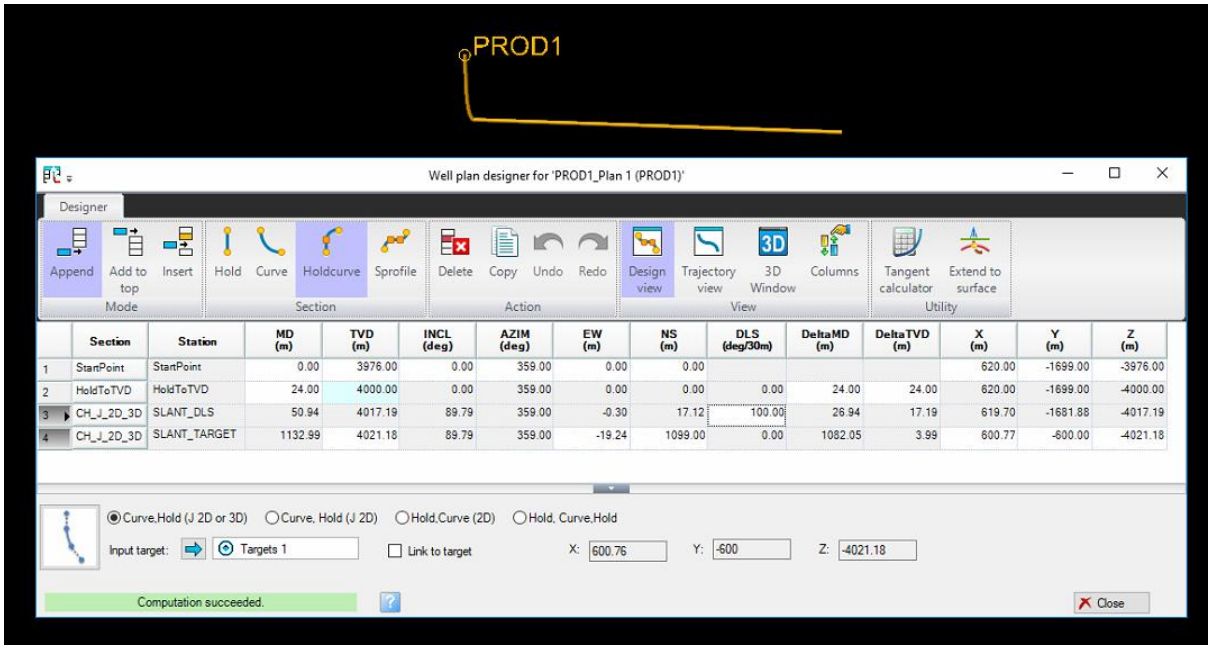

Image 3

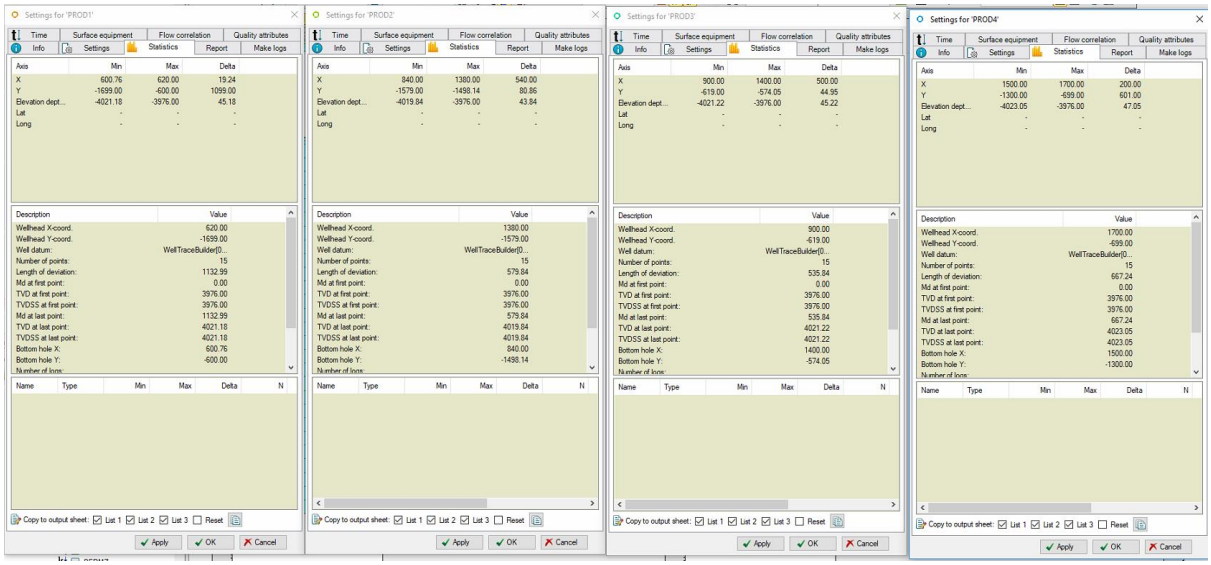

Image 4

Appendix G

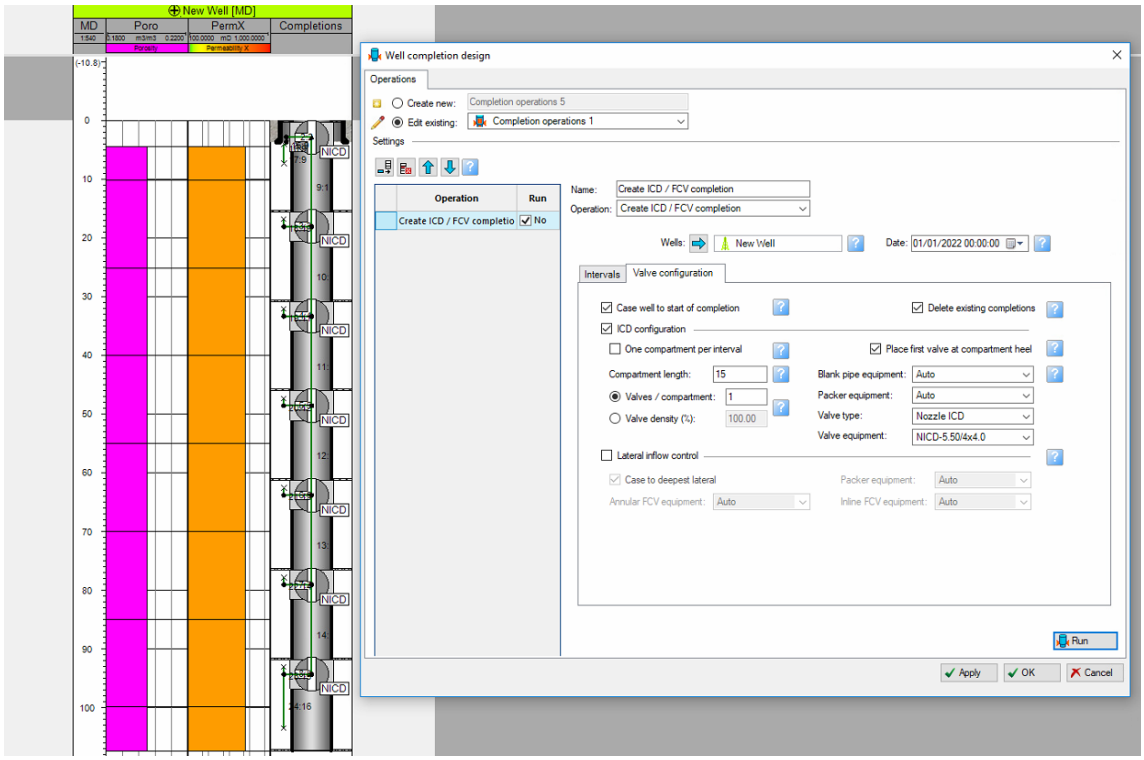

Image 1